ACE Deliverable 2.2D2

Future Trends in Terminal Antennas

Project Number: FP6-IST 508009

Project Title: Antenna Centre of Excellence

Document Type: Deliverable

Document Number:

Contractual date of delivery: 31st December 2005

Actual Date of Delivery: 19th December 2005

Workpackage: 2.2-1

Estimated Person Months:

Security (PP,PE,RE,CO): PU

Nature: Report

Version: 1.0

Total Number of Pages: 117

File name: ACE-A2.2.D2.pdf

Editor: M. Martínez-Vázquez (IMST)

Participants: A. Skrivervik (EPFL), L. Jofre (UPC), R. Serrano-Calvo (UPC), A. Sharaiha (IETR), P.-S. Kildal (Chalmers), C. Icheln (HUT), S. Schulteis (IHE), C. Kuhnert (IHE), C. Sturm (IHE), C. Luxey (LEAT), C. Peixeiro (IST), A.J. Johansson (LU), A. Derneryd (LU)

Abstract

The present document presents a review of future trends in mobile communications terminals, their repercussion in antenna design. New present and upcoming standards, such as 3rd generation mobile or broadcasting systems are analysed. The main requirements regarding their implementation and operation characteristics are also considered, along with some new applications, such as RFID, on-body antennas and implanted devices. Finaly, new technologies for antennas are analysed.

Keyword List

Mobile communications terminals, antennas, future trends.

Table of Contents

EXECUTIVE SUMMARY

Along the whole duration of ACE, a research was carried out in order to determine the future trends concerning personal communications devices. During this research it has been noticed that it is possible to enhance the performance of the networks and to provide the user with higher data rates and thus with better services by using multiantenna configurations at the base or mobile station or both. From the network operator as well as the user point of view the use of high-quality antennas is also important due to general enhancement of the performance of the radio system. During recent development work on mobile communications terminals emphasis has been directed towards devices working in several radio systems. As many as 10 or more radios can be expected in future devices, which sets a challenge for the antenna designer especially due to the very limited space available in handheld terminals.

The first chapter of this report will describe the situation of the latest and upcoming standards for cellular mobile communications. This includes not only a review of the requirements of thirds generation systems, such as UMTS (Universal Mobile Comminications Standard), but also some updated requirements for second generation devices. In this sense, some consideration will be given to the need for HAC (Hearing Aid Compatible) phones.

Chapter 2 deals with the trends in wireless, non-cellular communications. These include some standards designed for broadcast applications. Future handsets should be adapted to the reception of digital-TV and radio. The use of these broadcast technologies will also allow increasing the data rate in the downlink. The applications of UWB (Ultra Wide-Band) to short range communications and positioning applications will also be described.

Additionally, it was shown already many years ago that the use of MIMO (Multiple Input, Multiple Output) antenna systems to form independent parallel propagation channels between a transmitter and a receiver in theory yields a linear increase in the link capacity, when the number of antennas is increased. However, the initial assumptions were and are often also today quite ideal, i.e. the power and angular distributions of the different signals are commonly assumed to follow the traditional Rayleigh criteria with a wide angular distribution providing the richness of separate multipaths. Moreover, the antenna elements at each end of the link are typically assumed to form a simple array configuration and have equal radiation properties. In reality, placing several antenna elements on a handheld terminal is challenging and the usage condition of the terminal far from ideal due to the unpredictable holding position of the terminal. A lot of research is required to determine feasible multi-antenna implementations in a terminal and to be able to estimate their realistic performance.

In chapter 3, other emerging applications will be analysed. These include RFID (Radio-Frequency Identification) systems, which are rapidly spreading to cover many different fields, ranging from asset tracking to medical applications. The specific requierements of RFID antenna design will then be analysed. Body Area Networks (BAN) will also have an increasing importance in the next future, fostering the development of on-body devices that will satisfy the need for body-centric configurations. These devices will be distributed all over the body of the human user, and will therefore require novel antenna solutions. This applies also to antennas dor in-body devices, such as medical implants.

MIMO systems are designed for rapidly changing communications environments. Therefore, their performance is determined by their ability to adapt to the changing channel conditions. To analyse this problem, both the antenna arrays and the propagation channel should be considered as a whole. A Statistical description is needed, to take into account the different channel realisations of the propagation environment. For that, it is necessary to use a proper characterisation of the channel properties. This will be treated in chapter 4.

Finally, chapter 5 will be devoted to innovative technological solutions that can be applied to terminal antenna design. These technologies include on-chip and o-package antennas for RF applications, which could lead to higher integration. The use of MEMs (Micro-Electro-Mechanical Systems) would allow the design of reconfigurable antennas for terminals, whereas metamaterials can also be considered for enhancing the antenna performance.

INTRODUCTION

The first deliverable of WP 2.2-1 of ACE was dedicated to a review of the state of the art in terminal antenna design. It showed that, variety of factors had to be taken into account, which include: small physical size, mechanical robustness, operation on a small ground plane, input bandwidth, radiation patterns, efficiency, interaction with the user and cost. Current needs and requiremebnts where identifyied, to allow a clear vision of the present situation in Europe and around the world and a better understanding of the future trends for mobile terminals.

Nevertheless, the market is countinuously evolving, at a rapid pace. The design of antennas for mobile applications must evolve in parallel with the technology and the applications, in order to respond to new societal needs. In this document, some of the most significant trends are identified and analysed. This should help defining new lines of reseach in the field of mobile communications terminals.

Antenna design for terminals must be application-oriented. Therefore, the first three chapters of the report are devoted to define future needs and trends for different kinds of applications: cellular communications, wireless connections and other uses that require or may be improved by RF communication. Then, some attention will be given to the problem of propagation in muultipath environments, which is especially important for MIMO systems. Finally, a review will be made of new technologies that can be used to improve the performance of mobile terminal antennas.

1. ANTENNAS FOR FUTURE CELLULAR APPLICATIONS

1.1. UMTS and beyond

1. Description of the context

The International Telecommunication Union (ITU) started the process of defining the standard for third generation systems, referred to as International Mobile Telecommunications 2000 (IMT-2000). UMTS is one of the Third Generation (3G) mobile systems being developed within this ITU's IMT-2000 framework. The main characteristics of 3G systems are a single family of compatible standards:

- Used worldwide
- Used for all mobile applications
- Support both packet-switched (PS) and circuit-switched (CS) data transmission
- High data rates up to 2 Mbps (depending on mobility/velocity)
- High spectrum efficiency

In Europe, the European Telecommunications Standards Institute (ETSI) was responsible of UMTS standardisation process. In 1998, the Third Generation Partnership Project (3GPP) was formed to continue the technical specification work. Later, the Third Generation Partnership Project 2 (3GPP2) was formed for technical development of cdma2000 technology, which is also a member of IMT-2000 family.

ITU Recommendation ITU-R M.1457 specifies five types of 3G radio interfaces:

- IMT-2000 CDMA Direct Spread, also known as UTRA FDD. UMTS is developed by 3GPP.
- IMT-2000 CDMA Multi-carrier, also known as Cdma2000 developed by 3GPP2.
- IMT-2000 CDMA TDD, also known as UTRA TDD and TD-SCDMA.
- IMT-2000 TDMA Single Carrier, also known as UWC-136 (Edge)
- IMT-2000 DECT.

One of the main advantages of UMTS over existing cellular systems is the drastic increase in data rates that enables multimedia applications such as video streaming. In order to improve the link

reliability needed for reaching high data rates, multi-element antenna structures in the terminal are a popular way to achieve antenna diversity. A realistic number of antenna elements placed on the quite small mobile terminals is probably less than five. In this context especially dual-polarised antenna elements are interesting, as they enable locating two antennas in the same volume.

However, it is quite obvious that the 2G and 3G mobile networks will continue to coexist during a certain period. As a consequence, one antenna for each communication standards will have to be integrated above the same terminal [1] or at least, when the radio front-end modules will reach maturity, a multi-band antenna covering the involved standards [2].

UMTS will be upgraded with High Speed Downlink Packet Access (HSDPA), sometimes known as 3.5G. This will make a downlink transfer speed of up to 14.4 Mbit/s possible. Work is also progressing on improving the uplink transfer speed with the High-Speed Uplink Packet Access (HSUPA).

2. *Requirements: frequency allocation.*

In February 1992, the World Administrative Radio Conference WARC-92 allocated the frequency bands of 1885-2025 and 2110-2200 MHz for IMT-2000 use. The frequency allocation of the different standards around the world can be seen in Figure 1.

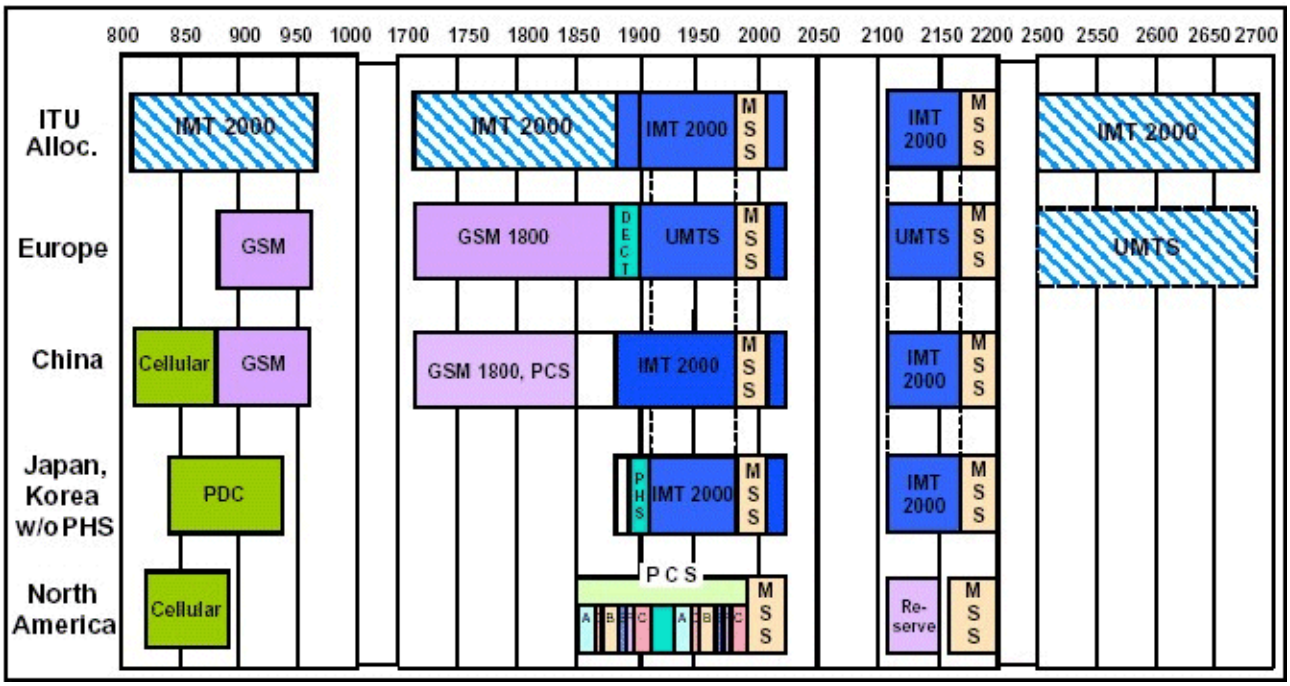

Figure 1: Frequency allocation (source: UMTS World)

In the case of UMTS, the frequency band is divided into three different blocks:

- 1900-1920 and 2010-2025 MHz: Time Division Duplex (TDD, TD/CDMA). Tx and Rx are

not separated in frequency.

- 1920-1980 and 2110-2170 MHz: Frequency Division Duplex (FDD, W-CDMA).
- 1980-2010 and 2170-2200 MHz :Satellite uplink and downlink.

In the USA, the frequencies allocated for 3G are:

- Uplink: 1850-1910 and 1710-1770 MHz.
- Downlink: 1930-1990 and 2110-2170 MHz.

Because the US has not provided new spectrum for UMTS, it must share spectrum with the existing 1G and 2G systems.

3. Antenna concepts

First, an example for a dual-polarised design is presented and evaluated. In Figure 2, a possible UMTS dual-antenna solution for a diversity antenna structure in a mobile terminal is shown. When the performance of the antenna prototype (and several similar designs) was estimated with the EPWBM method described in Chapter 4, it was seen that the link budget can typically be improved by about 5 dB by using the diversity technique [3]. The improvement was quite similar in several different radio-channel environments. In a few cases the improvement was not as good, and the most typical reason for the sometimes poorer diversity performance was noticed to be the power imbalance between the antenna branches. This may be caused either by incorrect polarisation or beam direction of one branch.

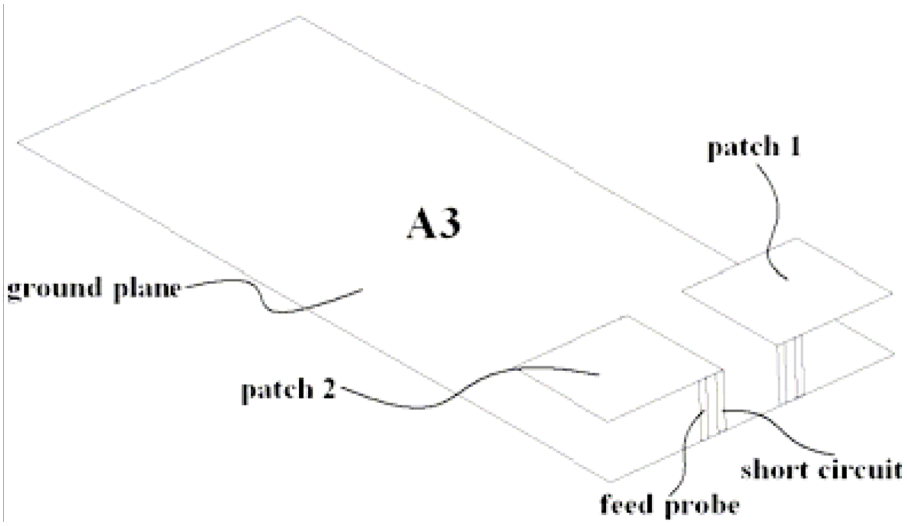

Figure 2: Dual element PIFA prototype for UMTS using polarisation diversity

In Figure 3, a possible multi-antenna solution for a multi-mode (GSM and UMTS) mobile terminal is shown [1]. The antennas are closely spaced at the top corner of a 100 x 40mm^2 Printed Circuit Board (PCB), which represents a realistic mobile terminal. The mutual coupling between these

antennas is around -10 dB in the DCS/UMTS bands. In order to increase their isolation and thus enhance their total efficiencies, a suspended transmission line can be inserted between the antennas. It will act as a neutralization device by picking some signal on one antenna and reinjecting it on the other, with a suitable amplitude and phase. This enhanced structure is presented in Figure 4.

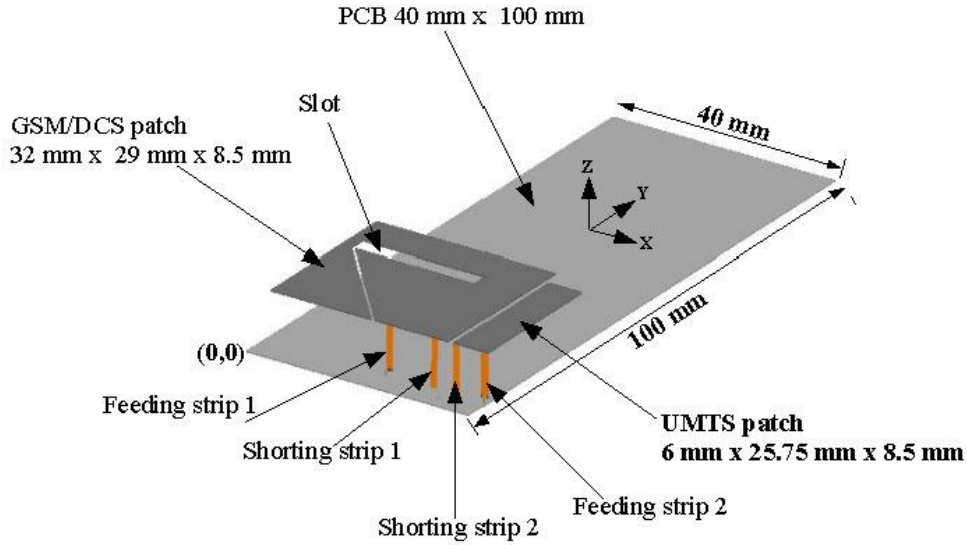

Figure 3: GSM/DCS and UMTS PIFAs without suspended line

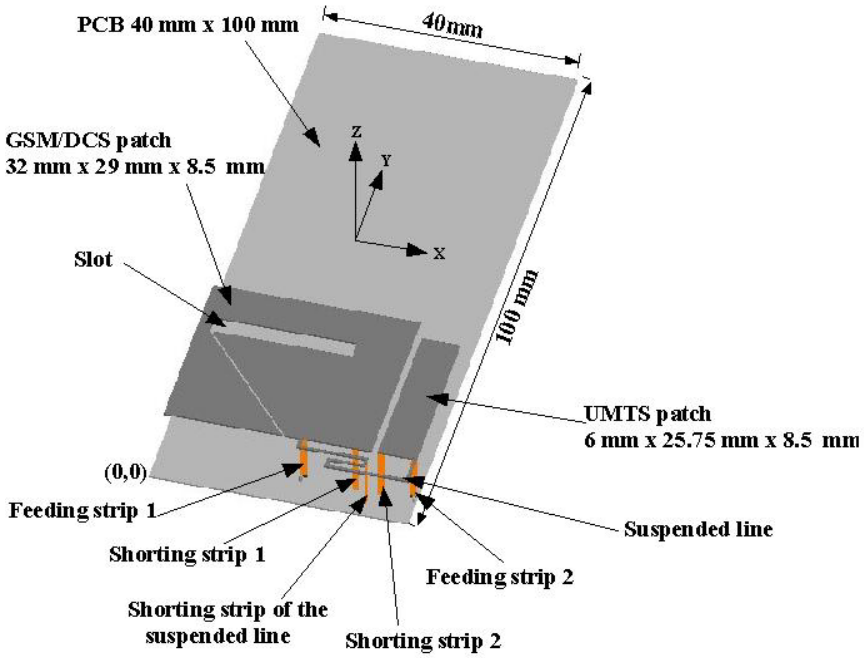

Figure 4: GSM/DCS and UMTS PIFAs with suspended line

By adding the suspended line, insertion losses drop to -15 dB in the higher frequency bands. A further enhancement of the isolation in the GSM band can be achieved by short-circuiting this suspended transmission line. The measurements of these antenna systems showed more than 15%

improvement in the total efficiency, to reach values as high as 90%, as displayed in Figure 5. Same kinds of solutions have been recently successfully implemented with two UMTS PIFAs working closely spaced on a small PCB. This gives some new opportunities for the implementation of efficient UMTS diversity antenna systems on small mobile phones.

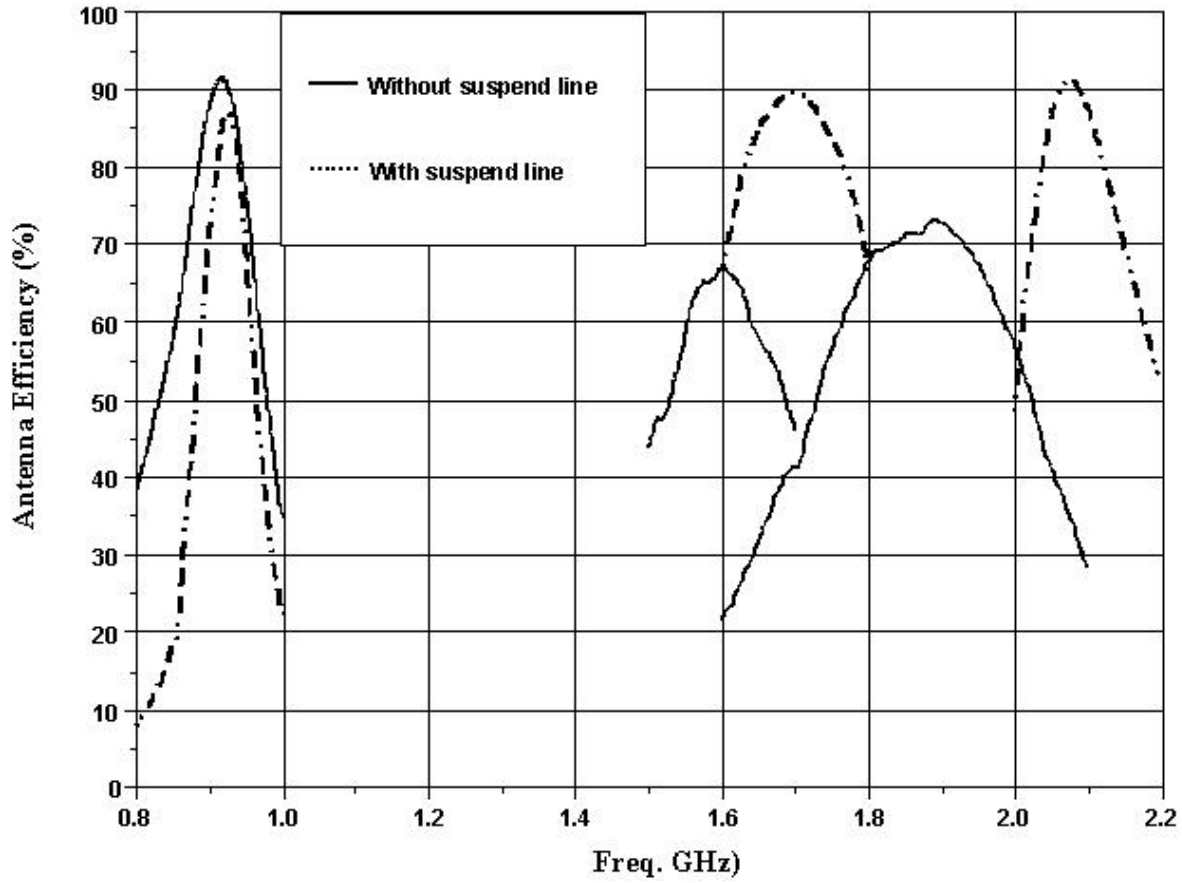

Figure 5: Measured total efficiencies of the GSM/DCS and UMTS PIFAs with and without suspended line

The emerging satellite personal communication networks will offer global communication coverage based on small handheld terminals. This terminals will also have to include third generation communications capabilities, such as UMTS connectivity.

The Printed Quadrifilar Helical Antenna (PQHA) is one of the most promising solutions as radiator for such applications. It it offers the advantage of light weight, low cost, circular polarisation, a good axial ratio and a radiation pattern which can be shaped in elevation as required with small structure changes. Figure 6 shows a compact PQHA with variable pitch angles, which includes an integrated feeding network [4], [5].

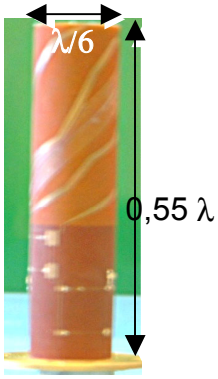

Figure 6: PQHA antenna for UMTS and satellite handsets.

The radiation patterns of the compact antenna, measured with a rotating dipole, are shown in Figure 7. Two different frequencies were considered: f=1.9GHz and f=2.2GHz {UMTS Band}. A half power beamwidth greater than 160° was obtained, with an axial ratio less than 3dB in all the coverage (cross polarisation < -15dB).

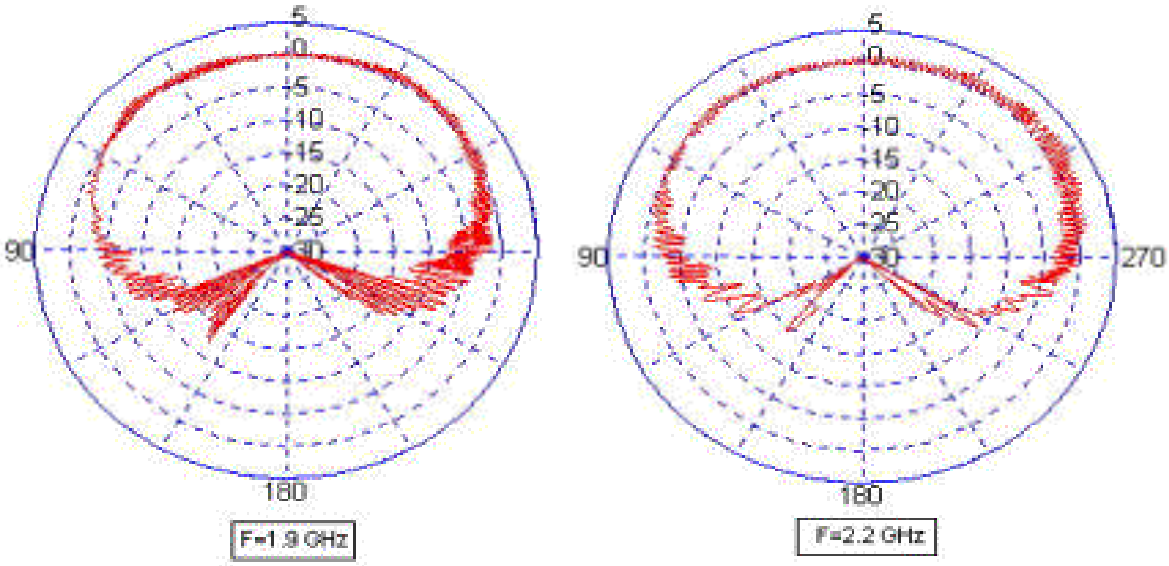

Figure 7: Radiation patterns in GPS (left) and UMTS (right) band.

4. *UMTS Measurements*

The performance of a mobile terminal in 3G systems will not only affect the quality of service to the user, but also the performance of the whole cellular network. The effect of terminal antenna performance on the UMTS system coverage/capacity in outdoor urban areas has been investigated in [6] and [7]. It was shown there that a 3 dB antenna performance degradation increases the number of required base stations by 40 %, and 6 dB degradation yield 100 % more base stations needed to cover the same service area. This motivates well-defined measurements of the mobile handsets performance including the antenna, or even multiple antenna systems.

Performance measurement require the definition of suitable figures of merit such as the total radiated power (*TRP*) and mean effective gain (*MEG*) (See [8]), as well as a definition of the different measurement methods. As in 2G systems, many aspects influence the accuracy of the measurement results, such as the user's hand, head and/or body, tissue-simulating liquids, number of samples. Due to the complexity of the issue, until now no standard performance measurement procedure has been defined for 3G terminal antennas, but the 3GPP standardization body (sub-working group RAN 4) [9] is currently working on suitable standard specifications for mobile handsets performance testing (See [8]).

1.2. HAC (Hearing Aid Compatible) terminals

A key challenge for the mobile industry is reducing the interference between some hearing aids and some digital wireless phones. Many hearing aid wearers still experience interference when using mobile phones, particularly if they use a telecoil[1] for telephone communication. The presence of noise affects the speech comprehension of people with partial hearing much more adversely than that of people with normal hearing. People with partial hearing thus require a high signal-to-noise ratio to optimize their speech discrimination. Telecoils help people with hearing loss achieve this high signal-to-noise ratio by coupling the Hearing Aid (HA) or Cochlear Implant (CI) inductively with Hearing-Aid Compatible (HAC) phones. Although there are no hard and fast rules, people with In-The-Ear (ITEs) or Completely-In-the-Canal (CICs) instruments generally experience less interference than people with Behind-The-Ear (BTEs) instruments, and newer, digital hearing aids are generally more immune to interference than older, conventional analogue hearing aids.

The radio waves emitted by the cell phone are referred to as radio-frequency (RF) emissions. The RF emissions create an electromagnetic (EM) field with a pulsing pattern around the mobile phone. This pulsing energy may potentially be detected by the microphone of the hearing aid or the telecoil circuitry, and perceived by the user as a buzzing sound. Besides, telecoil users may experience baseband, magnetic interference, caused by the electronics in the mobile phone (backlighting,

1 A telecoil is an induction coil. Placed in a varying magnetic field, an alternating electrical current is induced in its copper wire. The coil converts magnetic energy to electrical energy, retaining the original information, contained in the magnetic field around a telephone. The strength of the electrical current induced in the telecoil by the electromagnetic field is directly proportional to both the energy in the magnetic field and to the relative positions of the induction coil in the hearing aid to the magnetic field. The usefulness of telecoils includes detecting the electromagnetic field surrounding the earpiece of early telephones and current HAC phones.

display, keypad, battery, circuit board, etc). This baseband electromagnetic interference occurs in addition to the RF-interference, thus potentially increasing the effect perceived by the user. The amount of interference experienced by hearing-aid users also depends on the immunity of each hearing aid to these emissions. Moreover, the technology used for transmitting over a wireless network differs depending on the network, for example, CDMA or GSM, the interference may also have different characteristics, some of which may cause more annoying interference for hearing aid users than others.

In the USA, the Federal Communications Commission (FCC) requires that wireless phone manufacturers and wireless phone service providers make digital wireless phones accessible to individuals who use hearing aids. As ever more people have come to rely on wireless phones for safety, business, and personal uses, it is vital for individuals with a hearing impairment have access to digital wireless phones. The FCC has taken steps to increase access to wireless telephones by requiring wireless carriers and equipment manufacturers to make more digital wireless phones hearing aid-compatible. The ruling also requires a standard method for measuring digital cell phone emissions (i.e., ANSI C63.19 [10]) and product labelling on the outside packaging of the phone.

The latest timetable provided in June 2005 by the FCC includes the following points [11]:

- By **September 16, 2005**, the five largest wireless carriers must either make **four** hearing aid-compatible handset models available for each air interface or ensure that 25% of their handset models are hearing compatible.
- By **September 16, 2006**, the five largest wireless carriers must, per air interface, make **five** hearing aid-compatible handset models available for each air interface.
- **All** wireless carriers must ensure that 50% of their handset models are hearing aid-compatible by **February 18, 2008**.

The FCC defines Hearing Aid Compatibility (HAC) for cell phones in terms of two parameters: radio-frequency (RF) emissions and telecoil coupling. Cell phones that comply with the FCC's hearing aid compatibility rule must receive a minimum rating of M3 for RF emissions and T3 for telecoil coupling. "M" refers to the phone's RF emissions level and is intended for use with hearing aids in the microphone mode. The higher the "M" rating on the phone the more unlikely it will interfere with a hearing aid on the microphone setting. "T" refers to the phone's coupling ability and is intended for use with hearing aids in the telecoil mode. The higher the "T" number the more likely it will be to use the phone with a hearing aid on the telecoil setting.

This new HAC requirements translate into new problems related to antenna design. Indeed, the design of HAC terminals will have to be adapted to minimise the interaction with hearing aids. This will include not only the antenna, but also any element that could eventually interfere with a hearing device (loudspeaker, battery, display, etc.). EMC (Electromagnetic Compatibility) and nearfield

effects will also have to be considered, whereas measurement setups should also be defined to determine the behaviour of such devices.

The design of the telephone handset may be important for hearing aid users. HAC phones, as the examples presented in Figure 8, have often either a "clam shell" or "flip up" design, where the only part of the phone in the section that flips up is the speaker. This design provides some physical distance between the hearing aid and the components that may potentially cause interference. For telecoil users, it also provides physical distance between the cell phone electronics (another potential source of interference) and the hearing aid. The greater the distance between the hearing aid and these electronics, the less potential there is for interference experienced by the hearing aid wearer.

Figure 8: Examples of HAC mobile phones: Nokia 6255, LG VX4700 and Samsung SCH N330

Some of the suggested technically feasible solutions include [12]:

- Increase the strength of the radiated HAC field.
- Increase the size and effectiveness of the radiated HAC field with improved transmitting coils.
- Provide a user option to select HAC mode, to preserve the battery talk time.
- Reduce interference by the physical design and shape of the phone, for example using clam-phones in which the speaker is physically separated from other interfiering elements.
- Eliminate unnecessary interference from the display backlight and other hotspots.
- Design battery compartment and all associated battery supply conductors to cancel inductive EMI (Electromagnetic interference)/non-RF interference.

- Design shielding to reduce Inductive EMI/non-RF interference and RF at the earpiece/speaker.
- Ensure audio components are free of EMI.

2. ANTENNAS FOR WIRELESS COMMUNICATIONS

2.1. Digital Radio (DAB) and Digital Television (DVB-H)

1. Description of the context

One of the latest upcoming trends in mobile communications technology is the reception of digital-TV on mobile terminals. Besides the reception of public video streams it would also be possible to use this broadcast technology for other large-bandwidth data traffic (in the reception side), such as general or commercial localized information distribution.

2. Requirements and standards

Eureka 147 is a protocol for digital radio broadcasting originally developed in Europe and standardised by ETSI [13], but now being deployed in many countries around the world. It is more commonly known as Digital Audio Broadcast (DAB). Eureka 147 is operated in band III 174 to 240 MHz and in the L band, from 1452 to 1492 MHz, but can also operate in UHF bands. The scheme allows for operation almost anywhere above 30MHz. Antennas for DAB terminals must therefore be adapted to cover these bands with a reasonable performance.

DVB-H is the latest development within the set of DVB transmission standards. DVB-H technology adapts the successful DVB-T system for digital terrestrial television to the specific requirements of handheld, battery-powered receivers. The standard for terrestrial digital video broadcast, DVB-T, is not suitable for use in handheld TV reception due to an inherent high bandwidth and thus high power consumption of the receivers. Therefore, the adapted standard DVB-H (H as in handheld) was introduced recently to enable low-power receivers. The frequency range of the handheld digital video broadcast standard DVB-H is 470-702 MHz. Specifications for DVB-H receivers require a realised antenna gain of -10dBi at 470 MHz linearly increasing to -7dBi at 702 MHz [14]. This rather low realized gain specification was based on the common understanding of the realistic possibilities for implementing such a wideband antenna. It should be noted that in a transmitting antenna the matching has to meet the strict requirements of the RF power amplifier, whereas in a receiver antenna like for DVB-H, clearly higher matching losses (i.e. a lower total efficiency) can be accepted. This is because the radio environment is typically noisy in the DVB-H range [15], and in a noisy environment poor antenna matching does *not* deteriorate the signal-to-noise ratio. That is

why the only requirement set in the DVB-H specifications are for the realised antenna gain.

3. Antenna concepts

The lower end of the DVB-H frequency range is about half of the frequency used in the European GSM-900 system. This low frequency range makes the construction of antennas for the aspired small terminals very challenging. If for DVB-H the same antenna technologies were used that are popular in the GSM system, such as printed microstrip patches, the antennas alone would be almost as large as a current mobile phone.

To solve this problem, a small-antenna concept was developed that utilises the metal shield, which every mobile phone contains under the plastic cover, as an antenna [16]. A modular coupling structure ensures a good transfer of RF power between the radiating metal shield and the RF transceiver, see Figure 9. Since the coupling structure is non-resonant, the matching is achieved with an external lumped-element matching circuit, possibly dual-resonant and optimally overcoupled.

Here we present as an example the design of an antenna prototype intended for DVB-H reception in mobile terminals the size of current handheld computers (palmtops), see Figure 10. The coupling structure is very small (volume only 1.5 cm^3) compared to traditional antenna designs, and shows a sufficient performance across the whole DVB-H frequency band, even with a comfortable margin of 3 dB above the specifications given for the realized gain across the DVB-H band (see Figure 11). A margin like that is useful because in the final product a plastic cover and other lossy parts can cause significant losses, and also the user of a real terminal causes some additional losses.

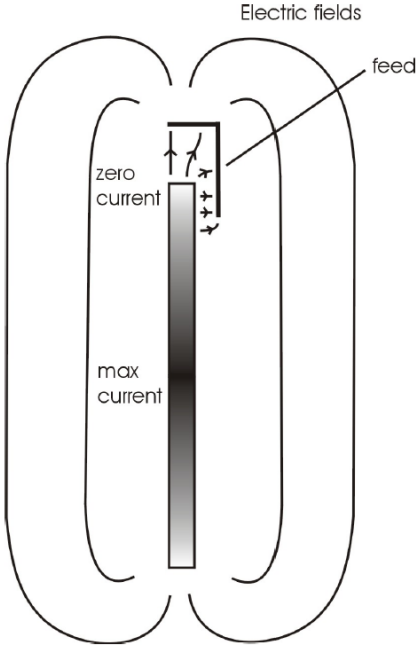

Figure 9: Chassis wave mode excited by the non-resonant coupling element structure.

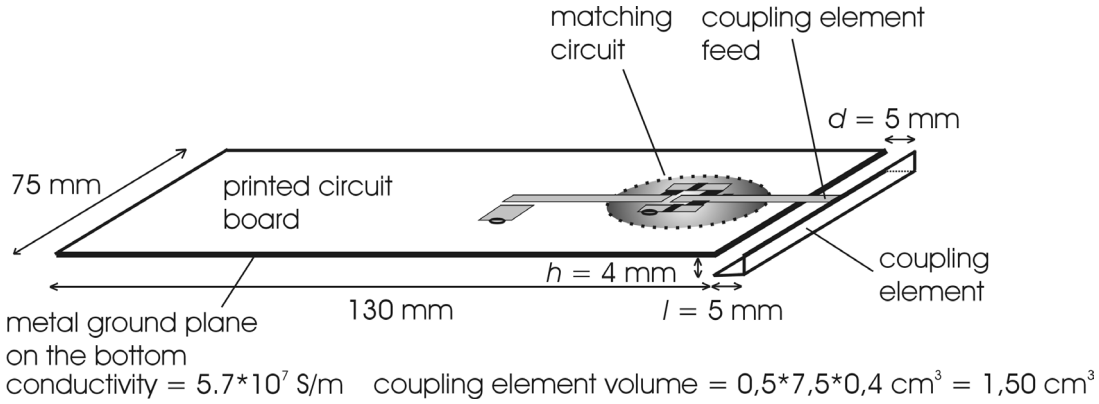

Figure 10: Prototype with matching circuit and coupling element structure for DVB-H reception on handheld terminals.

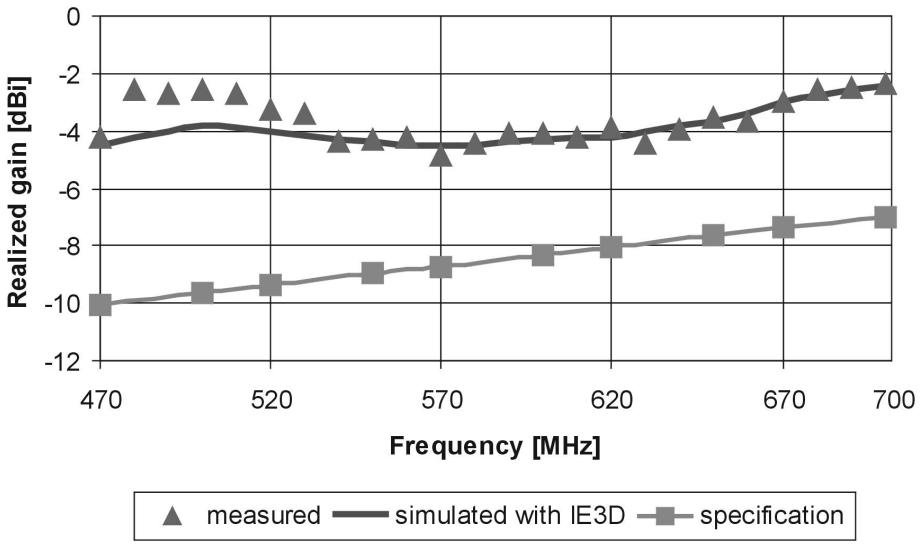

Figure 11: Simulated and measured realised gain compared to DVB-H specifications.

2.2. UWB systems

1. Description of the context

Recently ultra-wideband technology (UWB) has gained a lot of interest from industry and researchers. Although the very first wireless systems by Hertz and Marconi have in fact been ultra-wideband, the idea of applying UWB in consumer electronics and location and positioning systems has arised only a few years ago. Ultra Wide Band radio technology is one of the future technologies for mobile communication. It uses pulse position modulation of very short duration pulses, which results in a PSD (Power Spectrum Density), which, although very broad (over 1 GHz starting almost from DC), has only a few μW per MHz. This feature makes it resistant to interference,

which could be a key requirement for mobile computing. Due to the wide bandwidth (or very short pulses), it is easier to fight multipath effect. Also the signal has a higher penetrating power that makes it suitable for purposes other than simple data communication, like Ground Penetrating Radar, Position locator inside a building, in-house multimedia applications, as presented in Figure 12, etc.

The FCC gives the following definition for UWB systems [17]: Systems with a carrier frequency f_c > 2.5 GHz must have a -10 dB bandwidth of at least B = 500 MHz to be ultra-wideband, whereas UWB systems with f_c < 2.5 GHz need to have a fractional bandwidth of at least 0.20 (the fractional bandwidth is defined as B/f_c). These systems rely on ultra-short waveforms and do not need any IF (Intermediate Frequency) processing, since they can operate at baseband.

Figure 12: UWB scenario for wireless multimedia applications.

Until 2001 the application of UWB technology was primarily limited to radar systems, mainly for military applications. In 2002 the FCC released a spectral mask that allows the operation of UWB devices at very low power levels (-41.3 dBm/MHz) but with an enormous bandwidth of 7.5 GHz, which spans from 3.1 to 10.6 GHz [18].

Figure 13 shows a draft of the specifications mask in Europe and the USA [19]. This regulation gives the opportunity for the realization of new applications demanding huge bandwidth in communications as well as in sensing. By means of UWB technology short-range high-speed wireless data links can be established, that e.g. provide the possibility of high-quality video streaming. The current FCC regulations allow data rates above 100 MBits/s over a short range of

10-15 m with very low transmit power. For sensing applications UWB offers precise resolution and accuracy due to the high bandwidth that can be exploited.

2. *Requirements*

The antennas employed have a strong influence on the performance of UWB systems. Due to the high bandwidth that has to be covered, the antenna characteristics must not be regarded to be independent from frequency any more, as it is done in narrowband systems. Instead, the antenna has to be described as a selective filter providing different radiation patterns dependent on frequency.

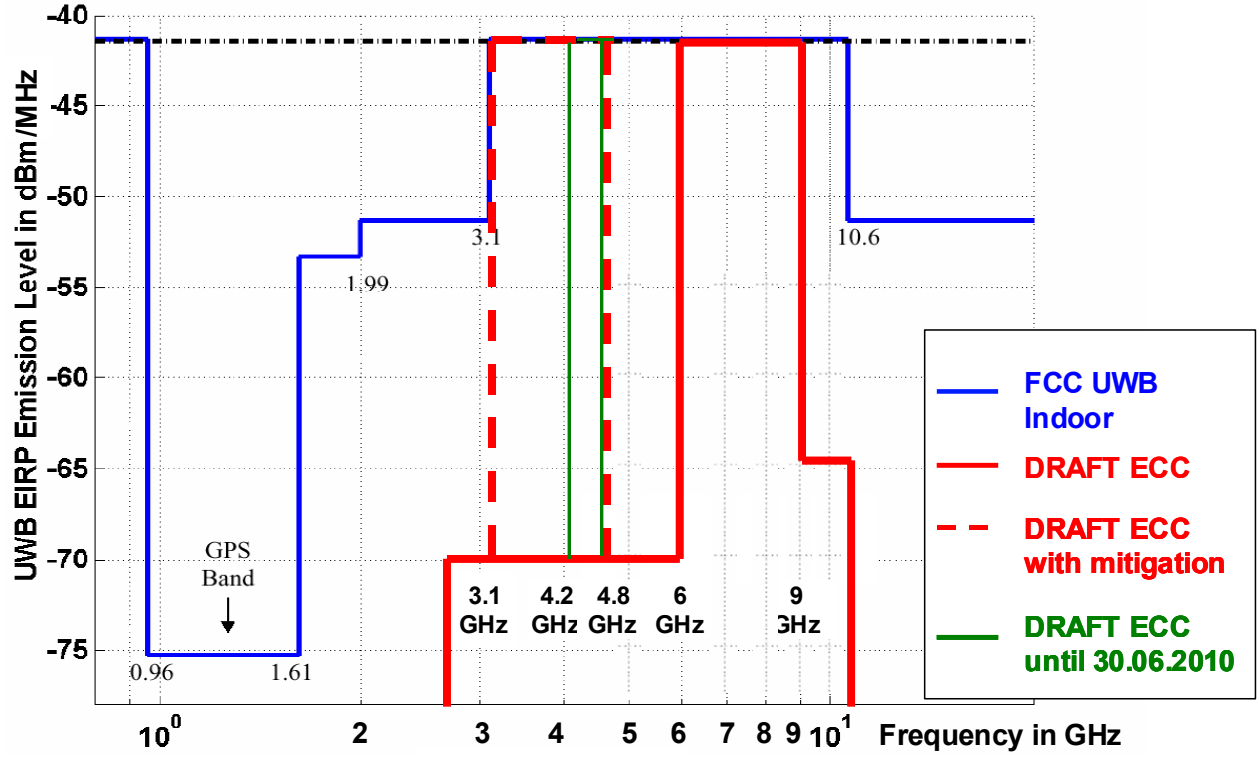

Figure 13: UWB regulation, draft specification mask

For high performance UWB operation two main requirements have to be fulfilled by the antennas [20]: First, the antenna has to support the complete frequency range of the ultra-wideband signal to be transmitted. Second, the antenna must have an impulse response as short as possible (which is equivalent to a constant group delay). Otherwise the transmitted signal will underlie dispersion. Figure 14 illustrates the distortion of the pulse due to the filtering properties of the transmit and receive antennas.

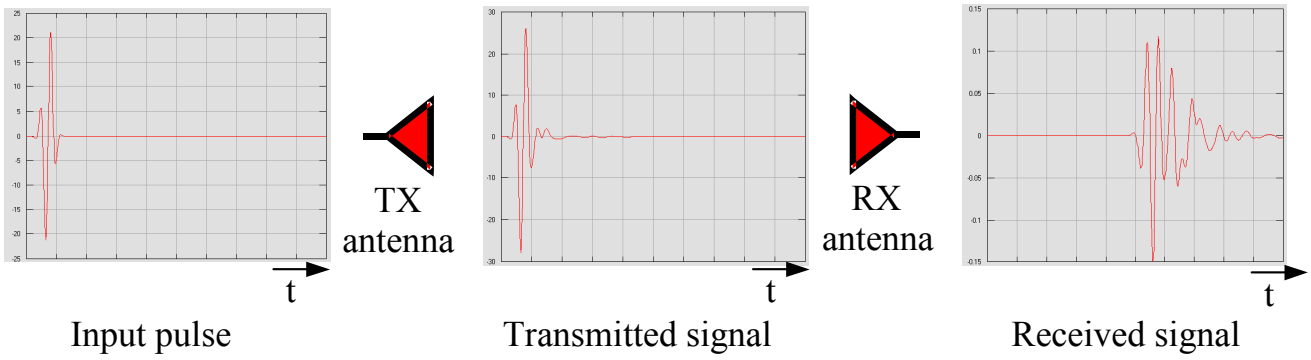

Figure 14: Pulse distortion due to antenna filtering.

Ultra wideband radio systems are expected to transmit and receive baseband pulse waveforms with minimum loss and distortion. Both transmit and receive antennas can affect the faithful transmission of UWB signal waveforms because of the effects of impedance mismatch over the operating bandwidth, pulse distortion effects, and the dispersive effects of frequency dependent antenna gains and spreading factors [21].

Some of the desirable antenna characteristics for UWB radio systems are:

- Wide impedance bandwidth: Good impedance matching over the operating frequency band is desired to minimize reflection loss, and to avoid pulse distortion.
- Fixed phase centre over frequency: If the phase centre (the point where spherical wave radiation effectively originates) of an antenna changes with the frequency, pulse dispersion will occur. This is the case with spiral, log periodic, and travelling wave antennas.
- High radiation efficiency: Some broadband antennas employ resistive loading, which reduces efficiency.

Since the antenna characteristics in the time domain are essential for UWB performance, usually UWB antennas are assessed by properties related to their impulse responses. Naturally, these properties reflect the characteristics in the frequency domain as well. Two important performance measures for UWB antennas are the Full Half Width Maximum $w_{0.5}$ (FHWM) of the magnitude of the envelope of the transient response, and the duration of the ringing. The FHWM is a measure of the linear signal distortion that will be induced by the antenna. The duration of the ringing $\tau_{r,\alpha}$ is the time duration until the envelope has fallen from the peak value below a certain level (e.g. below a fraction α of the main peak). Both measures characterize the dispersive properties of the antenna and are dependent on direction.

Other UWB antenna concerns include polarisation properties (versus frequency), physical size, cost, and feeding techniques (balanced or unbalanced). For example the electrically short dipole provides good pulse fidelity, but at a relatively low amplitude. The resonant dipole provides higher amplitude, but also greater duration. The log-periodic dipole array has very good impedance and

gain bandwidth, but the non-constant phase centre causes considerable ringing of the radiated field. In contrast, the constant phase centre of the Vivaldi antenna produces less ringing, and a very high amplitude pulse.

From a signal processing point of view the antenna can be considered a LTI (Linear Time-Invariant) system, which can be fully characterized by its transfer function [22]. This can be expressed by:

$$\frac{\mathbf{E}_2(\mathbf{r}_2,\omega)}{\sqrt{Z_{F0}}} = \frac{U_{1,in}(\omega)}{\sqrt{Z_L}} \mathbf{A}_{TX}(\hat{\mathbf{r}}_{12},\omega) \frac{e^{-jk_0 r_{12}}}{\sqrt{4\pi} r_{12}} \qquad \text{Eq. 1}$$

$\mathbf{E}_2(\mathbf{r}_2,\omega)$ denotes the electric field strength at a point $\mathbf{r}_2$ in the farfield of an antenna placed at $\mathbf{r}_1$. The antenna port is excited with a voltage $U_{1,in}(\omega)$. $e^{-jk_0 r_{12}}/\sqrt{4\pi} r_{12}$ describes the propagation of the wave from the antenna to the observation point in the direction $\mathbf{r}_{12}$. $\mathbf{A}_{TX}(\hat{\mathbf{r}}_{12},\omega)$ represents the transmit transfer function of the antenna,. Z_{F0} and Z_L are the free space and feed line impedance, respectively, and $\hat{\mathbf{r}}_{12} = \mathbf{r}_{12}/r_{12}$ the unit vector in the direction from the antenna to the observation point. Consequently, $\mathbf{A}_{TX}(\hat{\mathbf{r}}_{12},\omega)$ is independent from the distance between the antenna and the observation point. However, it has to be taken into account that the definition of the transfer function requires local plane wave propagation, and thus is related to farfield conditions only.

On the other hand, according to [22], the reception behaviour of the antenna excited by an incident plane wave can be expressed as:

$$\frac{U_{2,out}(\omega)}{\sqrt{Z_L}} = \sqrt{4\pi} \frac{\mathbf{E}_{1,inc}}{\sqrt{Z_{F,0}}} \mathbf{h}_{RX}\left(\hat{\mathbf{k}},\omega\right) \qquad \text{Eq. 2}$$

Where $U_{2,out}(\omega)$ denotes the output voltage at the antenna port when the antenna is exposed to a plane wave. $\mathbf{E}_{1,inc}$ represents the electric field strength of the incident plane wave, i.e., the field in absence of the antenna. With this definition, $\mathbf{h}_{RX}\left(\hat{\mathbf{k}},\omega\right)$ can be considered as the receive transfer function of the antenna. Figure 15 illustrates the above definitions.

The transmit and receive transfer functions of the antenna are related to each other by Lorentz theorem of reciprocity. In narrow band conditions, both functions are identical. An expression that takes into account the ultra wideband properties of the system has been derived in [22]:

$$2j\omega\mathbf{h}_{RX}\left(-\hat{\mathbf{k}},\omega\right) = c_0 \mathbf{A}_{TX}\left(\hat{\mathbf{k}},\omega\right) \qquad \text{Eq. 3}$$

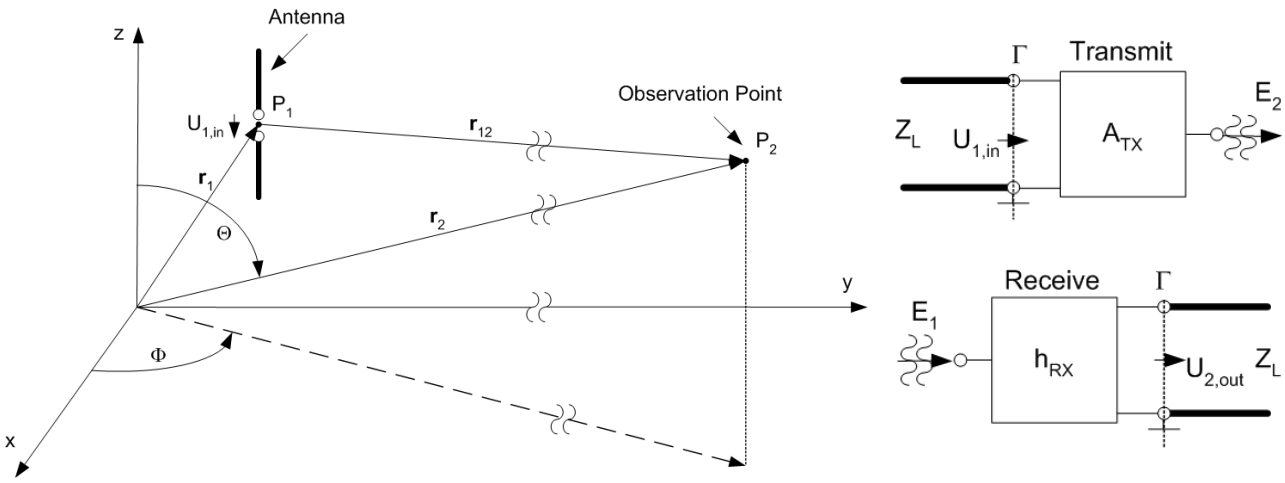

a) Definition of the coordinate system (transmit antenna). b) Transfer functions.

Figure 15: Representation of the antenna as an LTI system for transmit and receive mode [22].

3. *Antenna concepts and measurement issues.*

The applicability of different antenna concepts for UWB transmission has been investigated. The first antenna that was analysed for reference purposes is a broadband quad-ridged horn antenna, depicted in Figure 16.

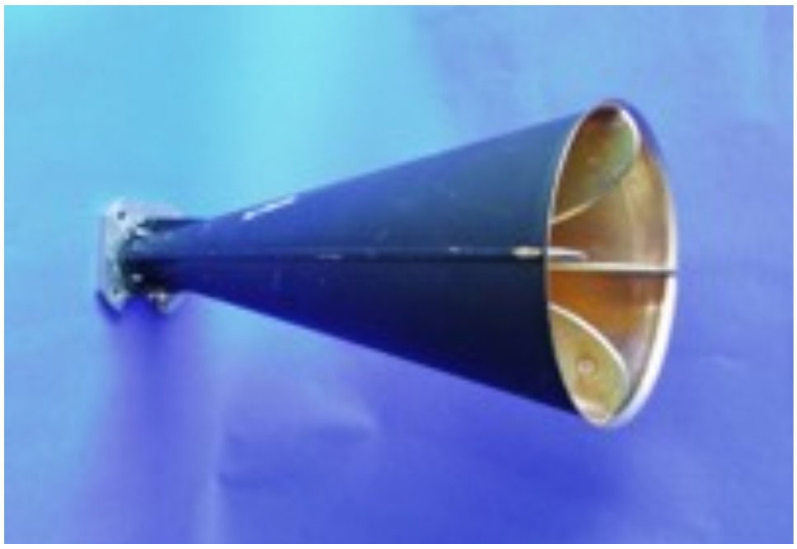

Figure 16: Quad-ridged horn (reference antenna)

The quad-ridged horn provides excellent performance for UWB applications but due to its outer dimensions it is not suited for terminal integration. Therefore, two more broadband antenna concepts have been investigated, which can be realised as planar structures with rather low size, and are hence applicable for integration into small terminals. These antenna concepts are the Logarithmic-Periodic Dipole Array (LPDA, Figure 17) and the Vivaldi antenna (Figure 18), which is a tapered slot antenna. The fundamental difference between these two concepts is the fact that the

LPDA is a broadband resonant structure whereas the Vivaldi is a travelling wave antenna. Both antennas are matched over the whole frequency range of the FCC regulation from 3.1 to 10.6 GHz.

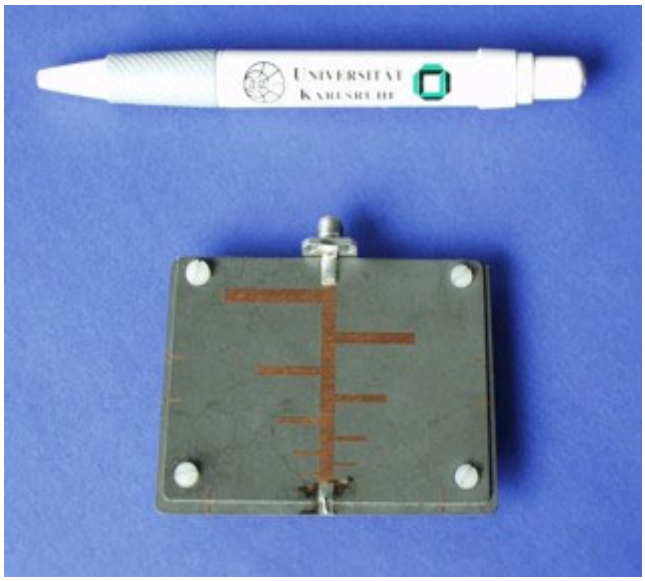

Figure 17: Logarithmic periodic dipole antenna

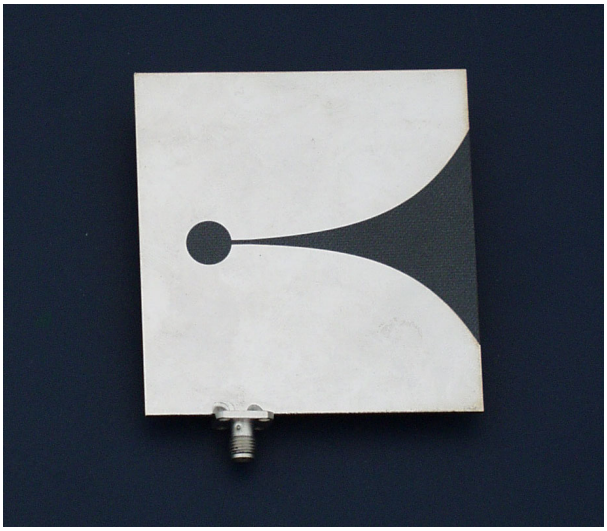

Figure 18: Vivaldi antenna

The transient responses of these three antennas have been measured. The measurements were conducted in the frequency domain in an anechoic chamber using a network analyser, and then converted into the time domain using a Fourier transform. From the measured impulse responses the important characterization parameters FHWM (Full Half-Width Maximum), ringing duration (with a threshold level of α = 0.22/-13 dB) and the medium gain were derived. The results for the main direction of radiation are given in Table 1. The noticeably smaller gain of the LPDA and the Vivaldi is a result of the smaller sizes of these antennas compared to the horn antenna. But for practical application it will be desired to have rather omni-directional radiation patterns, and consequently lower gain. The most striking result is the very high FHWM of the LPDA, which means that this antenna is highly dispersive and thus not well suited for UWB application although

it covers the whole frequency range. This can be explained by the fact that radiation is arising at different locations of the antenna structure for different frequencies, as the phase centre of the antenna changes with the frequency. The conclusion of this result is that the application of resonant structures for UWB antennas is not recommendable in general. In contrast to this the results of the Vivaldi antenna do not differ much from those of the reference horn antenna. Hence the Vivaldi can be regarded as an excellent candidate for UWB applications.

	Dimensions	$w_{0.5}$	$\tau_{r,0.22}$	G_{mean}
Broadband horn	28x14x14 cm^3	65 ps	355 ps	12.2 dBi
LPDA	4.8x4.5 cm^2	785 ps	440 ps	5.3 dBi
Vivaldi	7.8x7.5 cm^2	115 ps	475 ps	5.7 dBi

Table 1: comparison between the different UWB antennas.

To put into service an UWB communications system, different kind of devices, both desktop and handheld, must be considered. Some standard antenna solutions, those described above, show a good behaviour for common household devices such as TV-sets or DVD players, they are however too cumbersome to be integrated into smaller, portable terminals. In this case, smaller and higher-performance solutions are needed, as the one presented in [23]. Here, the problem to be solved will be how to integrate the antennas in handheld devices with reduced groundd planes without a significant loss of performance.

2.3. MIMO systems

1. Description of the context

It has been shown that multiple-input multiple-output (MIMO) wireless systems can provide increased capacity in rich multipath environments [24]. MIMO antenna systems can be used in a mobile terminal (MT) to combat the impairments of the propagation channel, and thus obtain additional gain over other well-established classical strategies.

2. Requirements

In MIMO antenna systems, the minimum physical separation between antenna elements for an appropriate limit in correlation between the multitude of received signals is commonly referred to

be λ/2. However there is not a minimum distance condition but rather a definition of the acceptable correlation level (or mutual coupling) to insure the effectiveness of the MIMO antenna system. Useful benefits are still obtained with coupling as high as -3 dB, and it has been proved that the mutual coupling can be compensated at the signal processing level [25]. Therefore, when necessary and appropriate, inter-element spacing less than λ/2 can be used. The distance can be very small especially if adjacent antenna elements use orthogonal polarisation.

In a small MT the number of antenna elements may range typically from two in a small handset, to four in a PDA, and up to sixteen or even more, in a laptop computer [26]. The most challenging case is the handset. In fact with very little space available for the antenna integration, it is very difficult, if not impossible, to have more than two antennas with reasonable efficiency.

An important indicator of the quality of a MIMO system is the channel capacity. This capacity depends on many factors, namely:

- The number of transmit antennas and their spacing,
- The number of receive antennas and their spacing
- The multipath environment and, in particular the spread of direction of arrival angles. In general, indoor and Pico cell environments are considered to have angle of arrival spreads that approach 360°, with multipath components likely to arrive from any direction.

Assuming a propagation scenario in which the incident field shows a uniform 3D random distribution, the envelope correlation can be obtained from the scattering parameters S of the antenna system [27], [28]. In the case of a 2-antenna system, the envelope correlation ρ_e can thus be defined as:

$$\rho_e = \frac{\left|S_{11}^* S_{12} + S_{12}^* S_{22}\right|^2}{\left(1 - \left|S_{11}\right|^2 - \left|S_{12}\right|^2\right)\left(1 - \left|S_{22}\right|^2 - \left|S_{12}\right|^2\right)} \qquad \text{Eq. 4}$$

Where S_{11} and S_{22} represent the input return loss of each port of the antenna system, and S_{12} the mutual coupling.

3. *Antenna concepts*

A MIMO antenna system with two elements were designed, fabricated and tested. It is based on the PIFA element presented in [29]. The system consists of two PIFAs, designed to be used in GSM1800 (1.710-1.880 GHz), UMTS (1.900-2.170 GHz), and IEEE 802.11b/Bluetooth (2.400-2.484 GHz). In order to cover this wide bandwidth, a 7 mm thick air gap was used. The spacing between the PIFA elements is 32.5 mm, which corresponds approximately to λ/5 in the worst case,

that is for the lower frequency (1.710 GHz). A photo of the prototype is shown in Figure 19.

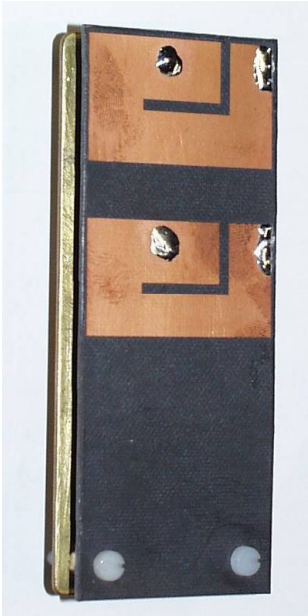

Figure 19: Handset antenna with 2 PIFA elements

The scattering parameters of the two ports (S_{11}, S_{22} – input reflection coefficients and S_{12} – mutual coupling) of the antenna prototype were measured using a vector network analyser. The obtained results are presented in Figure 20. The experimental results are in good agreement with the simulations, and fulfil the requirements of all the standards considered. Within the required frequency band (1.710-2.484 GHz), the maximum mutual coupling is -4.4 dB at 1.76 GHz. Yet, this high mutual coupling was expected, and can not be avoided, due to the small distance between the two antenna elements.

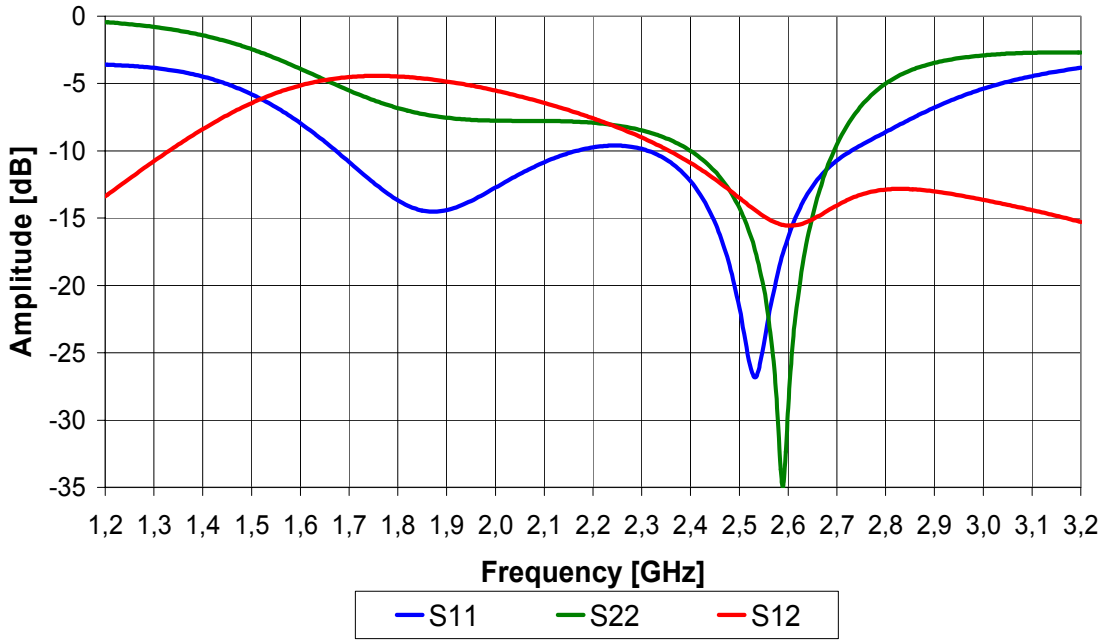

Figure 20: Experimental S parameters of the 2 PIFA antenna system.

The envelope correlation can be obtained from the scattering parameters represented in Figure 20, by using the expression given in Eq. 4. The obtained results are displayed in Figure 21.

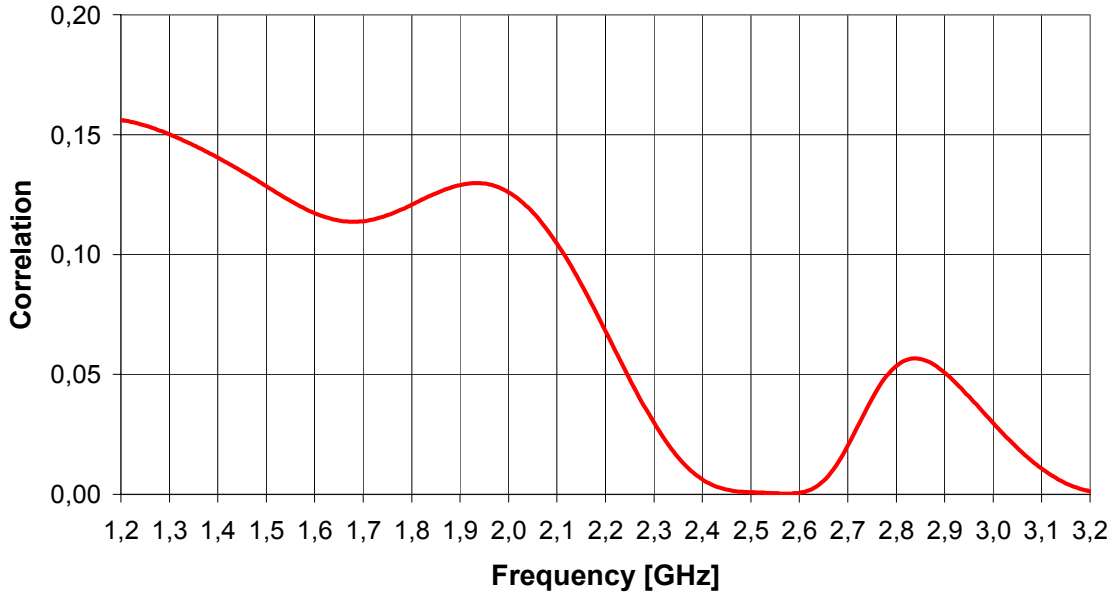

Figure 21: Envelope correlation for the 2 PIFA antenna system

Within the specified frequency band (1.710 – 2.484 GHz) the correlation is below 0.13 although the antenna elements are quite close (about λ/5 in the worst case). This proves that considerable improvement of the performance can be obtained with this MIMO system.

Another example is shown in Figure 22, where the two antennas are separated in both space and polarisation to achieve low coupling between the radiating elements. The ground plane size is 45 mm x 90 mm, and the slots are tuned to the 2 GHz band. Propagation measurements to evaluate the diversity performance have been performed in an indoor office environment [30].

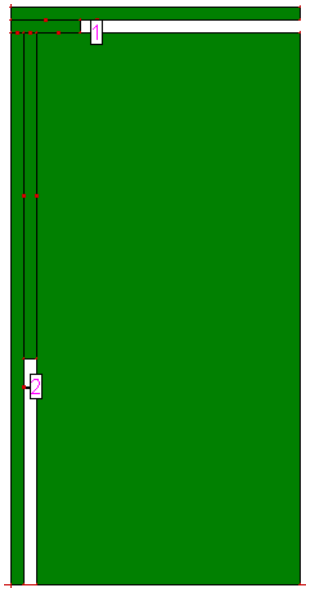

Figure 22: Two-slot antenna prototype (Simulation model)

The transmit sector antenna was either vertically or horizontally polarised and it was placed at the end of a corridor. The two-slot antenna was held in front of a user forming a type of data mode application while walking along the corridor, and in and out of the offices. The cumultative distribution functions of the received signals are plotted in Figure 23 and Figure 24 together with the combined signal level assuming ideal selection combining.

The distributions of the separate antenna signals follow each other very well in this environment. The diversity gain at the 1 and 50% levels are 5-7 dB and 1.6-1.8 dB, respectively, almost independent of the transmit antenna polarisation. However, the received signal level is slightly lower for the vertically polarised transmit case mainly due to the slot antenna implementation at the receive side.

Diveristy measurements have also been performed in a reverberation chamber The received signals at both antenna ports were recorded simultaneously. The signal level was increased by 7 dB and 1 dB at the 1 and the 50 % levels, respectively, compred to the strongest branch. These results are in close agreement with the indoor tests and the reverberation chamber may thus be used to evaluate antenna performance in a repeatable and controllable environment.

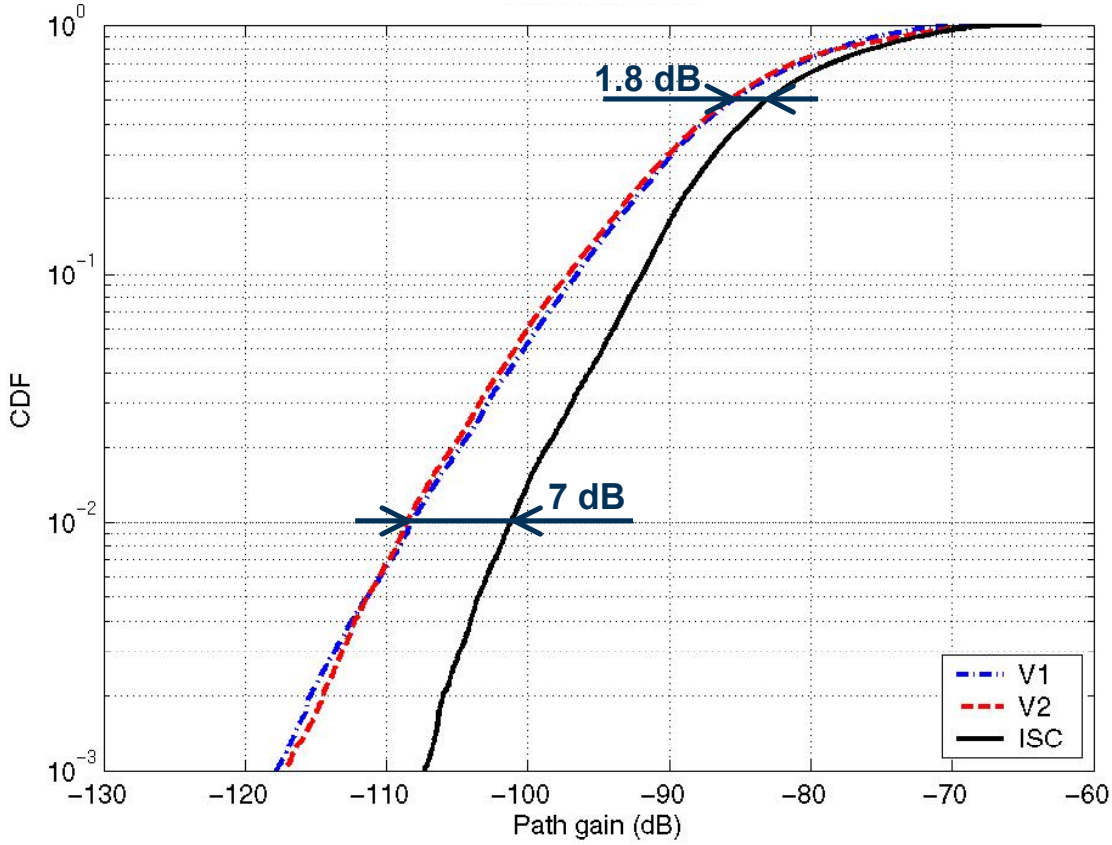

Figure 23: Cumultative distribution function of the measured received antenna signals for vertically polarised transmit antenna.

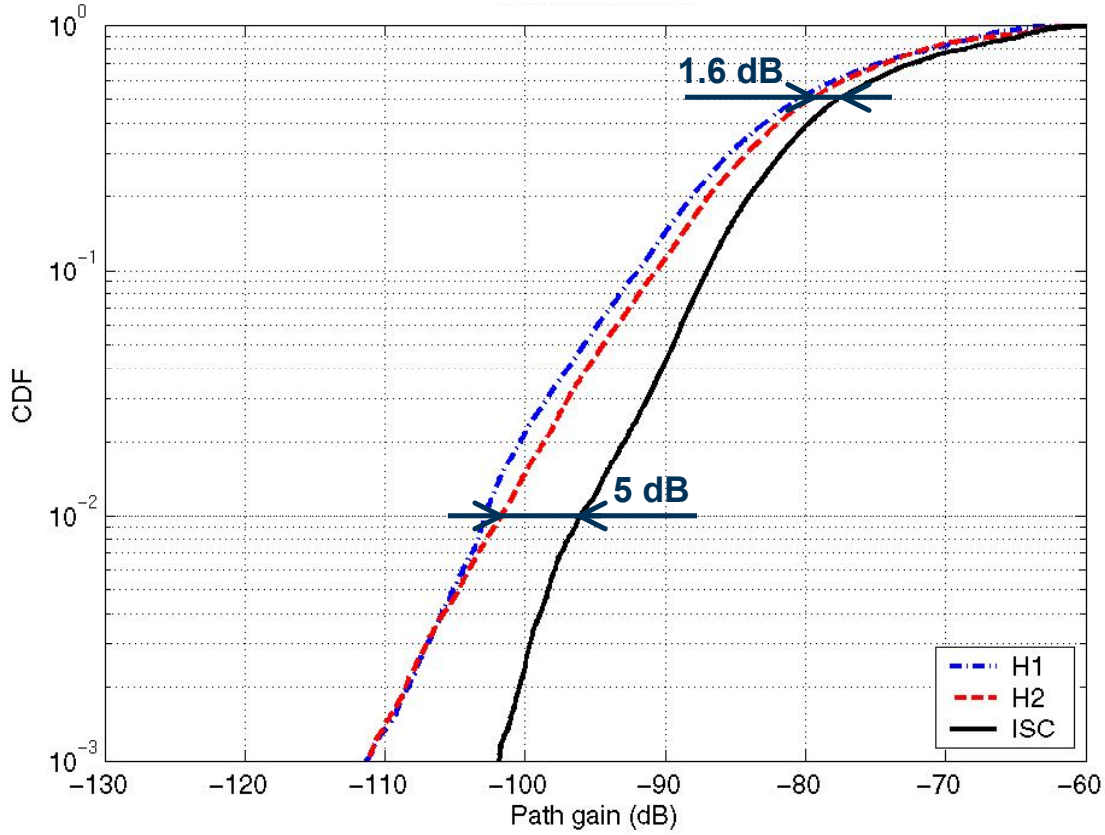

Figure 24: Cumultative distribution function of the measured received antenna signals for horisontally polarised transmit antenna

3. OTHER APPLICATIONS

3.1. RFID

1. Description of the context

In the last years, there has been a tremendous growth in the demand for Radio Frequency Identification (RFID) procedures in manufacturing units, purchasing departments, logistics and transportation, for which identification is a prime concern [31]. The use of RFID in tracking and access applications first appeared during the 1980s. RFID quickly gained popularity due to its ability to track moving objects. As the technology is refined, more pervasive and possibly invasive uses for RFID tags are in the works. Important applications, such the tracking of patients with life supporting gears within the hospital premises, should be developed and implemented in the near future. The main objective of such procedures is to provide location and identification information about people, animals, goods, products in transit.

Up to now, bar code and optical sensors are widely used in many supermarkets for identification of goods and commodities. However, these systems have limited range and require a clear line-of-sight. The great appeal of RFID technology is that it allows information to be stored and read without requiring either physical contact or a line of sight between the tag and the reader by using electromagnetic waves.

Some of the applications of RFID include:

- **Asset Tracking**: RFID tags can be used on assets to check that they are not lost, stolen, underutilized or hard to locate.
- **Manufacturing**: RFID can be used to track parts and work in process and to reduce defects, increase throughput and manage the production of different versions of the same product.
- **Supply Chain Management**
- **Retailing**: The use of RFID tags may help improve supply chain efficiency and make sure products are available for the customers. Among the most talked about potential applications are the ability to automate the checkout process to eliminate lines, and the ability to provide information to consumers while they are making purchasing decisions.
- **Payment Systems**: Automatic toll-paying in the roads is already broadly used. This concept

can be extended to further applications, such as payment in fast food restaurants. It is also a convenient way to pay for bus, subway and train rides, as RFID cards would allow more people to pass through turnstiles faster, and the lack of mechanical parts in readers would reduce maintenance costs. This system is already used in ski resorts in Europe for lifts.

- **Security and Access Control**: RFID has long been used as an electronic key to control who has access to office buildings or areas within office buildings.
- **Medical applications**: RFID tags and readers that can be combined with software systems to alert doctors and nurses of potential problems.
- **Insect tracking**: Design of miniature transceiver or tag for insect tracking has been proposed [32], [33].

The purpose of a RFID system is to enable data to be transmitted by a mobile device, called a tag, which is read by an RFID reader and processed according to the needs of a particular application. The data transmitted by the tag may provide identification or location information, or specifics about the product tagged.

The main components of a RFID system are thus the reader and the tag. In a typical communication sequence, the reader emits a continuous radio frequency (RF) carrier sine wave. When a tag enters the RF field of the reader, the tag receives energy from the field. After the tag has received sufficient energy it modulates the carrier signal according to the data stored on the tag. This modulated carrier signal is resonated from the tag to the reader. The reader detects and decodes the modulated signal. Finally, in case of traditional tags, information is relayed to a host computer. Lastest generation tags are also able to store and modify this information.

In this sequence of events, the job of the reader is to:

1. Provide energy for the tag,
2. Provide a carrier signal,
3. Detect and decode the modulated signal.

The job for the tag is to:

1. Utilize the energy provided by the reader,
2. Resonate the reader carrier signal,
3. Modulate the resonated signal that is sent back to the reader.

RFID tags can be active, semi-passive or passive.

- **Passive RFID tags** have no internal power supply. The electrical current induced in the antenna by the incident radio frequency signal provides the power necessary to activate the

integrated circuit in the tag, and transmit a response. Most passive tags use backscattering of the carrier signal from the reader to relay the information. Therefore, the antenna in the tag must be designed to both receive the power from the incoming signal and also to transmit the backscatter signal [34]. In this case, as the power available is very low, the information transmitted by a passive RFID tag must be very brief. This kind of tags can be kept very small in size, and their fabrication cost is very low.

- **Semi-passive RFID tags** are very similar to passive tags except for the addition of a small battery, which allows the integrated circuit in the tag to be constantly powered. In this case, the tag doesn't need to use the incoming signal to transmit the information, and the antenna can be optimised for the backscattering.
- **Active RFID tags** are equipped with an internal source, which provides the power for both the integrated circuits and the outgoing signal. Thus, not only the range can be increased, but also additional information can be stored and transmitted.

There are four different kinds of tags commonly in use. They are categorized by their radio frequency: low frequency tags (125 or 134.2 kHz), high frequency tags (13.56 MHz), UHF tags (868 to 956 MHz), and microwave tags (2.45 GHz). UHF tags cannot be used globally as there are different regulations for their usage in Europe or the USA.

A suitable antenna for the tag must have low cost, low profile and especially small size whereas the bandwidth requirement is less critical [35]. In the particular case of antennas for long range in the UHF band, the importance of reducing costs is very significant in order to make possible a wide spread of this technology.

2. Requirements: regulation and standardization

Whereas low-frequency (LF: 125 - 134.2 kHz and 140 - 148.5 kHz) and high-frequency (HF: 13.56 MHz) RFID tags can be used around the world without a license, this is not possible in the ultra-high-frequency band (UHF: 868 MHz-928 MHz), as there is no single global standard. For example, in North America, UHF can be used unlicensed for the 908-928 MHz band, although some restrictions exist regarding transmission power. In Europe, UHF can be used without license for RFID purposes only in the 869.40-869.65 MHz band, with transmission power limitations. The 865.6-867.6 MHz band is currently under consideration.

Some standards that have been made regarding RFID technology include:

- ISO 11784 & 11785 - These standards regulate the Radio frequency identification of animals, for example for tracking cattle with RFID
    - ISO 11784 defines how data is structured on the tag.

  - ISO 11785 defines the air interface protocol.
- ISO 14223/1 - Radio frequency identification of Animals, advanced transponders - Air interface
- ISO 14443 standard for the air interface protocol for RFID tags used in payment systems and contactless smart cards
- ISO 18000: RFID standards for automatic identification and item management. The ISO 18000 family of standards covers the major frequencies used in RFID systems around the world.
  - 18000–1: Generic parameters for air interfaces for globally accepted frequencies
  - 18000–2: Air interface for 135 KHz
  - 18000–3: Air interface for 13.56 MHz
  - 18000–4: Air interface for 2.45 GHz
  - 18000–5: Air interface for 5.8 GHz
  - 18000–6: Air interface for 860 MHz to 930 MHz
  - 18000–7: Air interface at 433.92 MHz

3. Basic antenna geometries

We have been focused on the development of antennas for tags, what is to say, small antennas able to work in a RFID system, especially in the UHF band.

Generally speaking, small antennas can be classified into three basic types, depending on the geometry: dipoles, patches and slots, even tough a conventional tag antenna has rather a strip-line structure, rather than patch antenna structure to fit to the RFID tag IC chip. From these fundamental types, more complex and smaller antennas are developed.

In its simplest form the dipole antenna consists solely of a straight piece of line of a defined length. By suitable shaping the geometry of the antenna, some characteristics, in particular, the radiation resistance and bandwidth, can be influenced [36]. The parallel connection of two λ/2 dipoles has an effect in the radiation resistance of the structure. The 2-wire folded dipole has around four times the radiation resistance of the single λ/2 dipole.

A patch antenna in its simplest configuration consists of a radiation patch on one side of a dielectric substrate, which has a groundplane on the other side. Patch antennas can therefore be manufactured cheaply and with high levels of reproducibility using PCB etching technology. The length of the patch (L) determines the resonant frequency of the antenna. We could approximate: L=λ/2.

Normally the substrate thickness is 1-2% of the wavelength. The width w determines the radiation resistance (R_r) of the antenna. When using patches, it is sometimes useful to use the carton and cardboard packaging of the pack as substrate material for the antenna [37].

Slot antennas, which are also called magnetic dipoles, can be seen as a long, narrow opening on a metallic surface. The radiated field can be seen as generated from a field distribution that is held on the slot itself.

4. Small antennas: fundamental limits

a) Downsizing techniques

At present, most of the RFID systems operate in the megahertz frequency range. Higher frequencies that utilize free microwave RFID system design antennas operate at their dominant mode, which is characterized by the lowest frequency of operation. The use of such modes of operation results in large size antennas, which are predominantly responsible for an increased size of an RFID tag. It becomes apparent that, in order to miniaturize a microwave ID system, the main assignment is to miniaturize its antenna.

A large number of downsizing solutions for small antennas can be found in literature. Some of the techniques applied are: folding, meandering [38] and bending [39] configurations but also use of surface etching, shorting walls or pins, high dielectric constant materials or tuneable ferroelectric thick films [40].

b) Bandwidth and efficiency. Fundamental Limits

The performance of electromagnetic passive devices is sensitive to its electrical size compared to the wavelength, i.e. given an operating wavelength and certain performance, classical antennas can not be made arbitrarily small, while keeping at the same time certain operative parameters. As a matter of fact, bandwidth, losses and dimensions of the antenna are closely interrelated in small antennas, as we will see further in this chapter.

Some losses in the antenna can be characterised by the efficiency, η which is defined as the ratio of total radiated power to the net power accepted by the antenna from the connected feed line [41].

A second parameter, called quality factor (Q), related to the bandwidth, can be defined, and, for lossless antennas, can be expressed by [42]:

$$Q \approx \frac{1}{BW} = \frac{f_{center}}{f_{upper} - f_{lower}} \qquad \text{Eq. 5}$$

Where BW is the fractional bandwidth.

The quality factor Q is defined as the ratio of time-average, non-propagating energy to radiated power of an antenna [43]. This parameter is a quantity of enormous interest when designing small antennas because of its lower bound, which provides knowledge of how small an antenna can be constructed, for a given fractional bandwidth.

There are laws that can be summarized in terms of the quality factor Q that restrict the performance of antennas fictitiously enclosed in a given volume. For linearly polarized antennas the fundamental limitation can be expressed by [44].

$$Q = \frac{1}{ka} + \frac{1}{(ka)^3} \qquad \text{Eq. 6}$$

Where a is the radius of the smallest sphere that encloses the antenna and k is the wave number at the operating wavelength λ ($k = 2\pi/\lambda$).

Recently, it has been published a paper [45] where a more realistic lower bound for the fundamental limit on the radiation Q has been estimated. This prediction is based on the assumption of a sinusoidal current distribution along an electrically small antenna, in contrast with the classical approach, where a Hertzian dipole with a uniform current distribution was considered. This realistic limit is compared in Figure 25, jointly with the classical fundamental limit.

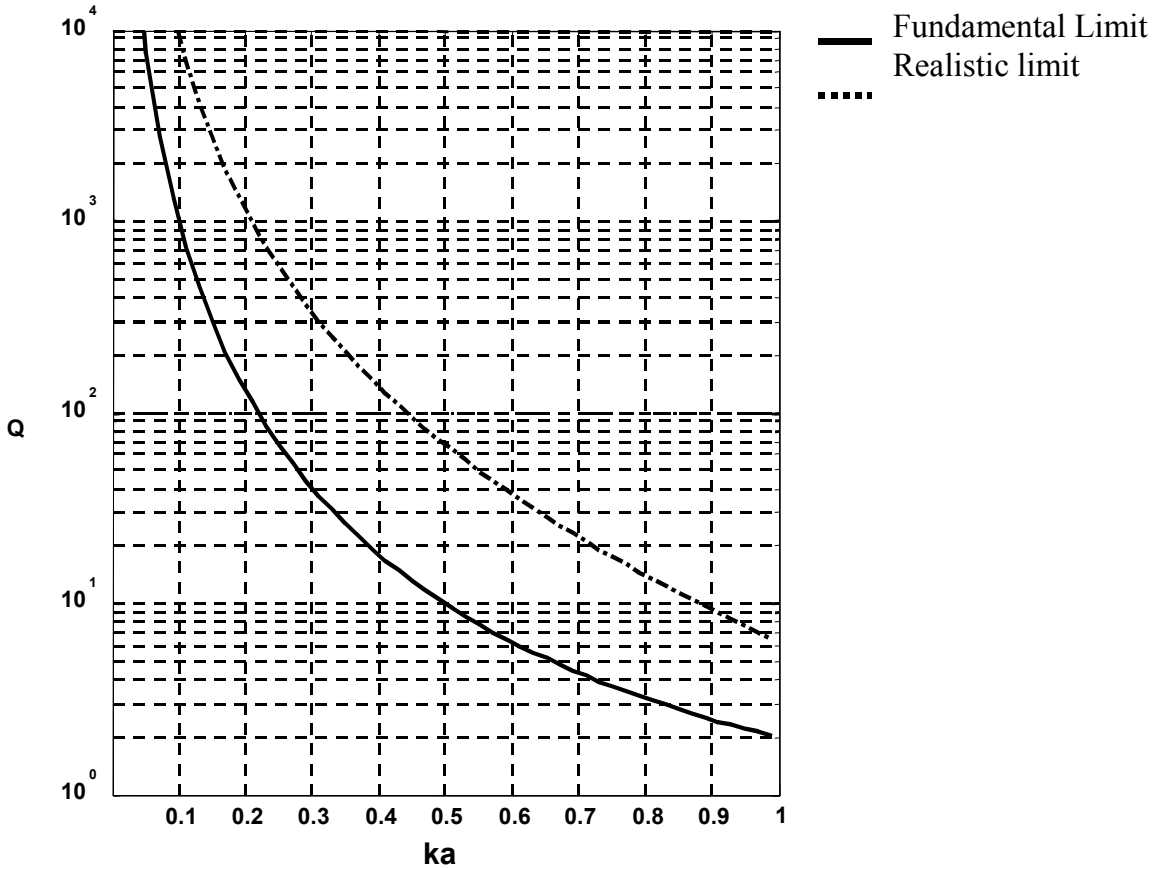

Figure 25: Fundamental Limit and Realistic Limit of quality factor Q

The former expressions of the limit *Q* have been formulated considering lossless antennas.

Taking into account losses (characterized by η), another fundamental relationship [46] between the radius *a* of an electrically small antenna, its maximum fractional bandwidth BW, and its radiation efficiency, can be written:

$$BW \cdot \eta \cong (ka)^3 \qquad \text{Eq. 7}$$

The former expression, which is valid only if $ka << 1$, implies that a larger bandwidth can be gained at the price of radiation efficiency, once size of antenna is constrained [41].

c) Radiation Pattern, Return Loss and Gain.

Other parameters such as radiation pattern, directivity, gain, polarisation and input impedance are important when designing an antenna.

Regarding radiation pattern, small antennas in free space do have a doughnut-like radiation pattern with a directivity of approximately 2dBi. Some small antennas have radiation patterns and directivities (D) with shapes and figures between elemental-short dipole (D = 1.76 dBi) and the λ/2 dipole (D = 2.15 dBi). These parameters do not vary much when dealing with electrically small antennas. Nevertheless, for a given size, if the operation frequency is increased, the former-mentioned antenna characteristics will be modified as well, with a tendency to higher directivity. It is important to remark that the ideal doughnut-like radiation pattern will be also distorted when locating the antenna on its place of operation (i.e. wireless device), since the surroundings of the antenna have a significant effect on the radiation.

As for antenna gain, the ohmic losses in the conductors have to be taken into account. Small antennas could have significant losses and quite different loss efficiencies can be expected according to their design.

Regarding return loss, it would be desirable that the antenna was matched at the input port. Therefore, the input impedance should be as close as possible to the output impedance of the transmitter [34].

Polarisation will depend on the orientation of the electric field radiated by the antenna and, in the end, is controlled by the flow of electric or magnetic currents on the structure of the antenna. The importance of this parameter relies on the application the antenna is intended for, and especially the position and distance of the reader's antenna. In urban environments and with a long interrogation distance no particular polarisation states are required, as multipath propagation will generate both vertical and horizontal polarisation of the emitted electromagnetic waves of the reader.

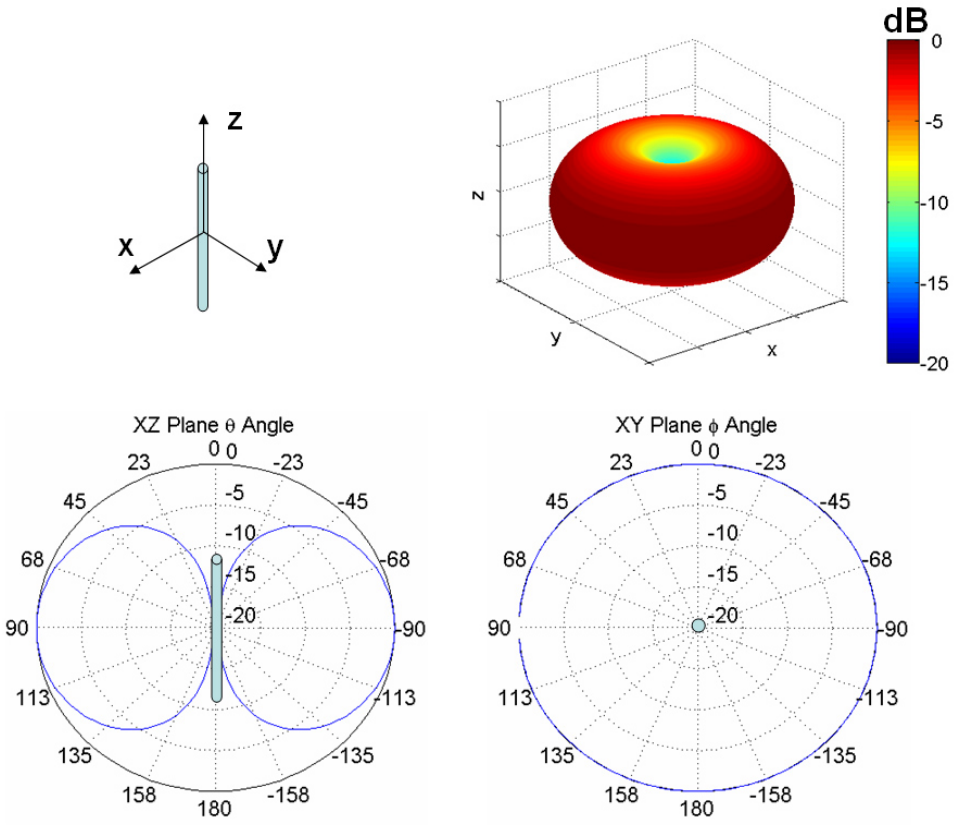

Figure 26: Doughnut –like radiation pattern

5. *State of the art*

Regarding the antenna of the reader unit must maintain a high degree of isolation between transmission (Tx) and reception (Rx) ports and, in some cases, have two orthogonal polarisations. Some examples of antennas for RFID readers that are currently commercialised are shown in Table 2.

With regard to the transponder chips, they have unique identification codes that can only realise the backscatter principle if the tag antenna attracts sufficient electromagnetic energy from the interrogating radio frequency (RF) of the reader. The antenna of the tag must be able to rectify sufficient energy from the interrogating EM field to activate the transponder chip. Generally, omnidirectionality for the transponder antenna is preferred to ensure the identification from all directions. But at very low frequencies (134 kHz, 13.56 MHz), these RFID systems rather work in magnetic coupling mode than electromagnetic wave propagations [47].

				
Dimensions (cm)	101.8 x 51.8 x 4.7	75 x 166.3 x 8.8	22.4 x 20.6 x 4.1	22.4 x 20.6 x 4.1
Operating frequency	134.2 kHz	13.56 MHz	900-928 MHz	900-928 MHz
Vendor	Texas Instruments (USA)	Texas Instruments (USA)	Symbol (USA)	Symbol (USA)

Table 2: Commercial antennas for RFID readers

The key design challenge has been to achieve tag antennas with sufficiently high gain. The tags are further required to be small in size and mechanically robust against vibrations. Planar antennas, which are low cost, simple to manufacture and have low profile, are suitable for the RFID systems. The most common types of antennas for tags, commercialized nowadays, are folded dipoles, Meander Lines Antennas (MLA) and spirals. In spite of the downsizing techniques that are used in order to design such meandered antennas, their dimensions are still quite large in comparison with the rest of the circuitry.

In Table 3 different antennas are shown. Since these are products available in the market, the complete tag is presented (antenna plus microchip).

Much work has been carried out to improve the existing methods of manufacturing the key RFID tag components, namely antenna, transponder chip, power supply and packaging. Concerning the antenna element, the big challenges pending to be reached could be summarised in two points:

- To achieve an antenna with small size and high efficiency: focusing on the UHF band (868 and 915 MHz), we can affirm that the sizes of the RFID antennas are still too big in comparison with the transponder.
- To achieve an antenna and, a complete tag, in applications involving liquids and metals: liquids absorb or attenuate RF signals while metal surfaces reflect and scatter the RF energy required to activate the transponder chip. Thus, there are still practical limitations in using passive RFID tags on numerous products or at least intensive research to smartly work with these surroundings.

					
Antenna type	Dipole	Meandered line (dipole)	Meander line	Meandered line (dipole)	Loop
Operating frequency	869-915 MHz	869 MHz and 915 MHz	915 MHz	2.45 GHz	13.56MHz
Vendor	Symbol (USA)	Intermec (USA)	Intermec (USA)	Intermec (USA)	Texas Instrument (USA)

Table 3: Commercial antennas for RFID tags

Different antenna solutions have been proposed, based on planar folded dipoles and meander lines (Figure 27) alone or combined with quasi-metamaterial surfaces in order to be able to work close to a metallic environment.

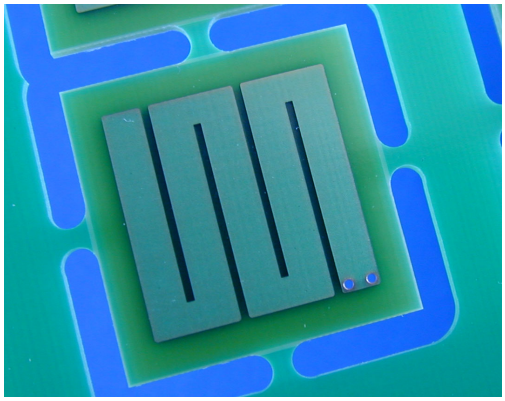

Figure 27: Meander Line Antenna (UPC)

6. *Measurement procedures*

The measurement procedure of the antenna is one of the most critical stage within the process of the design and development of a small antenna. Four main measurement techniques can be considered: The Wheeler-cap method, the transmission method, reverberation chambers or backscatter modulation.

a) Wheeler cap method

The radiation efficiency can be defined as:

$$\eta = \frac{P_{rad}}{P_{in}} = \frac{P_{rad}}{P_{rad} + P_{loss}} = \frac{R_{rad}}{R_{rad} + R_{loss}} \qquad \text{Eq. 8}$$

Therefore, we need to measure the total resistance and the loss resistance, since the radiation resistance can be obtained from those two:

$$R_{rad} = R_{tot} - R_{loss} \qquad \text{Eq. 9}$$

With the help of a Network Analyzer, we can obtain the input resistance of an antenna, so, we can easily measure what we have called total resistance.

The loss resistance can be acquired by removing the radiation resistance and measuring again the input resistance of the system. The radiation resistance is short-circuited by surrounding the antenna by a grounded sphere (the cap). In this way, if we measure the input impedance with the Network analyzer again, we obtain the loss resistance, assuming no RF leakage and no losses in the cap. The set up is shown in Figure 28.

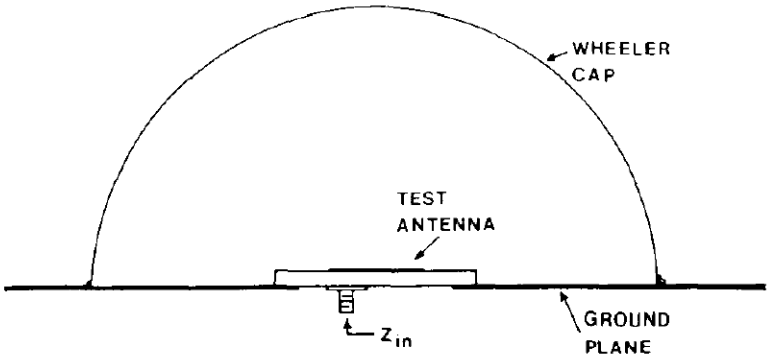

Figure 28: Wheeler cap method (from [48])

The advantage of this method is its simplicity. However, if the losses in the substrate are considerably high, the wheeler cap method is not accurate, so the reliability of the method is reduced. Moreover, if the equivalent circuit is more complicated than just an RLC series, some adjustments and approximations need to be done. We can find some cases of small antennas whose equivalent circuit is really difficult to obtain, for example when dual-resonance behaviour is observed.

Obviously, this method implies that the antenna has a ground plane of reasonable size, otherwise, the measurement procedure is not applicable, since the antenna performance will be modified due to the proximity of the metallic plate of the set up (Figure 28).

b) Transmission

Actually, another method that could be more reliable is the transmission method. In order to avoid spurious radiation from the cables connected to the antenna under test, we suppress them by connecting a VCO directly to the input port of the antenna. The information that we have a priori is the transmitted power at the output of the VCO (Pt), the gain of the receiving antenna. What we get from the measurement is the received power at the reference antenna. Following the simple transmission equation, we can deduce the gain of our antenna.

The measurement set up is shown in Figure 29. A Ridge antenna is placed as the reference antenna. We could use whatever reference antenna we wish, if we have perfectly characterized it.

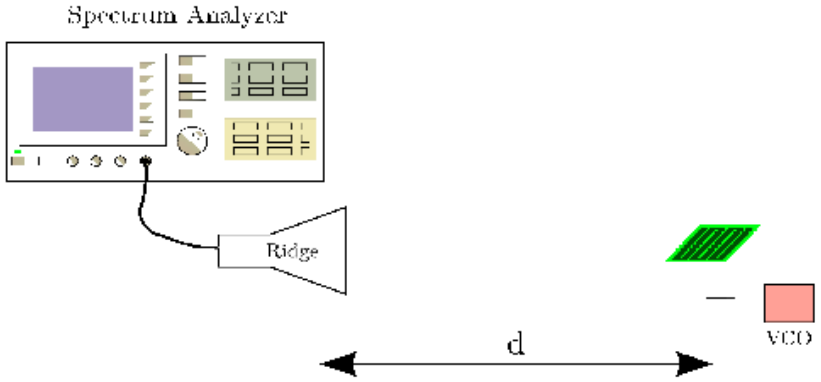

Figure 29: Gain measurement set up

The gain of the antenna under test has been calculated from the expression of the received power:

$$P_R = \frac{P_T G_T G_R}{(4\pi d/\lambda)^2} \qquad \text{Eq. 10}$$

Where P_R is the received power, P_T is the transmitted power, G_T the gain of the transmitter antenna, G_R is the gain of the receiver antenna, d is the distance between the two antennas and λ is the wavelength.

G_T is the gain of our antennas, so we can deduce its value in dB as follows:

$$G_{AUT} = G_T = P_R - P_T - G_R + L_{\substack{free \\ space}} \qquad \text{Eq. 11}$$

With $L_{\substack{free \\ space}} = 20\log(4\pi d/\lambda)$

c) Reverberation chamber

The Reverberation chamber is a metallic and electromagnetically isolated chamber. It can be seen

as a cavity where the cavity modes are stirred mechanically in order to obtain all possible plane wave excitation. This creates a Rayleigh distribution, between two antennas placed inside the chamber. This is approximately the distribution that exists in environments with unifom incident fields randomly distributed in 3D. Therefore, by having the total input power given to the reference antenna and measuring the received power in the antenna under test, with the help of the equation of transmission, it is easy to calculate the gain of the antenna under test.

d) Backscatter modulation

In spite of the relatively good accuracy of the last method, we can find cases in which the antenna is so integrated together with the rest of RF components that it makes no sense to characterise it alone. That is why we clearly are moving towards measurements of the antenna including the whole system, or, at least, a part of it. In case of RFID systems, one way to do it would be the backscatter modulation. By exciting our tag antenna, a backscatter field is generated. By measuring the backscatter signal with the help of a reference antenna, we can deduce how good the antenna is, in terms of efficiency [49].

3.2. Body Area Networks: On-Body applications

1. Description of the context

Future mobile communications systems will include so-called body-centric configurations, with modules distributed all over the body of the human user, forming a "Body Area Network" (BAN). Such wireless networks should provide a communication system available in all circumstances, with a high degree of reconfigurability, yet unobtrusive to the wearer. These systems, which in the beginning were conceived for emergency services and for disabled people, would in the future be available to all kind of users, as the examples shown in Figure 30.

2. Requirements

Such on-body networks have to respond to unique problems, related to the rapid changes in the communications channel. Indeed, the later will change depending on the subject carrying the equipment, and even on the position of the wearer, as described in [52]. Indeed, propagation close to the human user occurs due to both rays propagating around the body, or reflecting on different parts of it. Other effects should also be considered, such as multipath effects caused by multiple reflections in the environment of the user. UWB on-body communications are also of great interest and have been recently investigated [53].

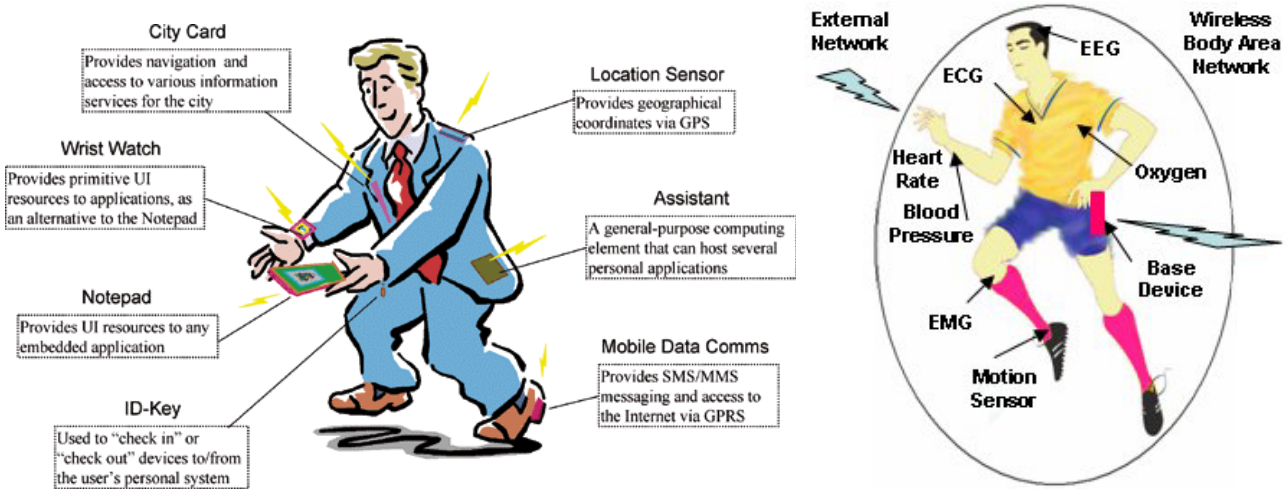

Figure 30: Example of wearable systems for Body Area Networks in everyday [50] (left) and sport [51] (right) applications.

3. *Antenna concepts*

Several different antennas such as monopole, patch, patch array, loop have been designed, built and tested in the on-body environment and their performances have been determined by measuring the path gain between two on-body paths for a range of body postures [54]. The results show that for most of the cases, the monopole-monopole combination gives lowest link loss. Link loss within 10 dB have been mathematically modelled and validated by measurement but prediction during body movement has been shown to be particularly difficult. For UWB communications the specific printed Horn shaped Self-Complementary Antenna (HSCA) and Planar Inverted Cone Antennas (PICA) have been used and their effect on the channel behaviour was studied [53].

Wearable antenna concepts are also currently under study for this kind of communications [55], [56]. Some other examples of wearable antennas on textiles are also presented in [57] (UWB half-disk antenna), and in [58] (dual-band E-shaped patch).

Figure 31: Mobile phone integrated on a jacket [55].

3.3. In-Body Applications

1. Description of the context

In-body antennas and applicators have been a hot topic in the last years [59]-[62]. The use of antennas as applicators for thermal therapy is today common practice at hospitals, whereas the use of high frequency communication to and from electronic implants is in its infancy. This in contrast to low-frequency bio-medical telemetry, which is a well-established filed [63]. Electronic implants are today already improving the quality of life of many patients. Modern electronic implants range through a variety of applications, as examplified in Figure 32, from the well-known pacemakers, to neurostimulators. "Temporary" implants are also of interest when speaking about measurements of the inner body temperature [64] or camera exploration of narrow body areas like the small bowel [66].

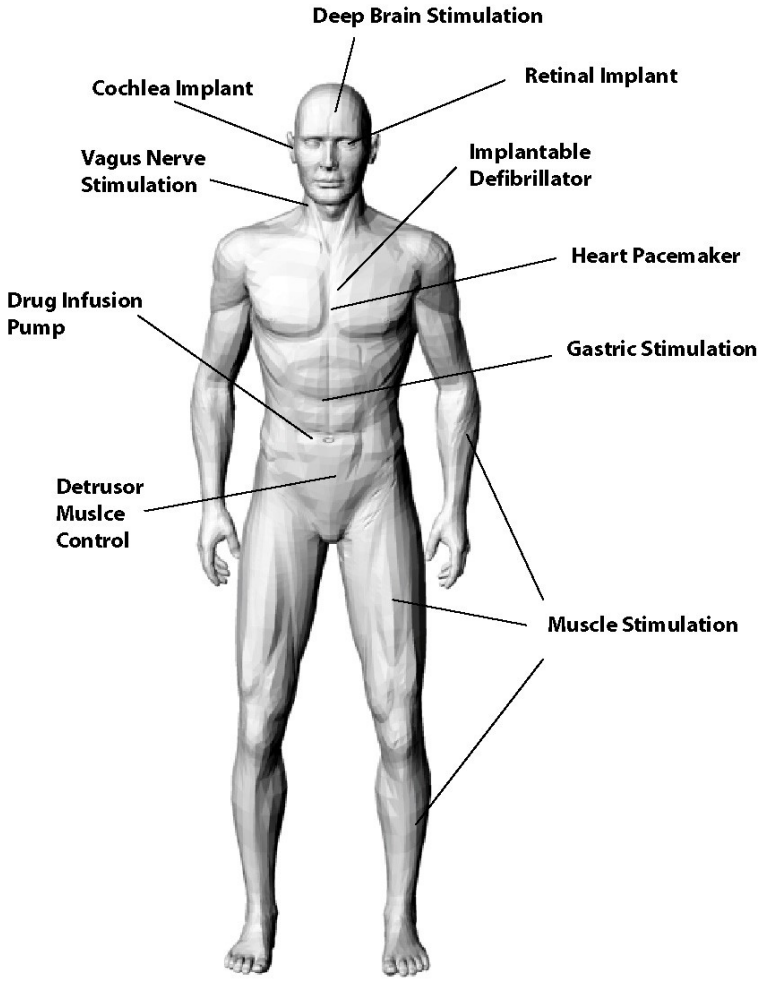

Figure 32: Examples of medical implants in the human body.

Yet, major developments in their use of RF communication technology are still ahead. Medical implants will in the future even more than today rely on miniature computers that employ sensitive,

low voltage, low power, Application Specific Integrated Circuits (ASICs) to measure, monitor, regulate physiological parameters, and control the delivery of drugs and electrical impulses to different organs in the human body.

To enhance also the quality of care, the advantages of wireless technologies should be used. Today an inductive link is commonly used to retrieve data from the implants regarding their performance and the health of the patient, and to make adjustments without any invasive operations. The drawback is that the inductive technology has a severely restricted range; the outside transceiver must touch the patient at the position of the implant, and the communication speed is very low. Using RF (Radio Frequency) links between the implants and the monitoring systems, doctors could more easily communicate with the implant, as shown in Figure 33. The communication sessions could also be made more comfortable for the patient, even taking place at home while the patient is sleeping. To accomplish this, low-power two-way RF communications systems must be employed.

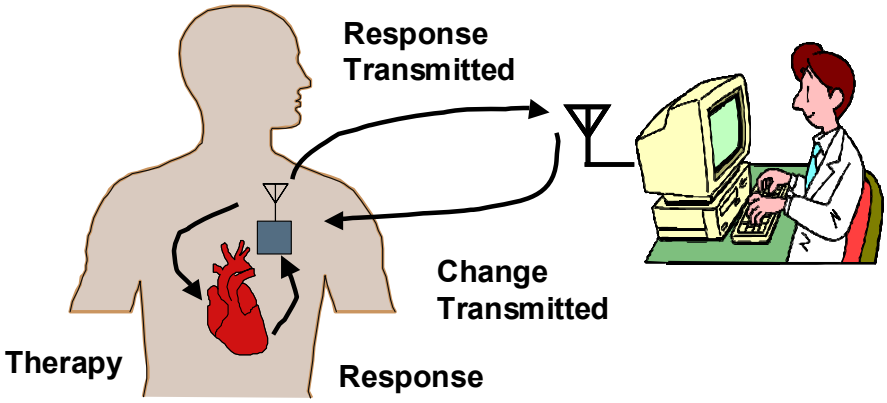

Figure 33: Two-way transmission between a pacemaker and the monitoring system (source: Zarlink Semiconductors).

To be able to produce efficient devices, the design of the communication system must run in parallel with the design of the implant itself. In this sense, the design of the antenna will partially be determined by the application, which will limit its shape, size or composition. It must also be taken into account that each body is different, and that the radio link will change with the position and posture of the bearer, and with time [60].

The human body is not an ideal electromagnetic transmission medium. The electromagnetic signals in the body will have to propagate through different tissue layers, before they are radiated into the air. These different tissues, such as muscle, bone and fat, all have different characteristics. This is exemplified in Table 4, with regard to permittivity, conductivity and characteristic impedance. The main influence of the tissue on the transmission link is the high loss that is due to the high conductivity of muscle and skin tissue. The varying permittivity will also give rise to internal reflections of the radio waves in the human body. The values of the tissue parameters are also dependent on the operating frequency, as displayed in Table 4.

Frequency (MHz)	Muscle			Fat		
	ε_r	σ (S/m)	Z_0 (Ω)	ε_r	σ (S/m)	Z_0 (Ω)
100	66.2	0.73	31.6	12.7	0.07	92.4
400	58	0.82	43.7	11.6	0.08	108
900	56	0.97	48.2	11.3	0.11	111

Table 4: Parameters of different tissues in the human body: dielectric constant, conductivity and characteristic impedance (Source: FCC and William Scanlon, Queens University Belfast).

2. Requirements and design considerations.

The European Telecommunications Standards Institute (ETSI) has reserved the frequency band from 402 MHz to 405 MHz for the Medical Implants Communications System (MICS), with a power restriction of 25 μW EIRP [67]. In the USA, the same frequency band is defined by the FCC in [68]. This allows for high-speed data exchange within a range of around 2m (6 feet). The 25 μW EIRP limit applies to the power of the signal that is transmitted into the air outside of the body. The power radiated by the antenna inside the body may be higher in order to compensate for the losses in the tissues.

In some applications, such as pacemakers, with a long life, the power available in the implants is very limited, and to increase the life of the batteries, the implanted device must be normally in a sleep mode, and activate only when needed.

There are also stringent constraints regarding the materials used for in-body antennas, as they must be biocompatible. That means that materials used must be non-toxic, mechanically stable and impervious to body liquids. Typically the antenna is isolated in order to reduce the losses in the surrounding tissue. This isolation then also acts as a barrier between the material of the antenna and the body tissue. If antennas are designed to be in direct contact with the body, then this need for biocompatibility restricts the use of the high-performance, low-resistivity conductors such as copper, silver and gold, usually employed in antenna design. Therefore, substrates such as alumina, titanium and zirconia must be used, whereas the conducting parts should be made of platinum or platinum/iridium.

3. Antenna concepts

As stated above, the antenna design for body implants is application driven. For example, low profile antennas as patches may be a good solution for devices with a flat surface, such as

pacemakers [69]. The most classic antenna for implant use is the coil antenna and the trailing wire antenna [63]. Other examples are F-antennas, PIFA (Planar Inverted-F Antennas), bent monopoles, circumference antennas [60], helix antennas, Vivaldi antennas, bowties and patches. Some examples are displayed in Figure 34. These antennas are all small, especially when compared to the wavelength in air of the MICS band frequencies, which is 74cm. But the wavelength inside the muscle tissue will only be 9.7 cm, and it is relation to this the antennas should be compared. Thus they all comply with the classic rule of thumb that a usable antenna should be larger than $\lambda/10$, or in the case of MICS: 1 cm.

A number of other antenna types have been investigated for special uses. Some examples are the spiral microstrip antennas and PIFAs with superstrate dielectric layers for implantation on the chest [70]. Very often, antennas have to be designed on purpose for better performances: a planar meander line dipole has been implemented and showed better performances than a classic microstrip antenna for use as intraocular element in a retinal prosthesis for telemetry links [71]. Implanted coils are also used in the same kinds of application when transferring power by inductive coupling. Bio-MEMS sensors are also strongly investigated for ingestible devices, intraocular sensors, visual prosthesis for epi-retinal stimulation, strain monitoring in orthopaedic implants, recording peripheral neural signals from axons, spinal implant. In [72], a silicon spiral chip antenna is recommended for these cases. Applicators antennas are mainly coaxial-slot for microwave hyperthermia [73], bowtie antennas for radar-based breast cancer detection [69].

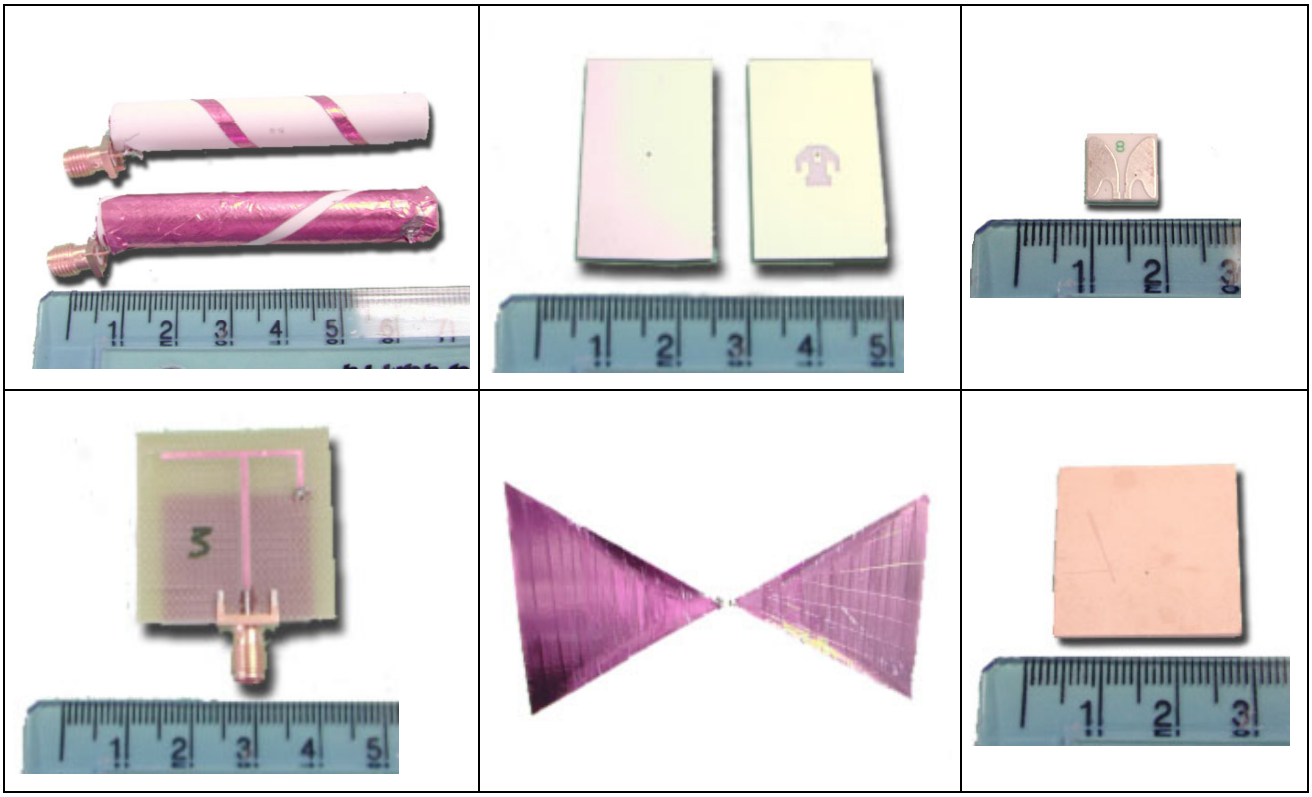

Figure 34: Examples of antennas for medical implants (Source: Zarlink Semiconductors)

4. PROPAGATION ISSUES

4.1. Description of the problem

Future mobile communication systems require reliability and high data rates. The use of multiple antennas, both at the transmission and the reception ends, promises to significantly enhance the capacity offered by conventional systems.

These multiple input multiple output (MIMO) systems exploit the spatial domain of the propagation channel. The combination of sophisticated signal processing and multiple antennas enables an adaptation of the smart antenna system to the multipath structure of the channel. In environments where MIMO systems can be applied, the propagation situation changes rapidly. Hence, it is not sufficient to investigate the performance of MIMO antennas at one specific moment, and using only one realisation of the propagation channel. The performance of a MIMO array is determined by the ability of the array to adapt to the changing channel conditions. Both the antenna arrays and the propagation channel should be treated together, with a statistical description, to take into account different channel realisations of a given propagation environment.

MIMO systems take advantage of the spatial properties of the propagation channel. Therefore, in the evaluation of MIMO antenna arrays, it is necessary to use a proper characterisation of the spatial channel properties. Parameters like the angular spread of the waves impinging at the receiver have a significant influence on the MIMO system performance. A meaningful conclusion from a comparison of MIMO antenna arrays can only be drawn if the spatial properties of a realistic propagation channel have been taken into account.

There are many studies addressing the properties of the MIMO propagation channel. These efforts have resulted in realistic characterisations of the propagation channel for different environments, e.g. indoor or outdoor, which are described in the following section.

4.2. MIMO aspects

1. MIMO channel characterisation in indoor environments

Statistical models reflect the time-variant channel behaviour, and they have the advantage of short

simulation times. Most channel models imply only channel impulse responses without any more detailed multipath information. MIMO systems require the consideration of the radiation directions of the multipath components at the transmitter and their angles of arrival at the receiver. In [74], a novel stochastic channel model based on physical wave propagation has been introduced which allows a fully polarimetric, wideband description of the multipath channel including path directions. The channel is described by multipath components, each characterised by its transfer matrix including loss, delay, direction of arrival and departure. The appearance and disappearance of multipath components over time is modelled as a birth and death process, a marked Poisson process, which enables the correct modelling of spatial and temporal correlations. In each modelling step, path properties change according to the motion of transmitter and receiver. The changing delay times of propagation paths yield a realistic Doppler behaviour of the channel. Data sets required for the statistical evaluation of the parameters of the model have been obtained by ray-tracing simulations and narrowband, wideband and directional channel measurements.

The channel models deliver the channel impulse response, the angle of departure of all paths at the transmitter and the angle of arrival of all paths at the receiver for the SISO (system with one transmit and one receive antenna) case. With this knowledge the MIMO channel matrix can be derived [75], as long as, first, the antenna spacing do not extend several wavelengths, thus the same plane waves impinge at all antenna elements. Second, the distances between transmitter and receiver and any obstacles in the channel are large enough to assume plane waves impinging at the arrays.

With these assumptions the MIMO channel matrix results from the coherent addition of the impinging waves at the different antenna positions. The channel impulse responses or in the flat-fading case the channel coefficients h_{ij} for the i-th receiving antenna and the j-th transmitting antenna are derived by placing virtual antennas in the vicinity of the SISO transmit and receive antennas. The phase difference of the incident plane waves at the different antenna positions is described by $\Delta\varphi$ (illustrated in Figure 35), which is a function of the angle of arrival of the waves and the antenna positions.

$$\Delta\varphi_i^k = \frac{2\pi}{\lambda}\left(\left(x_{SISO} - x_{vir,i}\right)\cos(\psi_k)\sin(\vartheta_k) + \left(y_{SISO} - y_{vir,i}\right)\sin(\psi_k)\sin(\vartheta_k) + \left(z_{SISO} - z_{vir,i}\right)\cos(\vartheta_k)\right) \quad \text{Eq. 12}$$

$$\Delta\varphi_j^k = \frac{2\pi}{\lambda}\left(\left(x_{SISO} - x_{vir,j}\right)\cos(\psi_k)\sin(\vartheta_k) + \left(y_{SISO} - y_{vir,j}\right)\sin(\psi_k)\sin(\vartheta_k) + \left(z_{SISO} - z_{vir,j}\right)\cos(\vartheta_k)\right) \quad \text{Eq. 13}$$

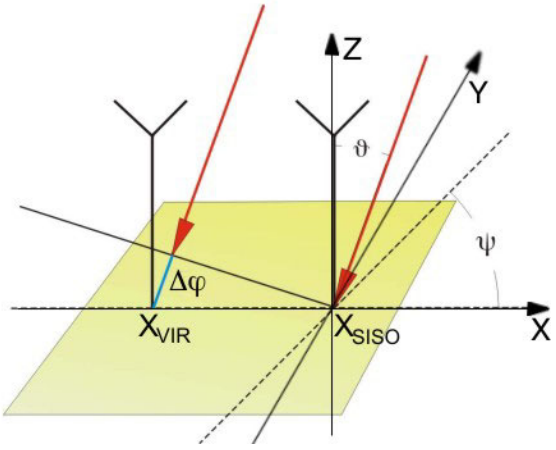

Figure 35: Plane wave impinging at the array. The phase difference of the plane waves at the different antenna positions is $\Delta\varphi$

The difference of the amplitude of the plane waves at the positions of the virtual antennas is neglected, in other words the amplitude is assumed to be constant for all antenna positions. The result is the channel coefficient for all virtual receive and transmit antennas:

$$h_{ij} = \sum_k A_1^k e^{j\varphi_1^k} e^{-j\Delta\varphi_j^k} e^{-j\Delta\varphi_i^k} \qquad \text{Eq. 14}$$

Where A_1^k is the attenuation of the *k*-th path in the SISO channel and φ_1^k is the phase.

The power azimuth profile of the stochastic channel model is composed of several Laplacian functions, each modelling a cluster of scatterers, see Figure 36.

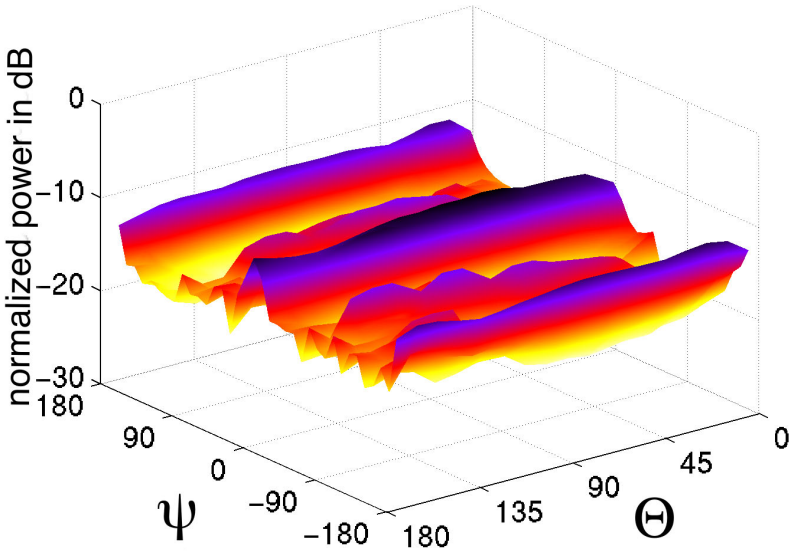

Figure 36: Azimuth ψ and elevation ϑ angle of departure and arrival in the stochastic channel model that is based on ray-tracing simulations and measurements.

The elevation profile is also modelled by Laplacian functions for paths with a short delay time, merging into a sinusoidal function for paths with a long delay time.

2. MIMO channel characterisation in outdoor environments

Ray-tracing provides an adequate means to model the multipath wave propagation for MIMO channels. In [76] a channel model for outdoor environments is introduced, which allows for an accurate narrowband and wideband characterisation of outdoor MIMO channels. The propagation phenomena taken into account are combinations of multiple reflections, diffractions and scattering from trees. The modified Fresnel reflection coefficients, which account for slightly rough surfaces, are used to model the reflections. Diffractions are described by the Uniform geometrical Theory of Diffraction (UTD) and the corresponding coefficients for wedge diffraction. Scattering from trees is considered to be totally incoherent, i.e. no distinct specular component is present. This assumption holds if the wavelength is smaller than the dimensions of the randomly distributed leaves and branches. Distinct scattering components resulting from tree trunks are neglected. To describe scattering from trees, the surface of the tree model is divided into small squared tiles. Depending on the energy, which is incident on the surface of the tree, each tile gives rise to a Lambertian scattering source. The amount of scattered energy per tile can be derived from measured normalised radar cross sections. Depending on the propagation phenomena, different approaches of ray-tracing exist. In order to trace pure reflection paths, the method of image transmitters (image theory) is implemented. Since the proposed propagation model supports full 3D diffraction, Fermat's principle is used to determine the diffracted ray paths. For mixed paths, image theory and Fermat's principle are combined. As only single scattering from trees is taken into account, the scattering paths are defined by the position of transmitter and receiver and the position of the central point of the tiles, in which the tree model is subdivided.

Figure 37 shows the result of the ray-tracing for one snapshot of an urban road traffic scenario. Receiver and transmitter are positioned on two consecutive cars with a truck in between resulting in a NLOS (Non Line Of Sight) condition. In order to keep track of the result, only the 30 strongest propagation paths are indicated (bright lines). It can be seen that part of the transmitted energy is diffracted around the truck. Since there are many buildings next to the road, the expected street canyon effect arises. Scattering from single trees contributes to the received signal as well.

For MIMO systems, ray-tracing can be applied for the calculation of the channel between each pair of transmit and receive antennas [77].

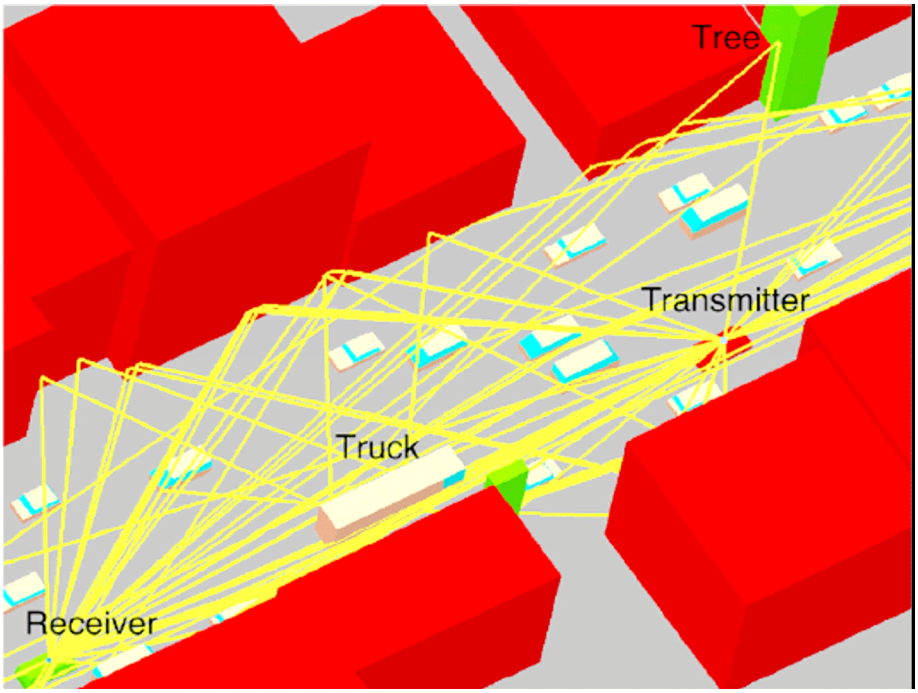

Figure 37: Ray-tracing result.

4.3. Other considerations

An experimental plane-wave based method (EPWBM) for the evaluation of multi-antenna systems has been studied [78]. The methods is based on a representative database of many radio-channel environments that is obtained from directional radio wave propagation measurements [79], [80] to record the signals approaching the mobile terminal in each environment, and combining this information with the measured or simulated antenna patterns of a terminal antenna system (see Figure 38). It has been shown that this method is accurate enough for comparing the performance of different antenna configurations (single-antenna, diversity, MIMO). A statistical antenna evaluation is possible without the need to separately perform long routes of radio channel sounder measurements for each antenna prototype.

The results of the EPWBM utilizing the joint contribution of environmental data and the radiation pattern of an antenna have been compared with the results of direct radio channel measurements. The average difference between the methods is below 1 dB in estimating diversity gain of two-element antennas. Further, the maximum difference between the methods in Multiple-Input Multiple-Output (MIMO) analysis has been found to be below 1 bit/s/Hz in estimating mutual information.

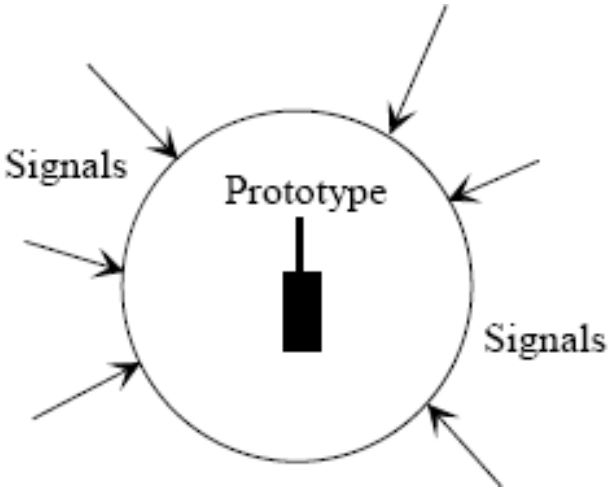

Figure 38: Illustration of how extracted radio channel signals are combined with the pattern of the antenna.

5. INNOVATIVE SOLUTIONS

5.1. On-chip/On-package antennas

One of the major issues in integrating RF System-on-a Chip (RF-SoC) is selecting the proper substrate resistivity, die thickness, and backside connectivity. This is because of the significant impact of these parameters on the substrate coupling and consequently, on the overall RF and mixed-signal system integration and performance. For low-resistivity substrate, thinning the die and grounding its backside are some of the options to reduce the substrate coupling. However, in case of Rf-SoC, the low-resistivity substrate is not preferred due to high substrate coupling and degradation of the quality factor of monolithic inductors. In this case, backside grounding is ineffective with thicker substrate. In the same time, the high-resistivity substrate degrades the latchup performance, which is a major concern for digital blocks.

A lot of patch antennas have been designed on high permittivity Silicon (Si) or GaAs substrate to reduce the dimensions of the resonator and reach a "chip-scale" [81]. But recently, a 2.4 GHz on-chip antenna with a T/R-switch has been indeed designed and fabricated in a 0.18 μm CMOS chip for RFID applications [82]. The study of on-chip integration of a 10 GHz dipole antenna with a VCO using standard BiCMOS7 (0.25μm) has been reported in [83]. But today, a very hot topic is currently about the feasibility of intra-chip communications [84]. Use of on-chip antennas as an alternative interconnect for clock distribution is investigated in [85], UWB communications in Si Ultra Large Scale Integrated Circuits (ULSIC) are studied in [86], and even as high as 13.5 Gbps ultra-wideband signal transmission on Si chips was recently demonstrated by wireless interconnects silicon integrated linear dipole antennas [87].

In contrast, only few attempts have been made for packaging antennas etched on high permittivity substrates [88]. In the development of dielectric chip antenna known as Integrated Circuit Package Antenna (ICPA), one antenna of this type has been designed and fabricated in a Ceramic Ball Grid Array (CBGA) package format [89].

5.2. Reconfigurable antennas with MEMS

1. Introduction

New engineering endeavours for many applications needing antennas, like wireless communications [90], military communication systems [91], space communication platforms, collision avoidance systems [92], [93], involve the resolution of specifications with conflicting requirements. For example, the need for higher data rates, increased radiated power and multimode, multiband, multifunction radio is in direct conflict with requirements for higher levels of integration, smaller size and lower power consumption. A keyword in the resolution of this conflict of requirement is *reconfigurability*, meaning the ability to instantly change the operating frequency, bandwidth, protocol, modulation, illumination etc.

If we consider the example of wireless communications, the denominated Software-Defined Radio (SDR) seems to be the ultimate merging solution for the low-cost appliances of the future. With SDR, multimode, multifunctional wireless devices can be upgraded via software, thus addressing the different issues with low cost.

To date however, one of the most important bottlenecks in the development of the SDR on handsets or other conventional devices is the RF front-end. That is, low cost, low consumption, highly integrated and digitally reconfigurable RF systems (antennas, filters, phase shifters, etc. or embedded configurations) are key points in the success of the current trend. The problem is the same if we consider other communication systems: the bottleneck in reconfigurability is in the front end.

The traditional approach to provide reconfigurable RF systems is based on switching devices built with ferrite materials or solid-state components, like p-i-n diodes or field-effect transistors (FET). These switches present good solutions for traditional microwave systems but they have important drawbacks in terms of losses and power consumption. A moderate amount of dc power (3-10mW per diode) is consumed by p-i-n diode but provides a low-loss switch especially at X-band frequencies. FET-based switches, on the contrary, consume virtually no dc power and can be integrated with low-noise or medium power amplifiers on the same chip, thereby reducing the assembly cost of the overall system. However they introduce a lot of loss in the front end.

Today, the Micro-Electro-Mechanical Systems technology applied to RF systems (RF-MEMS) is emerging and offers a substantially higher performance for reconfigurable systems than the traditional solutions. The MEMS switches, with electrostatic actuators, use mechanical movement, which can be controlled electronically, to achieve short-circuits or open circuits in a transmission line. Some of its outstanding characteristics are:

- *Very Low Power Consumption*: Electrostatic actuation requires 20-120V but virtually does not consume any current.
- *Very high isolation*: The devices are fabricated in air and the non-contact or OFF-state provides excellent isolation.
- *Very low insertion loss*: Using low loss metals in the MEMS fabrication, the losses in the switches become very small
- *Very low intermodulation products*: The traditional problem encountered in solid-state switches is avoided due to the "passive" structure of the MEMS.
- *Very high level of integration*: RF MEMS are fabricated using surface micromachining techniques and on-chip integrated with other electronic components.

There are however still limitations in existing MEMS, which have to be resolved prior to a wide scale commercial launch of MEMS based reconfigurable systems:

- *Packaging issues:* the parasitics due to packaging are not yet fully mastered in the microwave and millimetre wave ranges.
- *Reliability*.
- *Power handling capabilities (in hot switching applications).*

However, it is expected that these problems might be overcome by technological design improvement in the near future.

The possibilities of MEMS are not only restricted to switching (throw or reject) but they can also be used to provide variable loads, which can be electronically tuned. A famous configuration is the shunt capacitive MEMS implemented on coplanar-waveguide (CPW) transmission lines. But the combination of MEMS and antennas opens perspectives for still other types of elements, which are not circuit elements but which are directly part of the antenna itself, making the latter mobile in order to achieve polarisation or beam diversity [see for instance [94].

In the following of this section, we will thus distinguish between three different type of use of MEMS in antennas, which also represent three different levels of integration: we will first consider the use of MEMS in the antenna feeding network, then the use of MEMS to interconnect different radiating elements (in an array, or a space diversity antenna for instance) and finally the use of MEMS devices directly embedded in the radiating element. We will also illustrate that as the level of integration between MEMS and antenna increases, the model used to describe the MEMS goes from Kirchhoff to Maxwell, leading to the need of an increased collaboration between MEMS and antenna specialists.

A very thorough review of MEMS technology used in microwaves and millimetre waves can be

found in Deliverable 2.1D3, chapter 5 of the ACE network of excellence [95].

2. MEMS in antenna feeding networks

There are currently three main application fields for antennas using MEMS in their feeding network: Phased arrays, where the phase shifters in the array are realized with MEMS [96]- [99], miniature terminal antennas, where the impedance match is tuned in frequency using MEMS elements [90], [100], [101], and certain types of reflectarrays [102]-[104]. The MEMS devices used are usually switches, tuneable capacitors, tuneable inductors, and true time delay lines. We will concentrate mainly on MEMS in terminal antennas.

The specific characteristics of this type of reconfigurable structures are the following:

- This type of devices has existed generally prior to the introduction of MEMS. Traditional tuneable elements like PIN diodes, FET transistors and varactors are replaced by MEMS.
- The MEMS device is considered as a circuit element, and can be described using traditional impedance, admittance or scattering matrices.
- Radiating elements and MEMS can be fabricated on opposite faces of the same substrate, or on separate substrates depending on the configuration. This may lead to technological challenges such as double face processing if a fully integrated solution is required. In the non-integrated case, packaging and mounting of the MEMS is a major issue, as the parasitics can become severe at very high frequencies.

The main challenges for MEMS in these systems are:

- Power handling
- Packaging
- Availability of a good circuit model of the packaged MEMS
- Reliability

There are different examples of MEMS in the feeding network of terminal antennas. The first example is a diversity antenna operating at 2.3 GHz [93], where the switching device between the two antenna elements is made with a MEMS circuit. It consists on two planar antennas mounted on a vehicle, connected by a feeding network incorporating MEMS switches. The second example [100] depicted on Figure 39 shows a handset antenna where two different feeding networks can be selected using a switch (in the case of the example a PIN switch), allowing for dual frequency operation.

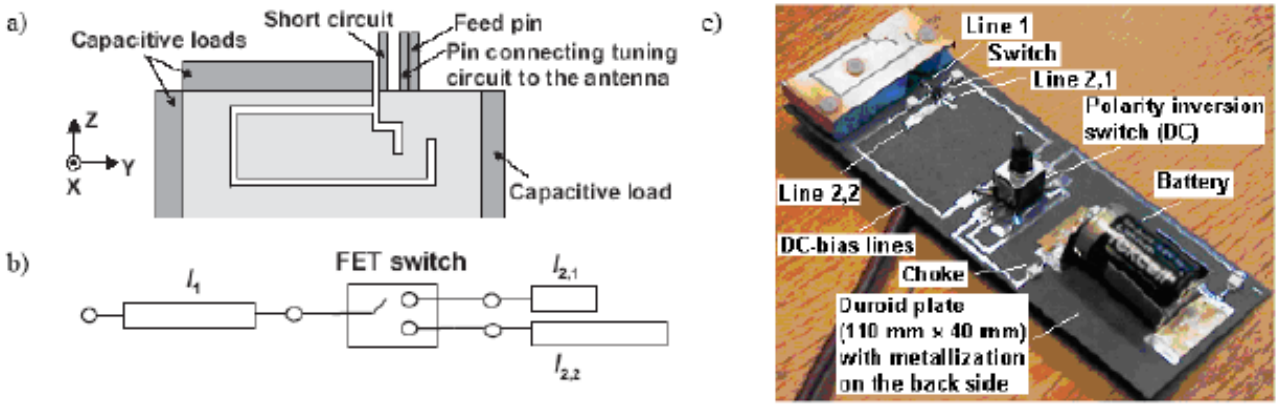

Figure 39: Dual frequency handset antenna using a switch.

The narrow impedance bandwidth of small antennas for personal mobile communications can be alleviated with electrical frequency tuning, which increases the effective bandwidth and can enable the use of a single antenna element in several radio systems without increasing its size. To date, the main emphasis has been on the achievable tuning range while power loss caused by the tuning circuitry is a major problem of frequency-tuneable antennas. The minimization of power loss and caused by the tuning circuit have received special attention from HUT [100] in a frequency-tuneable shorted patch antenna (Figure 40). The antenna is based on a shorted patch with $Q_0 = 20$. A PIN-diode was used as the switch. The prototype is capable of switching between the transmitting (TX, 880…915 MHz) and receiving (RX, 925…960 MHz) band of an E GSM900 mobile station. The goal was to minimise the power loss in the tuning circuit and to obtain approximately equal and high radiation efficiencies at both bands. With the help of a circuit model (Figure 40), an optimal configuration for the tuning circuit can be determined. Both in simulations and in measurements, the necessary frequency tuning was obtained at the expense of roughly 3 % reduction in efficiency compared to the antenna without the tuning circuit.

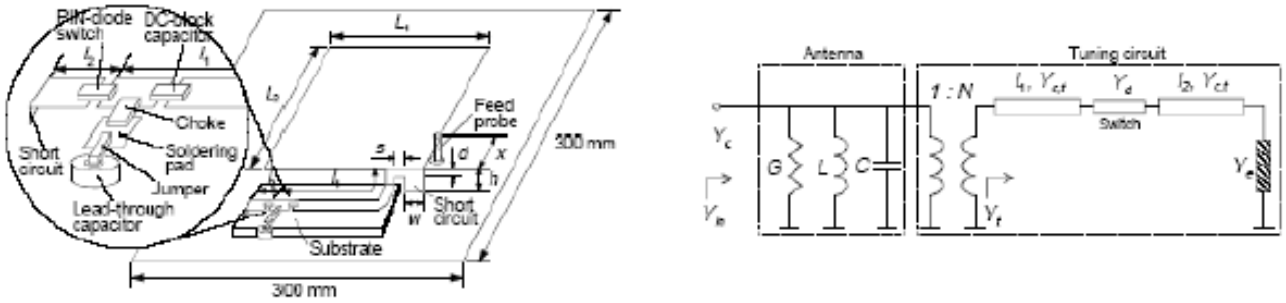

Figure 40: Geometry of frequency-tuneable shorted patch antenna and corresponding circuit model [100].

3. *MEMS connecting radiating elements*

This second category of tuneable antennas is when MEMS switches or capacitors are used to connect radiating elements. In this case, the MEMS are not directly part of the radiators but are

usually located very close to them. A simple circuit model for the MEMS is in general sufficient for the design of such structures, as for the first category described above.

An example of this concept is illustrated in Figure 41. It consists of a dipole, in which the two branches are interrupted by switches. The resonant frequency of the dipole can be selected by playing with open/closed states of the switches. Due to the technology employed in the fabrication of MEMS, the printed antennas seem to be the most appropriate for this kind of applications.

Figure 41: Tuneable dipole

Two main structures are currently found in the literature: elements tuneable in frequency (usually dipoles or slot antennas) [105]-[108] and arrays that are reconfigurable in frequency and sometimes also have a reconfigurable beam [98], [109]-[113].

There are two challenges in the design of these structures: the design of the structure itself, with the selection of the different radiating elements, the best way to interconnect them and the MEMS which will be used to do so (usually switches or capacitors), and the design of the feeding structure for the elements with the appropriate excitation amplitude and phase in the various configurations. In addition, impedance matching must be done in order to minimize reflection loss. What complicates the design of the feed structure of such antennas is that the same feed mechanism must work for all antenna configurations, or the feed mechanism must adapt as the antenna is reconfigured, adding loss and volume, which we want to avoid in terminal antenna applications. The challenge is thus to design multi frequency terminal antennas by connecting several radiating parts, and a feeding network providing a good match in all frequency bands.

The main characteristics of these antennas are:

- This type of devices has existed generally prior to the introduction of MEMS. Traditional tuneable elements like PIN diodes, FET transistors and varactors are replaced by MEMS.
- In most cases, the MEMS device can be considered as a simple circuit element, and can be described using traditional impedance, admittance or scattering matrices. In some cases however, the coupling between the power radiated by the antenna and the MEMS has to be taken into account.
- The feeding network has to be designed carefully.

The main challenges for the MEMS devices are the same as for the first category described above.

Some examples of terminal antennas of this category are shown below. The first one is a reconfigurable antenna for MIMO systems, which was proposed in [114]. It consists of a square array of printed patches interconnected by MEMS switches, as depicted in Figure 42 to Figure 44.

As we can notice on Figure 43, the feeding network of the array is also tuneable in this case. According to the frequency selected for the reconfigurable system, groups of patches are connected or disconnected, as illustrated in Figure 44.

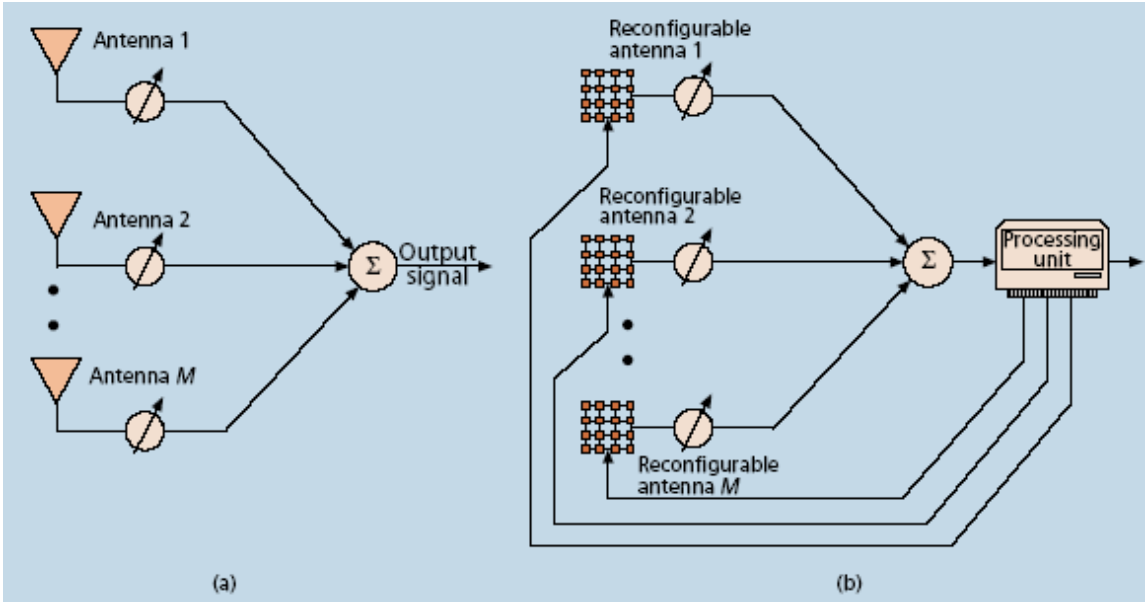

Figure 42: MIMO antenna system [114].

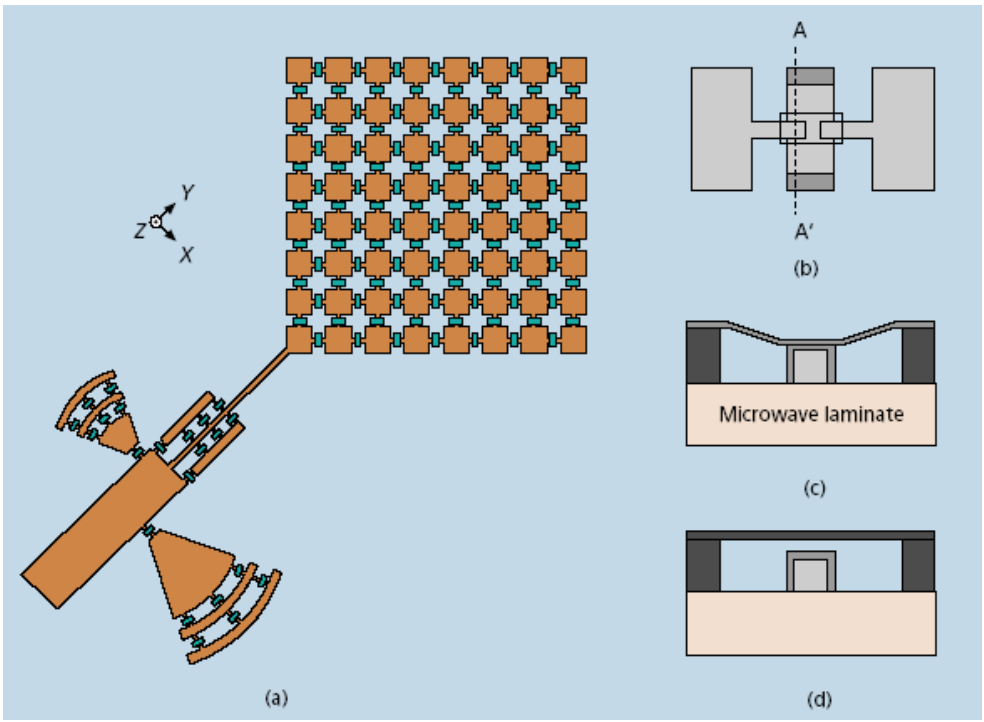

Figure 43: Reconfigurable MIMO antenna [114].

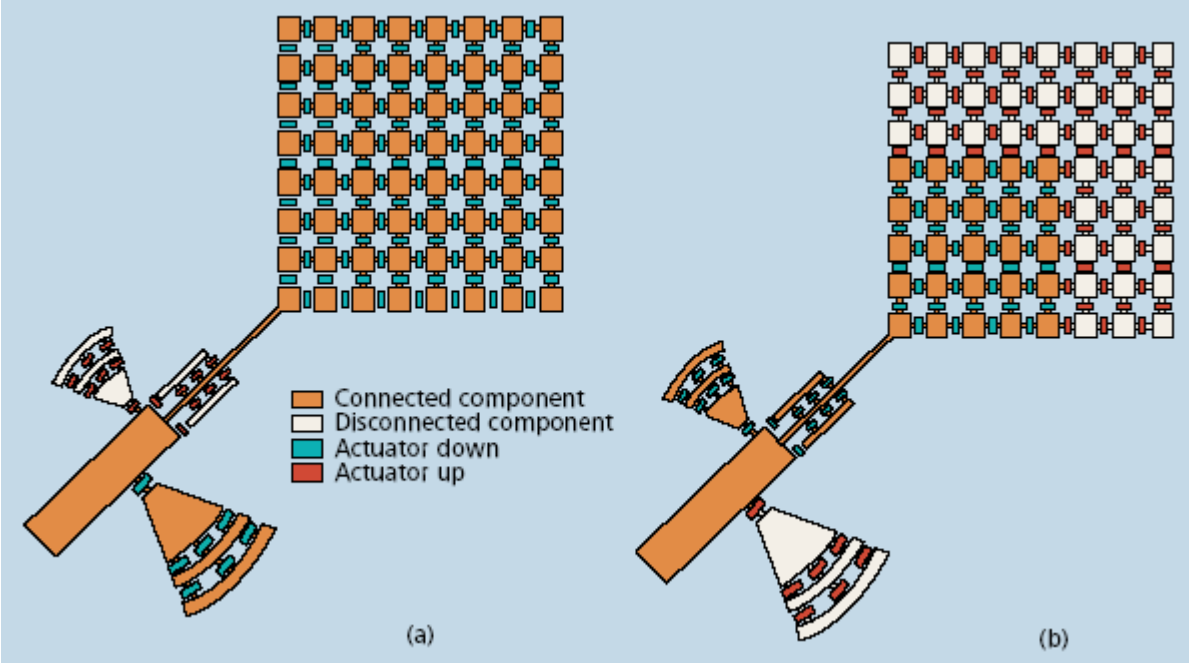

Figure 44: Reconfigurable pixel-patch antenna schematics for dual frequency operation at a) 4.1 GHz (mode21); b) 6.4 GHz (mode11).

Another example of this class of antennas is the tuneable slot (or dipole) antenna, where different parts of a slot (or dipole) are connected using switches. Such a design is proposed in [107] and illustrated in Figure 45.

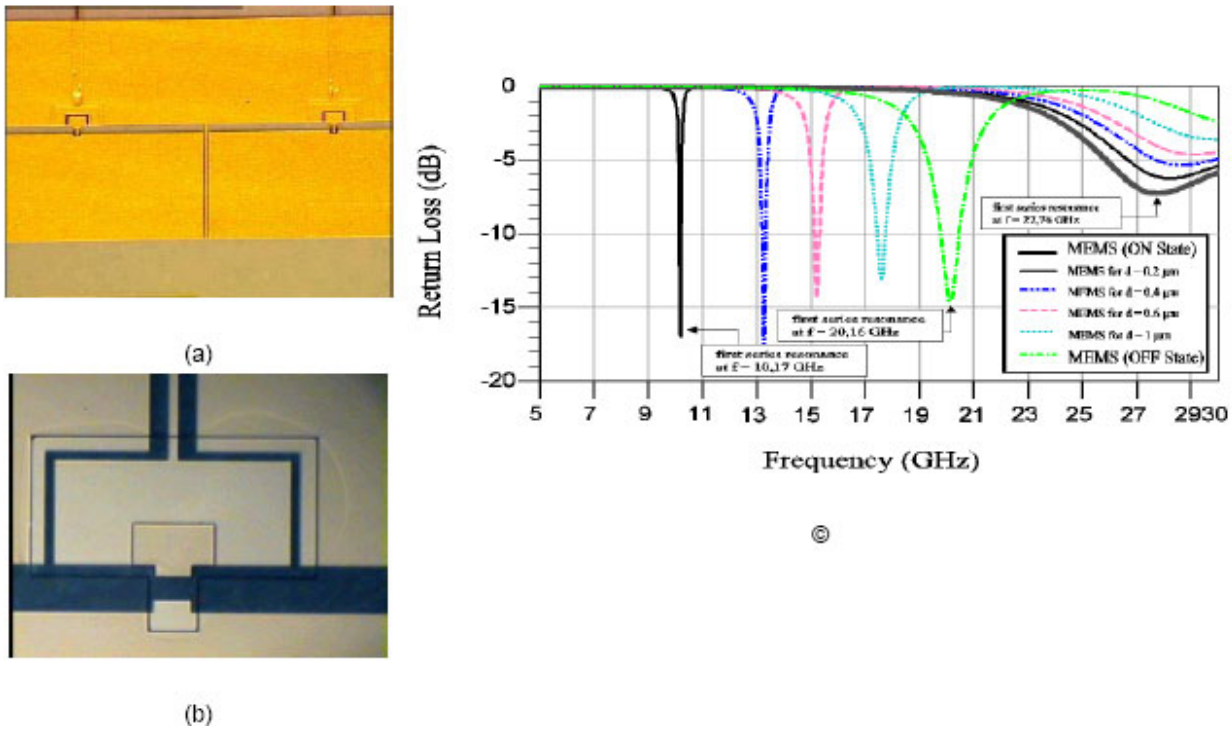

Figure 45: Tuneable MEMS-based CPW-fed slot antenna. (a) MEMS-based cavity-baked CPW fed slot-antenna on quartz. (b) Details of the MEMS area and bias circuitry. (c) Influence of the MEMS height on the return loss [107].

4. MEMS in radiating elements

The reconfigurable antennas having the highest degree of integration between MEMS devices and a radiating element are this third category, where the MEMS are located directly in the radiating element, and thus change its characteristics [101], [113], [115]-[120]. Three types of reconfigurability can be achieved using this mean: polarisation diversity, as is illustrated by the example of Figure 46, frequency tuneability and beam tuneability.

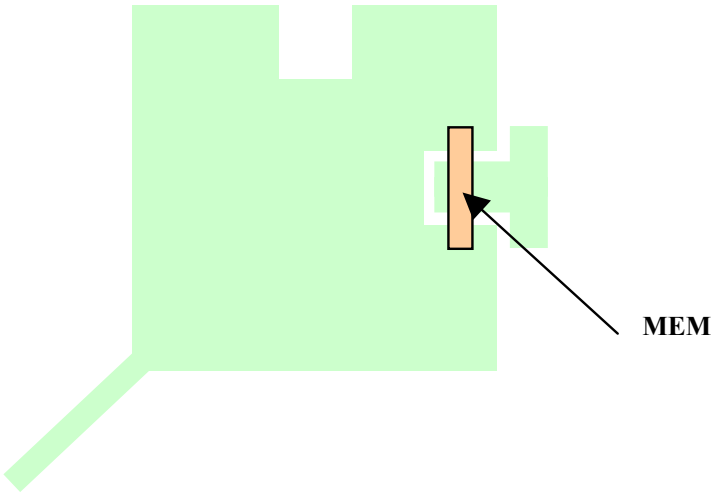

Figure 46: A patch antenna with a contact switch actuator is able to reconfigure the polarisation of the antenna between a linear or circular polarisation.

In this kind of structures again, the frequently used MEMS devices are switches and capacitors. There is however an interesting trend to go to completely novel structures, where the tuneability is obtained by moving parts of the antenna or the entire antenna itself (see for instance [115], [116]. This concept is especially interesting for mm-wave applications, where the physical size of the antenna is small enough to allow the complete integration of the antenna on a mobile device.

The main challenge in the design and realization of reconfigurable antennas having such a high level of integration is that the MEMS and the radiating elements have to be completely co-designed. A simple circuit model for the MEMS is not sufficient, and the structure has to be modelled globally, usually needing a complete full-wave field description (Maxwell's model).

A good example of a terminal antenna having polarisation diversity is given in [118]. It consists of a nearly square patch antenna, fed by on its corner, as is depicted in Figure 47. This type of antenna supports two degenerate orthogonal modes, and the notches are designed in order to provide 90° phase shift between the modes. When the actuator covering one of the notches is in off state, it does not perturbate the mode and the antenna is radiating circular polarisation. When it is on, the phase relation is perturbed and the antenna radiates a dual linear polarisation.

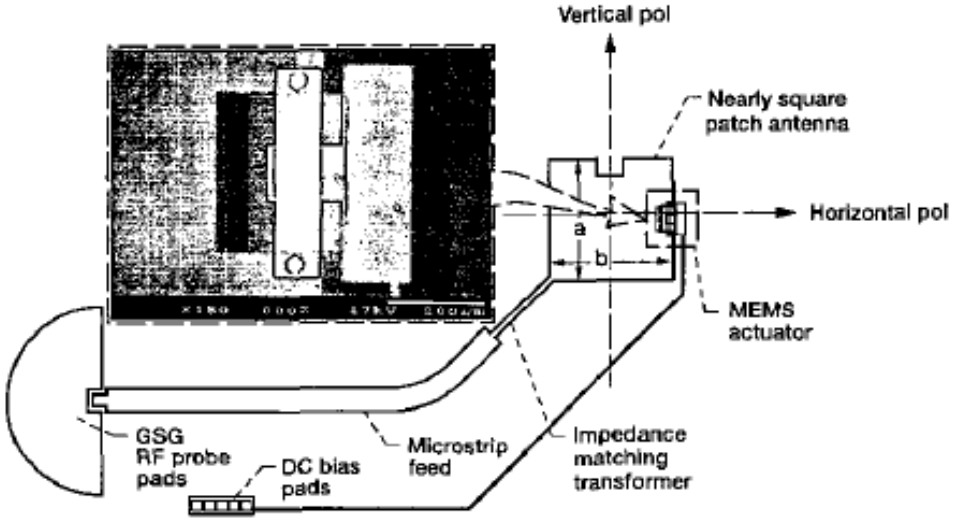

Figure 47: Polarisation diversity through MEMS switch

An example of frequency tunability is given in [121]. Again, the design starts from a microstrip patch antenna fed by a microstrip line, where a slot is incorporated into the patch to obtain a second resonance frequency. The electrical length of the slot is tuned by MEMS switches, as is depicted in Figure 48.

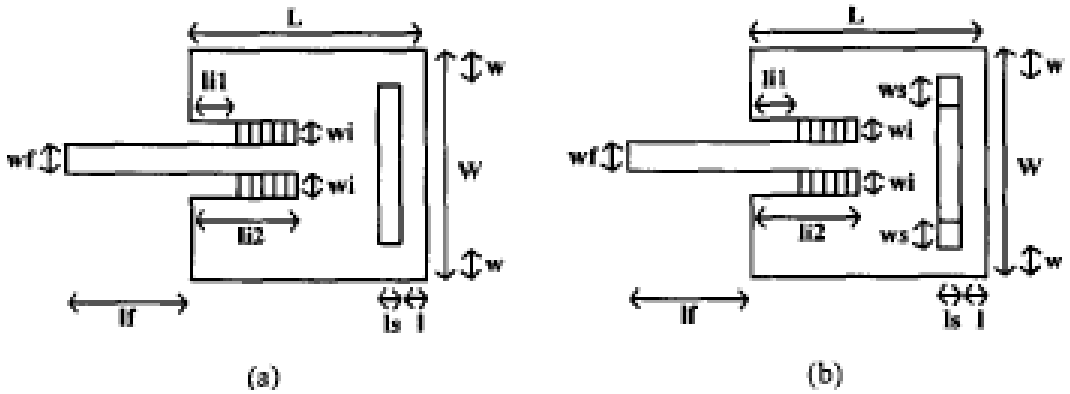

Figure 48: Multi frequency patch using MEMS.

The third family of terminal antennas with MEMS incorporated directly in the radiating element are antennas with beam diversity. It is in this family that we find the most novel design, where the radiating parts themselves are moving. A nice example is given in [115], and is depicted in Figure 49. It consists of a dipole antenna fed by a symmetric line, where the two arms of the dipole can be actuated through a MEMS device. By moving these arms, the dipole is changed to a Vee antenna, the central angle (and thus the beam) being adjustable.

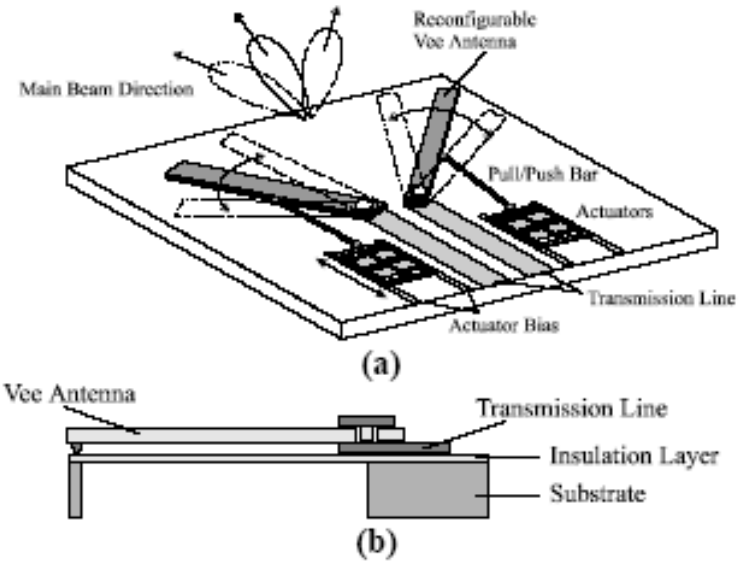

Figure 49: Planar Vee antenna with moveable lines. Tuneable beam antenna

5. Application examples

e) Pattern agility

The performance of a re-configurable CPW-fed slot microstrip array has been investigated. The radiation pattern can be controlled using MEMS switches [111] with independent actuations (Figure 50 and Figure 51) to optimize the possibilities of reconfiguration. Another challenge consists in optimizing the design of the feeding network to ensure a sufficient matching for the different possible states of the switches.

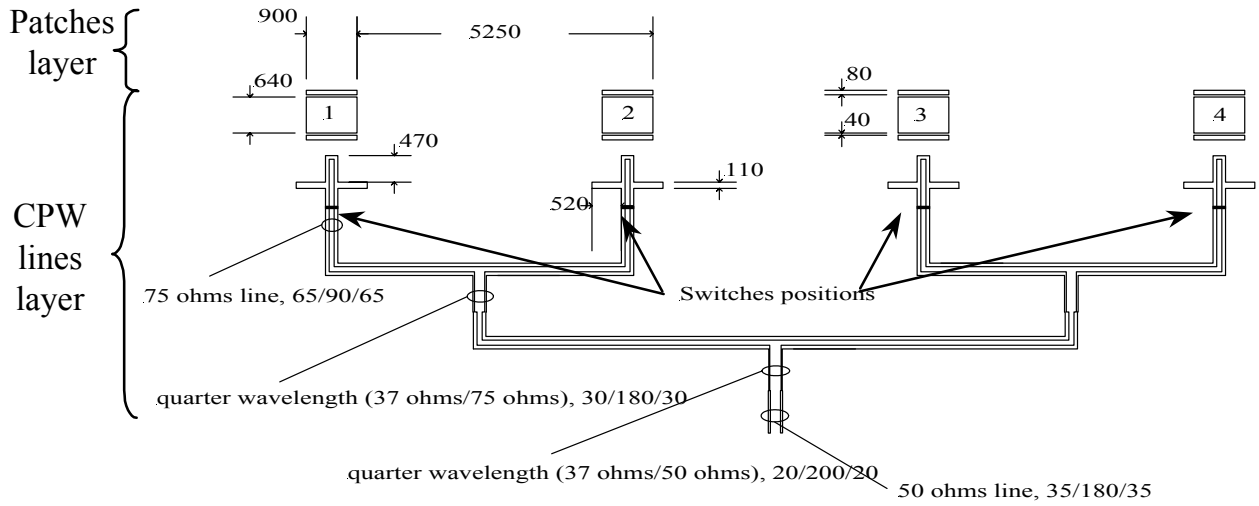

Figure 50: "Passive" configuration of a CPW-fed patch antenna array. Dimensions are in micrometers.

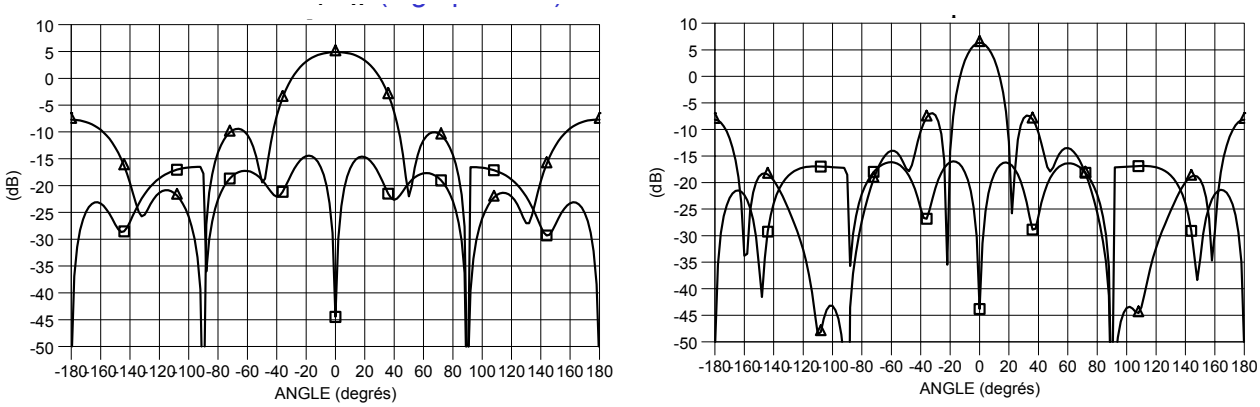

Figure 51: Antenna array (MEMS allow to change directivity)

f) Polarisation agility

A new re-configurable antenna application of Scratch Drive Actuator (SDA) [102] is reported here. Micro-actuators are associated to metallic parasitic plates and pushed it toward the truncated corners of a circularly polarized microstrip patch antenna. SDAs are constructed from a standard process in which we included the fabrication of the metallic plates and the antenna. The antenna operates in the 47 GHz band and is processed on a 200 µm silicon substrate (ε_r=11,8 ; σ=3,38.10^5 Ω.cm). A 150 µm cavity depth is then etched under the patch in order to reduce surface wave losses (Figure 52 a). The antenna is initially circularly polarized. The use of 2 SDAs arrays moving the metallic plates close to each truncated corner of the patch enable to generate a linear polarisation (Figure 52 b).

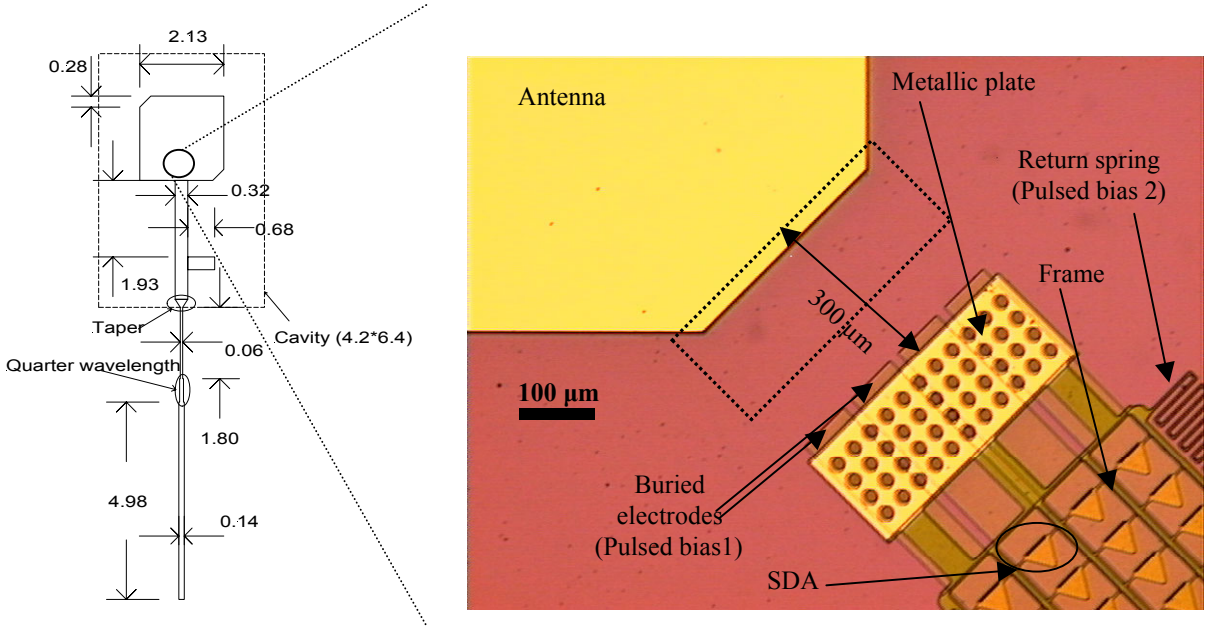

(a) (b)

Figure 52: (a) Schematic view of the microstrip antenna (all dimensions are in mm), (b) Optical microscope photograph of the system before the releasing.

g) CPW-fed slot MEMS-based frequency agile patch antenna

A new solution [122] (Figure 53) is applied with which the operating frequency of a printed antenna can be controlled (Figure 53 a). Its main advantages are: a conservation over all the frequency band of the antenna size, the antenna feeding network and its radiation characteristics. Such antenna was fabricated on a 400 µm high-resistivity silicon (ε_r=11,8 ; tanδ=2.10^{-3}) substrate on which we polymerise on each side 20 µm of BCB (ε_r=2.65, tanδ=2.10^{-3}) in order to reduce surface wave losses. This system is then associated with MEMS switches for discrete frequency shift (Figure 53 c). They are bridged onto the radiating element to rely or note parasitic pieces localized in the E-plane of the antenna. We can obtain for the position of the MEMS described on Figure 53 b frequency shift of one octave (Figure 53 d).

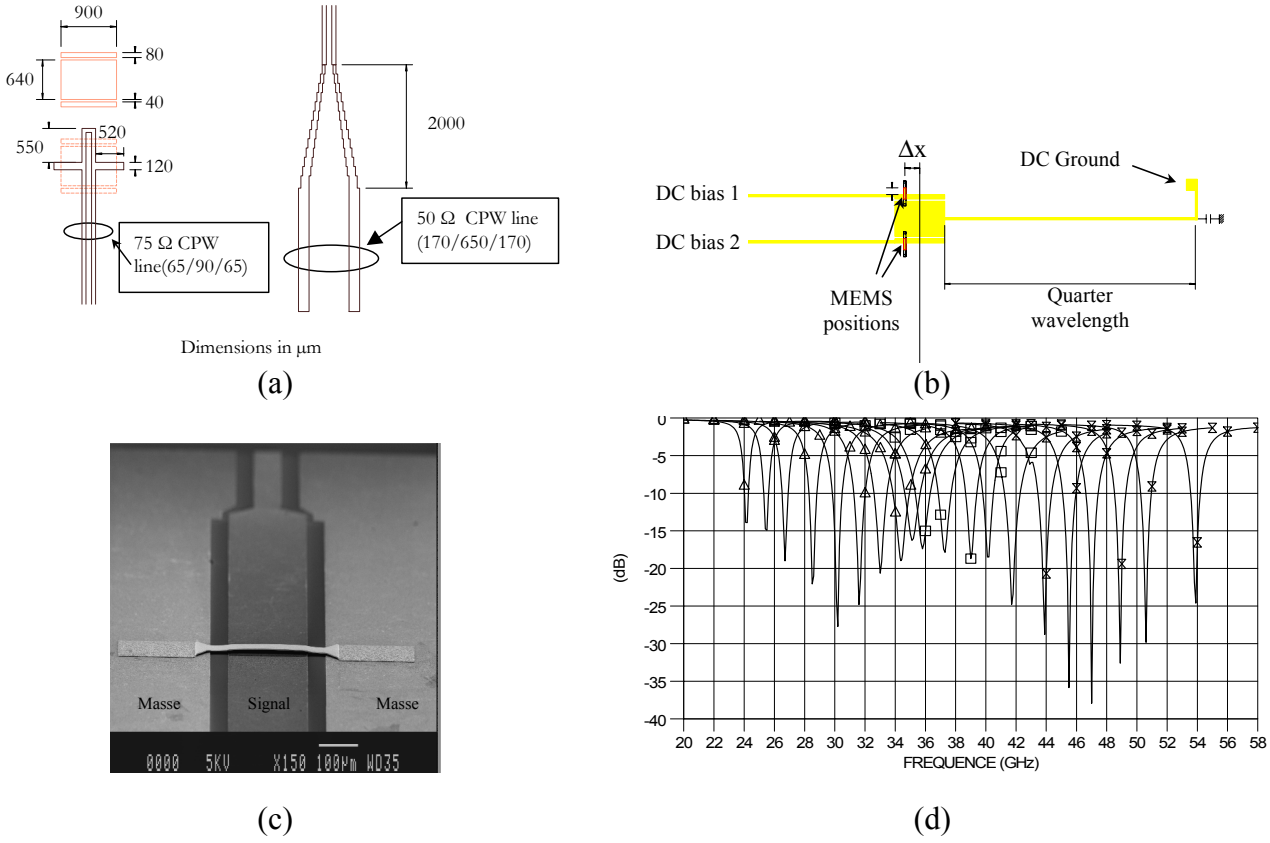

Figure 53: (a) Passive version of the frequency tuneable antenna. (dimensions are in µm). (b): Top view of a frequencies tuneable antenna. (c) Capacitive micro-switch. (d) Return loss versus switch positions

6. *Conclusions*

Reconfigurable antenna and using MEMS elements have a large potential for future applications [123]. Indeed, they open new opportunities and give novel and original solutions to complex problems.

However, a successful future for these devices depends on three key points: Improvements of

classical RF and microwave MEMS (power handling, reliability, good packaging solutions), creations of MEMS dedicated to microwave and millimetre-wave frequency bands (distributed MEMS), and a better understanding and cooperation between antenna and MEMS specialists.

5.3. Metamaterials for antennas

1. Basic concepts on metamaterials

There is not a unique way of defining such a vague term as "metamaterial", but we can however give a general description of the corresponding structures.

Metamaterials are artificial composite materials fabricated from repeated dielectric and/or metallic elements, specifically engineered to produce a desired electromagnetic behaviour. As suggested by the prefix "meta", we expect metamaterials to exhibit emergent electromagnetic properties, more precisely properties that the constituent elements do not exhibit when they are considered separately. These emergent properties are related to the fact that the periodic elements interact with electromagnetic waves in a subtle manner. Indeed, waves are not sensitive to each detail of the structure, but they "see" an equivalent homogeneous medium, for which it is possible to define equivalent permittivity and permeability: this is the equivalent (or effective) medium approach.

This approach relies on a homogenization procedure, which consists in defining equivalent macroscopic parameters from a microscopic description of the medium, which is nothing new. As a matter of fact, for a conventional material the permittivity and permeability are already macroscopic parameters that describe the average response of the material to electromagnetic phenomena, whereas microscopic models describe these interactions by taking into account the molecular and atomic structure of the material.

From that point of view, it can be considered that the arrangement of periodic elements in a metamaterial plays a role which is similar to the role played by the molecular structure in a conventional material, but at a different length scale.

Further considerations on the concept of metamaterial and on the circumstances under which such a term is appropriate can be found in [124].

There is also great interest in another type of periodic structures: photonic band gap structures (PBG) or electromagnetic band gap structures (EBG). A key difference between the concept of metamaterial and PBG/EBG structures is the electrical size of the unit cell:

- The electromagnetic properties of PBG/EBG rely on the periodicity, which should be of the order of the radiation wavelength. In that case, the electromagnetic behaviour of the

structure is essentially governed by diffraction phenomena[2].

- The properties of metamaterials can be deduced from the electromagnetic properties of its elementary constituents through an appropriate homogenization procedure. To make possible this homogenization, the electrical size of the unit cell should be much smaller than the radiation wavelength in the equivalent medium.

It can be deduced from this distinction that a given periodic structure can be used as both PBG/EBG and metamaterial, depending on the operating frequency.

Among all the emergent properties metamaterials can exhibit, the present summary focuses on structures where both the permittivity and the permeability can be simultaneously negative. Such structures were referred to as "Left-Handed Media" (LHM) by Veselago in 1968 [125]. He also predicted that LHM would have quite interesting and unusual electromagnetic properties, like negative refractive index, reversed Doppler effect and Reversed Cherenkov-like radiation.

Figure 54 illustrates the type of media we are interested in. It is a simplified representation because only real values for ε and μ are considered.

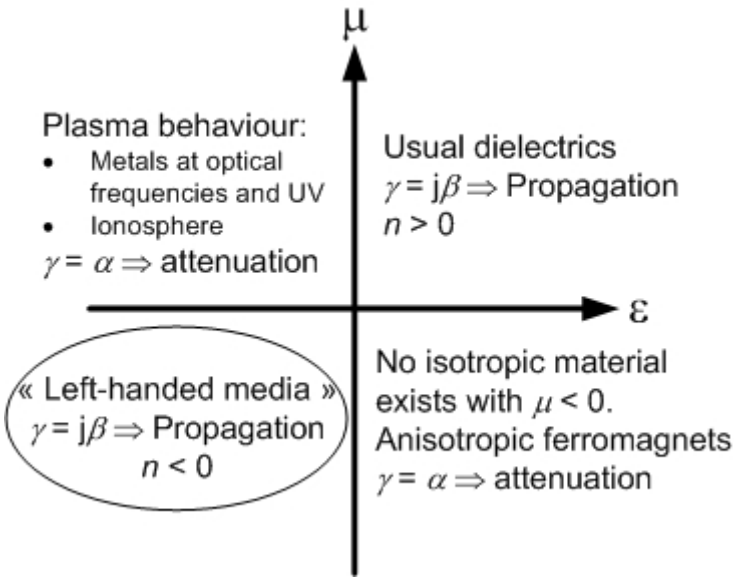

Figure 54: Simplified ε-μ diagram (ε and μ are real).

It can be seen that propagation is also possible when both ε and μ are negative, which leads to unusual propagation characteristics (like negative refractive index). The possibilities of taking

[2] The period of the EBG surface may also be much smaller than a wavelength. They can create resonances in the structure by using capacitances between patch edges and inductances of vias, thereby reducing the requirement to the period. Thus, the difference is that the EBG surface relies on a resonance in the surface, which the metamaterial does not require. The start of the bandgap is associated with a resonance.

advantage from these phenomena for small antenna application are under consideration in following sections.

General information about meta-materials can be found in [124]-[127], while different type of meta-materials and their properties are reported in [127]-[153].

2. Terminology

Several terms are used to characterize the media we are considering in this study. The most regularly used are:

- **Left-Handed Media (LH media or LHM)**: This term was coined by Victor Veselago [125]. It refers to the orientation of the vector triple *E*, *H* and *k*: in a conventional medium this triple follows a "right-hand" rule, whereas it follows a "left-hand rule" in a LHM. With this terminology, a conventional medium is called a "Right-Handed Medium", or RHM.
- **Negative Refractive Index media (NRI media)**: This term is used for media in which the refractive index is negative. With this terminology, a conventional medium is called a "Positive Refractive Index medium", or PRI medium.
- **Backward Wave media (BW media)**: This term is used for media that can support backward waves, i.e. waves for which the wave vector *k* and the Poynting vector *S* are in the opposite direction. With this terminology, we do not find in the literature a particular name for conventional media.
- **Double Negative media (DNG media)**: This term is used for media for which both the real parts of the permittivity and permeability are simultaneously negative. With this terminology, a conventional medium is called a "Double Positive Medium", or DPS medium.

All these definitions point out a particularity of these media. On a first glimpse, it seems that all these terms are equivalent, but ambiguities arise when we are looking to them in greater detail. For example, it has been shown that negative real parts of permittivity and permeability was a sufficient but not necessary condition to obtain backward waves (see [126]). Moreover, the term "backward wave" supposes that there is a forward and a backward direction of propagation, a terminology that can be suitable for a one-dimensional structure, but which is less intuitive in the general three-dimensional case. At this stage of the work, it is not worth spending too much time on choosing the best definition. In this report, we have chosen to use the term "Left-Handed Media" (LHM) because it is the most frequently used in the literature.

3. The two conceptual approaches for left-handed media

There are nowadays two rather different ways of considering and realizing LHM:

- Periodic arrays of dielectric and/or metallic elements.
- Periodically loaded transmission line networks.

The first approach is treated by field calculations, whereas in the second one the propagation characteristics are deduced from equivalent electric circuit models, like transmission lines. The first approach can be conceptually applied to 1D, 2D or 3D structures, whereas it seems not to be so evident with the second approach. Although 1D or 2D loaded transmission lines have been successfully investigated, the extension to a 3D network has not been reported yet.

Are these two approaches really conceptually different? This question is hard to answer because there are essentially two distinct communities that have investigated the subject of metamaterials: the physicists' community rather uses the first approach and they are more interested in optical applications, whereas the engineers' community rather uses the second approach and are more interested in microwave applications. As a result, the terminology and the way of presenting results and performances of structures can be rather different. Moreover, results are usually reported in distinct periodicals depending on the approach used by the authors.

We believe that doing a link between these two approaches would be of great interest for the general understanding of metamaterials.

4. Antenna applications using left handed media

The main advantages offered by LHM for the antenna applications reported here are:

- Size reduction, for a given level of performances.
- Higher directivity, for a given size.
- Increase of the radiated power.
- Novel functionalities (backward-wave radiation from a leaky-wave antenna, additional filtering effects, possibilities of tuning by an external signal, ...).

The reported antenna applications have not all been experimentally tested. Certain applications consist more in theoretical concepts than on a practical antenna realization.

We have decided to concentrate more on LHM antenna applications than on EBG (Electromagnetic Band-Gap) or FSS (Frequency Selective Surfaces) antenna applications. However, for certain structures it is not clear which category they belong to.

5. *Application to leaky-wave antennas*

a) Principle of forward and backward-wave radiation from a guiding structure

It is known that when a wave propagates along an open guiding structure with a phase velocity v_{p1} greater than the phase velocity of electromagnetic waves in the surrounding medium (v_{p0}), a cone of exceeds the speed of light in the medium. The angle θ between the normal to the phase velocity of the guided wave (v_{p1}) and the phase velocity of the radiated wave (v_{p0}) (direction of radiation, see Figure 55) is given by [154], [155]:

$$\sin\theta = \frac{v_{p0}}{v_{p1}} \qquad \text{Eq. 15}$$

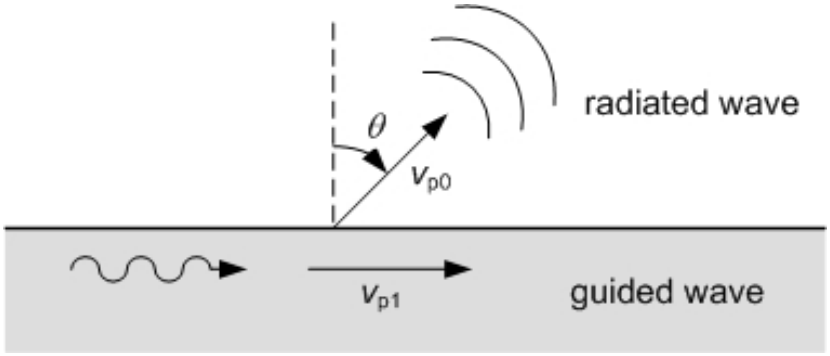

Figure 55: Radiation from a guiding structure, definition of angle θ.

Using the relations between the phase velocity v_p, the phase constant β and the refractive index n can be written:

$$\sin\theta = \frac{v_{p0}}{v_{p1}} = \frac{\beta_1}{\beta_0} = \frac{n_1}{n_0} \qquad \text{Eq. 16}$$

Assuming that $n_0 > 0$, we have the four following cases:

1) $n_1 > n_0 \quad \Rightarrow \sin\theta > 1 \Rightarrow$ no radiation + RH behaviour in the guiding structure.

2) $0 < n_1 < n_0 \quad \Rightarrow$ forward-wave radiation ($0° < \theta < 90°$) + RH behaviour.

3) $-n_0 < n_1 < 0 \quad \Rightarrow$ backward-wave radiation ($-90° < \theta < 0°$) + LH behaviour.

4) $n_1 < -n_0 \quad \Rightarrow \sin\theta < -1 \Rightarrow$ no radiation + LH behaviour in the guiding structure.

The conditions on n can also be expressed on β. It can be seen that only positive angles of radiation ($0 < \theta < 90°$) can be obtained with conventional structures ($n_1 > 0$), but the use of a negative refractive index medium as guiding structure allows obtaining negative angles of radiation ($-90° < \theta < 0°$). This reversed Cherenkov-like radiation from a left-handed medium was first predicted by

Veselago in 1968 [125].

b) Principle of transmission line leaky-wave antennas

Transmission line leaky-wave (TL-LW) antennas are essentially travelling-wave structures, which are based on the principle described above. Modes for which the radiation condition is met are dispersive and then the angle of radiation is frequency dependent. This resulting frequency scanning capability is a particularity of TL-LW antennas. Conventional TL-LW antennas use a higher-order mode with positive phase constant ($\beta_1 > 0$). As a consequence, they have the drawbacks of scanning only the half space from broadside to endfire ($0 < \theta < 90°$) and requiring special feeding structures for suppression of the dominant mode.

The utilisation of metamaterial TL to realize TL-LW antennas presents essentially advantages [156]:

- The structure can radiate in the dominant mode, and then it does not require any special feeding structure, which therefore reduces the size of the antenna.
- Using a left-handed TL, the structure can radiate in the backward direction, from broadside to backfire ($0° > \theta > -90°$).

c) Realization of a TL-LW antenna in CPW technology [154], [157].

A left-handed TL-LW antenna has been built using coplanar waveguide CPW technology, as shown in Figure 56 (a). This structure is a practical implementation of a loaded TL shown. The series capacitive loading elements are realized with gaps in the central conductor and the shunt inductive loading elements are realized with narrow connections between the central conductor and the ground planes. The antenna contains 16 unit cells of length a = 4.3 mm and the structure is designed to radiate around 15 GHz. Then, the ratio λ_0/a is about 4.7.

The measured far-field radiation pattern is shown in Figure 56 (b). A beam emerges in the backward direction at an elevation angle S of -38.5° from broadside. With increasing frequency, the main beam scans from the backfire direction toward the broadside direction.

LHM can also be obtained in coplanar technology by a different realization, which consists in a CPW waveguide periodically loaded with split ring resonators (SRRs) (printed on the other side of the substrate) [158]. Such structures can also act as a leaky-wave antenna, as described by simulations in [159].

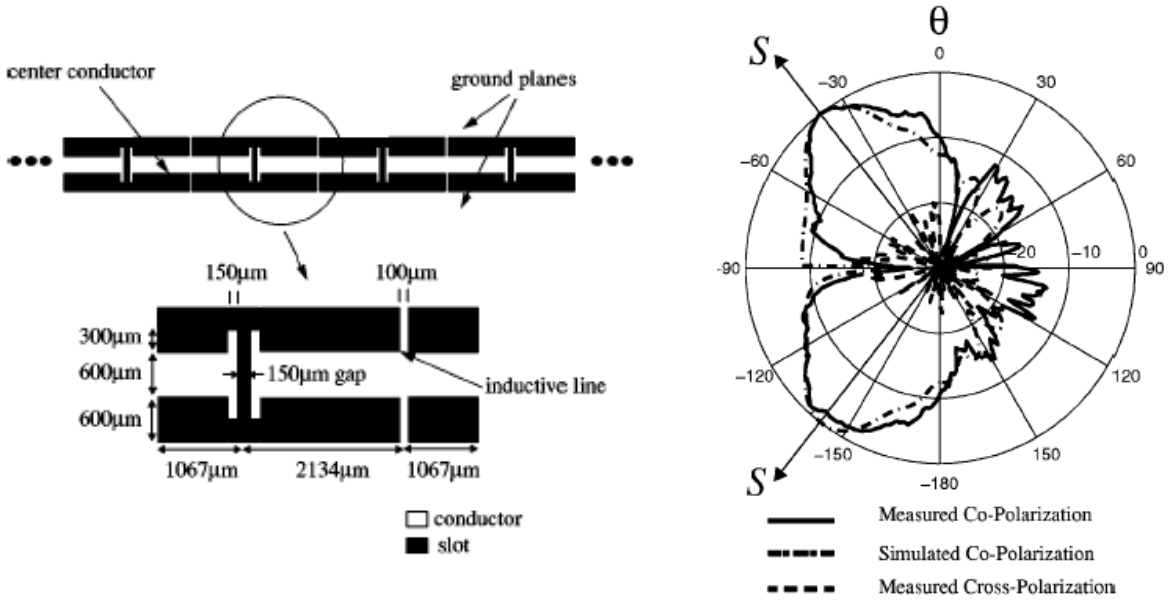

(a) (b)

Figure 56: Backward-wave radiating LHM in coplanar waveguide (from [154]): (a) graphical description (the antenna port is on the left) ; (b) E-plane far-field radiation pattern at 14.6 GHz (plane along the TL).

d) Realization of a TL-LW antenna in microstrip technology [156].

A left-handed TL-LW antenna has been built using microstrip technology, as shown in Figure 57. This structure is a practical implementation of the loaded TL. The structure is designed to be a balanced composite right/left-handed (CRLH) TL. The unit cell is shown in Figure 57 (b). The antenna contains 24 unit cells.

This antenna presents a backfire to endfire scanning capability: backward radiation occurs from 3.1 GHz (backfire: $\theta = -90°$) to 3.9 GHz (broadside: $\theta = 0°$) and forward radiation occurs from 3.9 GHz (broadside: $\theta = 0°$) to 6.3 GHz (endfire: $\theta = 90°$). The measured bandwidth ($VSWR < 2$) is 61 % and the measured gain is larger than 6 dB at all radiation frequencies.

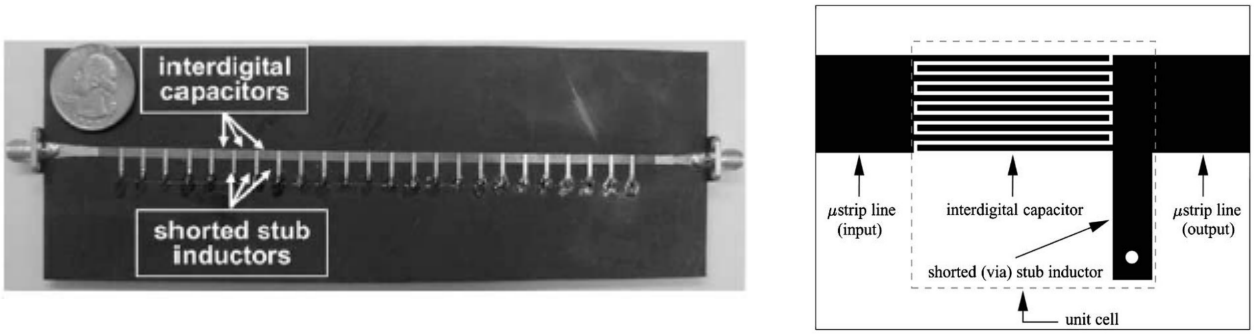

(a) (from [160]) (b) (from [161])

Figure 57: Composite Right/Left-Handed (CRLH) TL-LW antenna: (a) picture of the antenna (one of the two ports has to be loaded with a matched load in order to avoid reflections); (b) unit cell.

Combined with a heterodyne mixing system, this antenna can be used as a leaky-wave reflector, as proposed in [162]. This system has the advantage of using a single antenna (compared with conventional retrodirective reflectors which consist in antenna arrays), and it can scan the entire space (compared with conventional leaky-wave antennas which can only scan a half-space).

An improved version of this system is proposed in [163]. It uses two separate antennas: a patch antenna at reception and the CRLH TL-LW antenna at transmission.

The use of interdigital capacitance allows only small capacitance values; as a result the size of these elements has to be quite large to obtain sufficient values. The use of MIM capacitances in the series branch allows to reduce the size of the unit cell by a factor 2, as described in [164].

A laterally-shielded version of this TL-LW antenna can also be considered, as mentioned at the end of [165].

e) Electronically scanned CRLH microstrip TL-LW antenna [166]-[168].

First concept of conventional LW with scanning the radiated beam at fixed frequency was proposed in [169]. The antenna presented here (Figure 58 (a)) is an improved version of the CRLH TL-LW antenna reported in the prefious paragraph. Varactors are included in the shunt loading elements allowing modulating the propagation constant with an external DC voltage (V_{DC}). The objective is to scan the radiated beam at fixed frequency. With this antenna, continuous scanning is possible at 3.23 GHz over a range of 17.5° (from +7.5° to -10°) by changing V_{DC} from 0 to 35 V. The antenna contains four unit cells for a total length of 0.753 λ_{eff} (guided wavelength), then the ratio between the wavelength and the lattice constant (λ_{eff}/a) is 5.3.

Figure 58 (b) shows how the unit cell of the usual CRLH TL has to be modified to take into account the varactor and the DC feeding system. Figure 58 (c) shows the measured radiation patterns at a fixed frequency of 3.23 GHz for three different values of VDC. The input return loss in these three cases is shown in Figure 58 (d).

At VDC = 0 V, the measured Half-Power BeamWidth (HPBW) is 73° and the measured gain is -6.1 dB. As conventional LW antennas, the HPBW and gain can be improved by simply increasing the length of the line. Full-wave simulations showed that the HPBW decreases from ~70° to ~25° as the number of cells N increases from 4 to 20 cells, and that the gain increases from -4.8 to 5.7 dB as N increases from 4 to 27 cells.

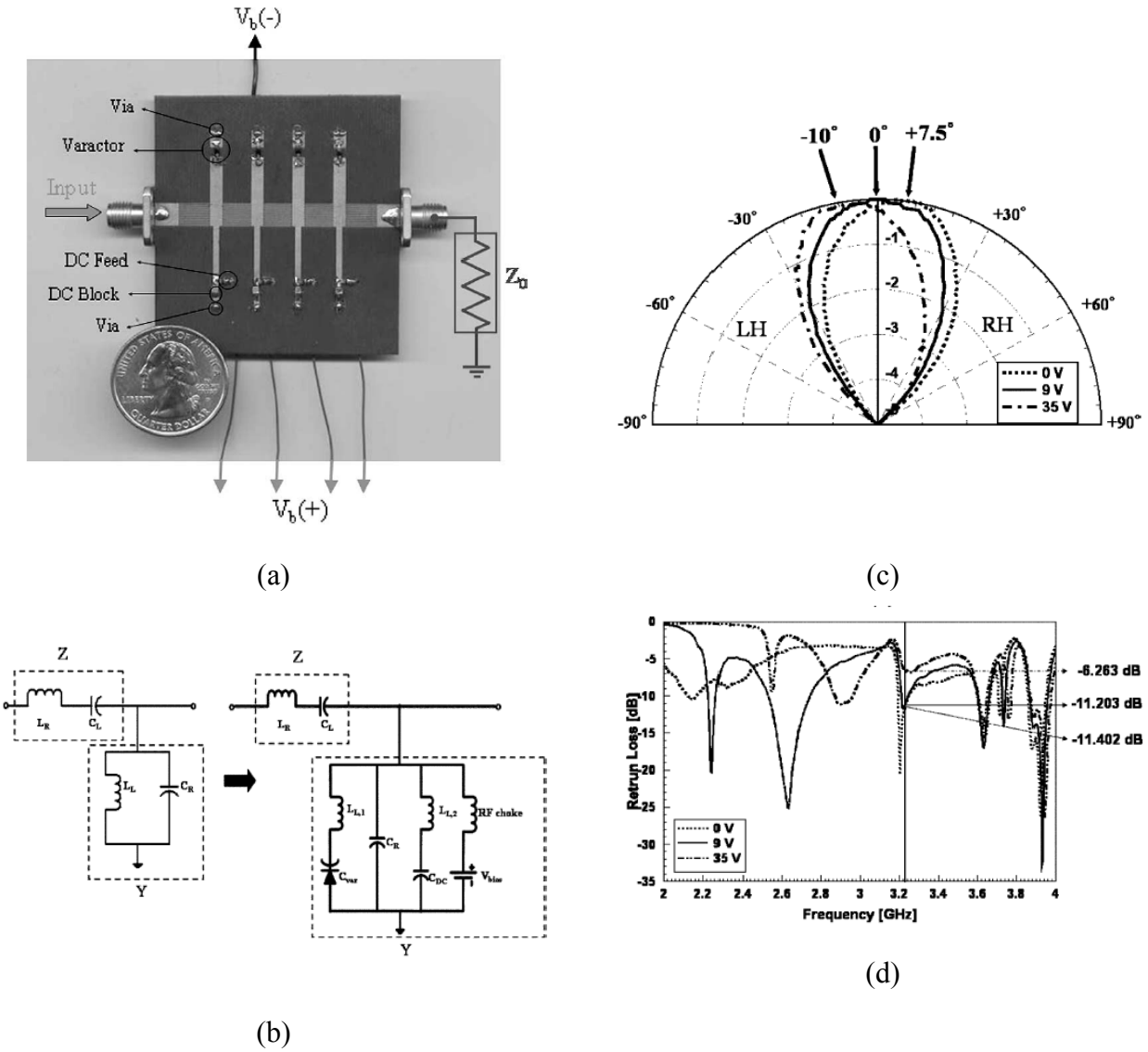

Figure 58: Electronically scanned CRLH microstrip TL-LW antenna (from [166]): (a) picture of the antenna ; (b) model of the unit cell ; (c) measured radiation patterns at 3.23 GHz ; (d) Measured input return loss.

An improved version of this electronically-controlled antenna has been proposed in [167]. The scanning range is improved by introducing series varactor in addition to shunt varactors. The antenna operates at a fixed frequency of 3.1 GHz and exhibits the capability of continuous scanning from backward to forward angles over a range of 77° (from -41° to +36°). The antenna contains six unit cells of length a = 12.3 mm. The ratio λeff/a is 5.8. The measured HPBW varies between 41° and 65° depending on the radiation direction.

Another improved version of this kind of electronically controlled antenna has been reported in [168], where both the radiation angle and the beamwidth can be tuned. This structure also contains both series and shunt varactors. On the one hand, angle scanning at a fixed frequency is achieved by adjusting the uniform bias voltage applied to the varactors. On the other hand, beamwidth tuning is obtained by making the structure non-uniform by applying a non-uniform bias voltage distribution

to the varactors. The antenna (shown in Figure 59) is designed to operate at 3.33 GHz. It contains 30 unit cells of length a = 12 mm (the ratio λ_{eff} /a is 5.6). The total length is 38.34 cm (5.87 λ_{eff}).

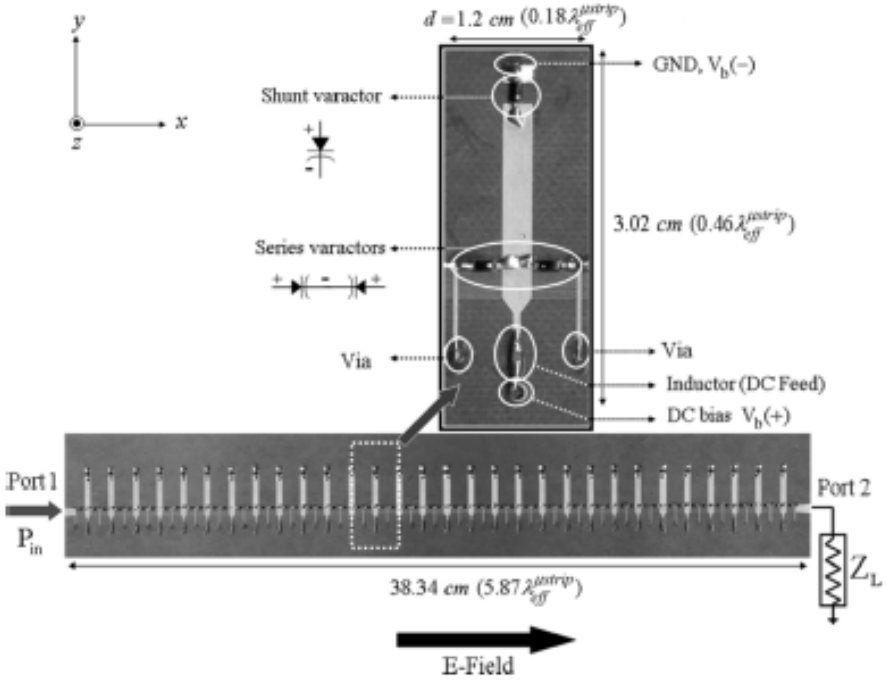

Figure 59: Electronically tuneable CRLH microstrip TL-LW antenna (from [170]).

This antenna exhibits the capability of continuous scanning at a fixed frequency of 3.33 GHz from backward to forward angles over a range of 99° (from -49° to +50°). The HPBW can also be electronically tuned. The maximum gain of this quite long antenna is 18 dB at broadside.

f) Two-dimensional CRLH leaky-wave antenna

Recently, the concept of 1D CRLH leaky-wave antenna has been extended to 2D. It was observed that the CRLH mode cannot be the fundamental mode of the structure [170]. A possible implementation of a 2D CRLH is the mushroom structure, as shown in Figure 60 (a).

This antenna can be either fed in its centre by a single port, resulting into conical beam radiation, or fed in its edges by several ports, allowing full-space scanning.

A first practical implementation has been reported in [172] using a classical mushroom structure (not the interdigital one shown in Figure 60 (a)). A similar structure has been used as an electrically tuneable impedance surface for beam-steering [173]. The antenna contains 19 x 19 unit cells of size 5 x 5 mm (= *a*). It is fed by a single port in its centre and it radiates a cone in the left-handed mode from 9.3 to 10.1 GHz and in the right-handed mode from 11 to 15 GHz (the structure is not balanced, therefore there is a stop band between the LH and the RH band). At the maximum operating frequency of 15 GHz, the ratioλ_0/a is 4.

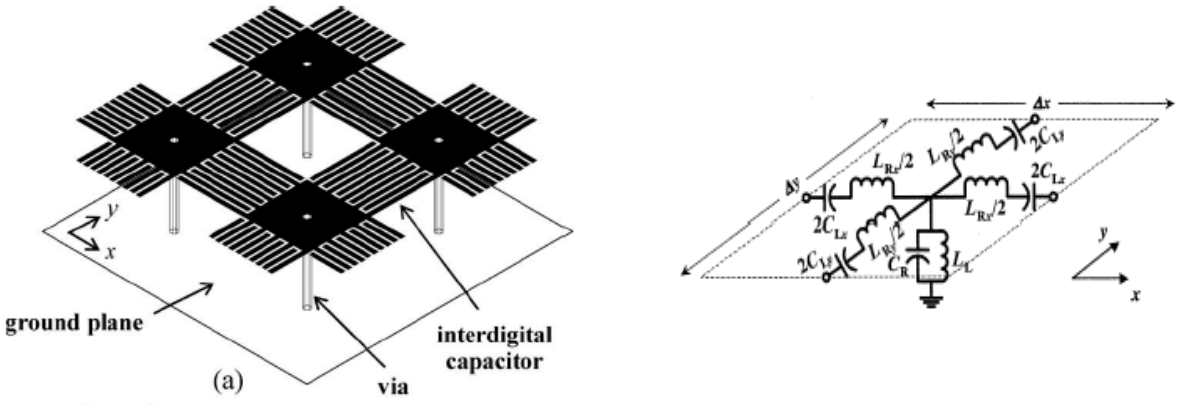

(a) from [160] (b) from [171]

Figure 60: 2D CRLH leaky-wave antenna: (a) capacitively-enhanced mushroom structure; (b) 2D CRLH TL model of the unit cell.

An analytical approach based on the array factor has been proposed in order to calculate in a simple way the radiation pattern of 1D or 2D CRLH leaky-wave antennas [160].

g) Further readings on leaky-waves with LHM

Analytical study of leaky-waves related to LHM:

- An investigation on dispersion and radiation properties of leaky-waves supported by LHM grounded slabs has been presented in [174].
- An analytical analysis of the radiation produced by a travelling wave infinitely-extend sheet of current that is placed at the interface between a conventional lossless dielectric and a lossless LHM has been presented in [174].
- The mathematical solution for Cherenkov radiation of a charged particle in a LHM can be found in [175], for both lossless and lossy situation.

In these works, a macroscopic vision of the LHM has been adopted. It means that the LHM has been considered as a homogeneous isotropic medium with negative permittivity and permeability.

6. *LHM as an antenna substrate or at proximity of a radiating element*

a) Electrically small antenna in a shell of LHM (theoretical study)

Small dipole antennas in free space are inefficient radiators and have large capacitive reactance. A theoretical study on the possibilities of increasing the power radiated by electrically small antennas by using LHM has been reported by Ziolkowski in [176]. The structure under investigation is a small dipole antenna surrounded with a shell of LHM, as suggested in Figure 61 (a). It is supposed here that the LHM is an isotropic non-dispersive medium with simultaneously negative permittivity

and permeability.

The fields generated by an infinitesimal electric dipole in free space were compared to those generated by a dipole embedded in a LHM. It was observed that while the radiated power in both cases was equal, the reactive power in the LHM case was equal in magnitude but opposite in sign to the free space case. This property led the authors to investigate whether the capacitive effect associated with an infinitesimal electric dipole in free space could be matched by an inductive effect associated with a LHM shell surrounding it.

Analytical and numerical results of the proposed structure showed that the radiated power could effectively be increased by orders of magnitude compared with the corresponding free space case. Moreover the reactance decreases by similar orders of magnitude.

A circuit model of the antenna was also proposed (Figure 61 (b)). It illustrates the fact that the LHM shell provides a kind of natural matching network to the antenna.

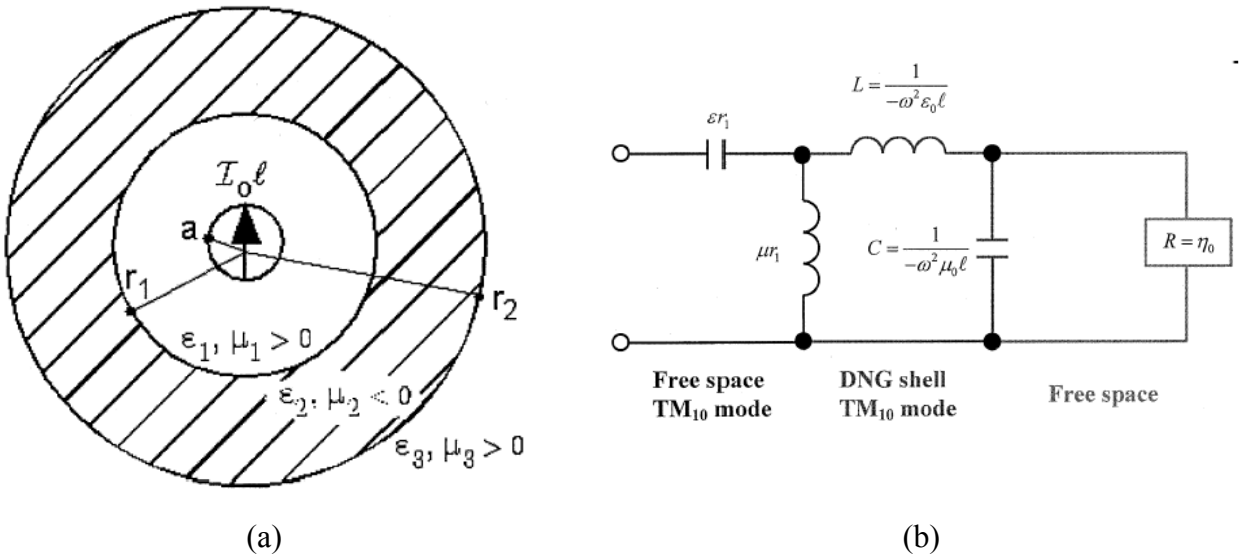

(a) (b)

Figure 61: Small dipole antenna in a LHM shell (from [176]): (a) shape of the structure; (b) equivalent circuit model for this antenna (here, $l = r_2$-r_1).

These results were obtained considering a non-dispersive isotropic LHM, which is something that cannot exist. It is anticipated in [176] that the dispersive nature of LHM will certainly have a negative impact on the dramatically increase of the gain of the dipole LHM-shell antenna, nevertheless the increase of the gain will still be significant.

The realization of this structure would require a fully 3D isotropic LHM. The effect of a more realistic anisotropic LHM on the possible increase of the radiated power has not been considered in this study.

Based on the same idea, another analytical study has been reported in [177]. It is shown that it is possible, in principle, to increase the radiated power of an infinite line source when surrounded by

cylindrical shells of LHM, compared to the case where the line source is surrounded by free-space. The idea to use several concentric shells has also been proposed.

Yet, the results reported in [176] are contested in [178], stating that the authors haven't taken into account gain, matching and efficiency.

b) Miniaturized microstrip annular ring patch antenna

Inspired by the idea of Engheta on a thin sub-wavelength cavity resonator using a sandwich of LHM/RHM slab between two perfect reflectors, a miniaturized annular ring patch antenna on an inhomogeneous substrate with LHM has been studied [179]. The structure is shown in Figure 62. Its substrate contains two parts: an inner ring made of LHM and an outer ring made of conventional material (RHM).

It has been theoretically shown that the resonant frequency of the dominant TM_{110} mode can be made as small as desired by adjusting the thickness of the LHM ring relative to that of the outer ring.

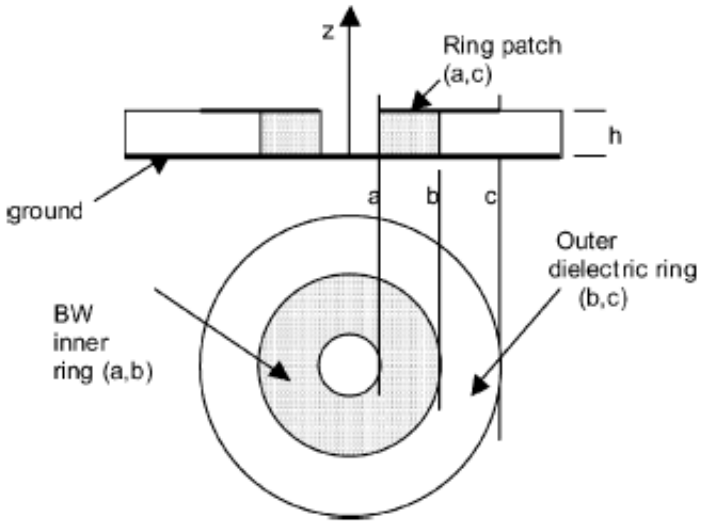

Figure 62: Annular ring patch antenna on an inhomogeneous substrate that contains LHM (in grey) (from [179]).

A design example has also been proposed for a resonant frequency of 1.8 GHz. The outer ring of the substrate is air and the parameters of the inner ring are $\varepsilon_r = -0.5$ and $\mu_r = -1$. The dimensions are $a = 4.2$ mm, $b = 7.5$ mm and $c = 15$ mm. Thus, the outer diameter ($2c$) of the patch corresponds only to 0.18 of a free-space wavelength λ_0. This is to be compared with the diameter $2c = 0.43\ \lambda_0$ for the case when the LHM ring is absent.

An idealized homogeneous isotropic LHM has been considered in this study. The performances of this antenna with a more realistic anisotropic LHM have not been investigated.

c) LHM as super-substrate to enhance dipole antenna performances [180], [181]

A LHM similar to a SRRs/wires medium has been used as super-substrate (substrate that is placed over the antenna) to enhance the performances of a half-wavelength dipole antenna. The unit cell of the LHM is shown in Figure 63(a). The LHM is placed over a dipole antenna as shown in Figure 63 (b). An improved version where two different sizes of unit cells are used in the LHM is shown in Figure 63 (c).

The LHM act as a filter: it has a small passband around 10 GHz and then at this frequency the dipole can radiate through the super-substrate with good performances (high directivity, low back radiation). At other frequencies, the power is essentially reflected by it and high back radiation is obtained.

With the antenna shown in Figure 63 (c) a directivity of 7.3 dB has been obtained at 10.1 GHz (the dipole radiates through the LHM super-substrate). Compared to a conventional dipole (with a directivity about 2 dB) an enhancement of 5.3 dB has been obtained.

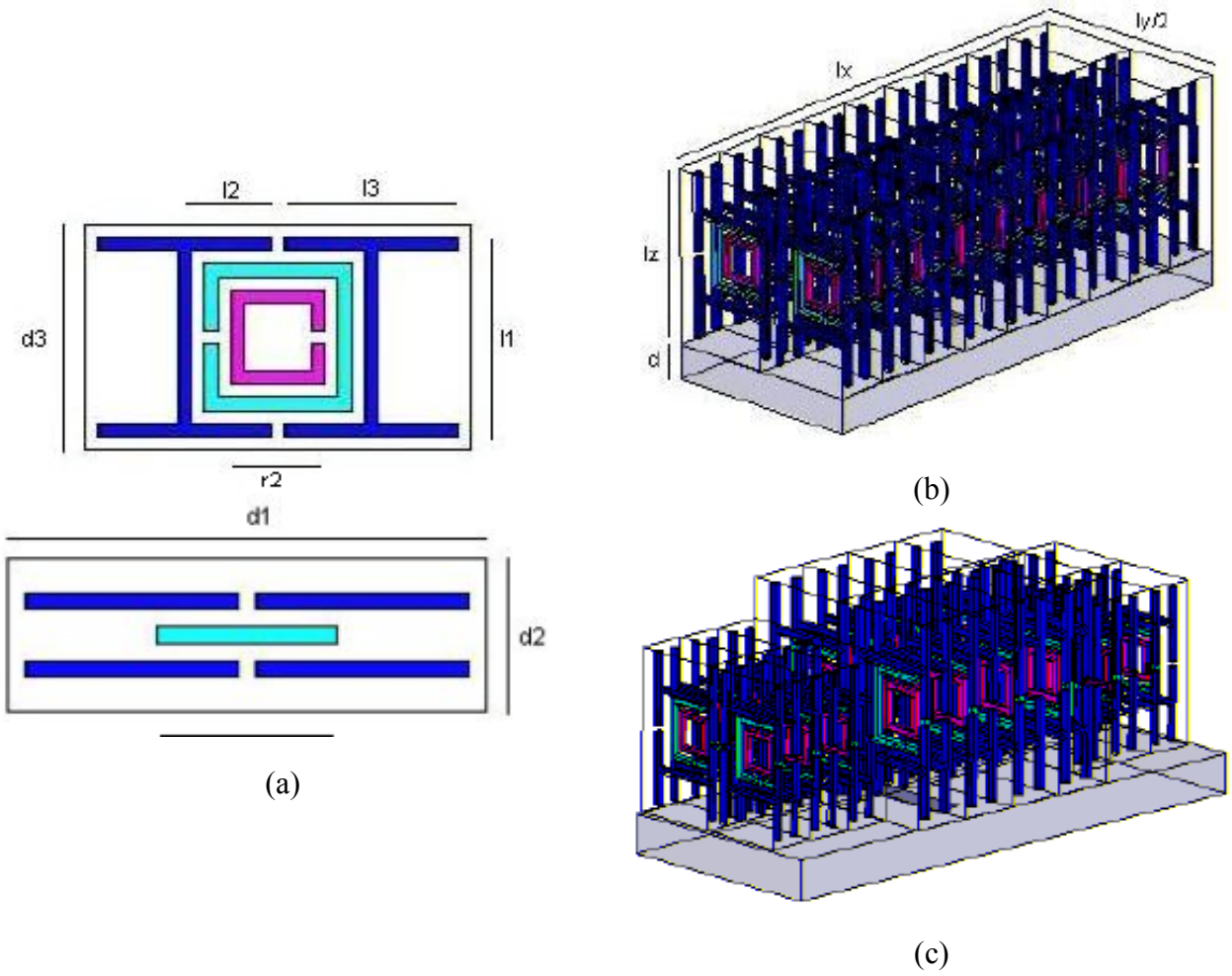

Figure 63: LHM super-substrate over a half-wavelength dipole antenna (from [182]): (a) unit cell ; (b) super-substrate with identical unit cells ; (c) super-substrate with two different sizes of unit-cells (the ones in the middle are slightly bigger). The dipole antenna can be seen under the superstrate.

d) Directive emission from a metamaterial

This application uses a metamaterial which is not directly a LHM (negative refractive index), but more a composite structure that exhibits a very low, but positive, refractive index. This can be achieved with a wire-mesh structure, just above the plasma frequency. A highly directive antenna can be obtained by placing a source inside such a medium, as suggested by the simple geometric image shown in Figure 64 (a). According to Snell's law, if the refractive index is close to zero in the metamaterial the rays in the medium above will be refracted in a direction very close to the normal. Then all the refracted rays will be in almost the same direction around the normal, resulting in a highly directive antenna.

A particular realization of such a structure is proposed in [183]. The metamaterial consists in six planes with a 2D wire-mesh in each plane. The lattice is square with a lattice constant of a = 5.8 mm. The plasma frequency is about 14.5 GHz. The distance between the planes is 6.3 mm. This metamaterial is placed above a ground plane and is excited by a monopole antenna placed between the 3rd and the 4th grid, as shown in Figure 64 (b). The best directivity has been observed at 14.65 GHz (i.e., just above the plasma frequency). The corresponding measured radiation patterns are shown in Figure 64 (c).

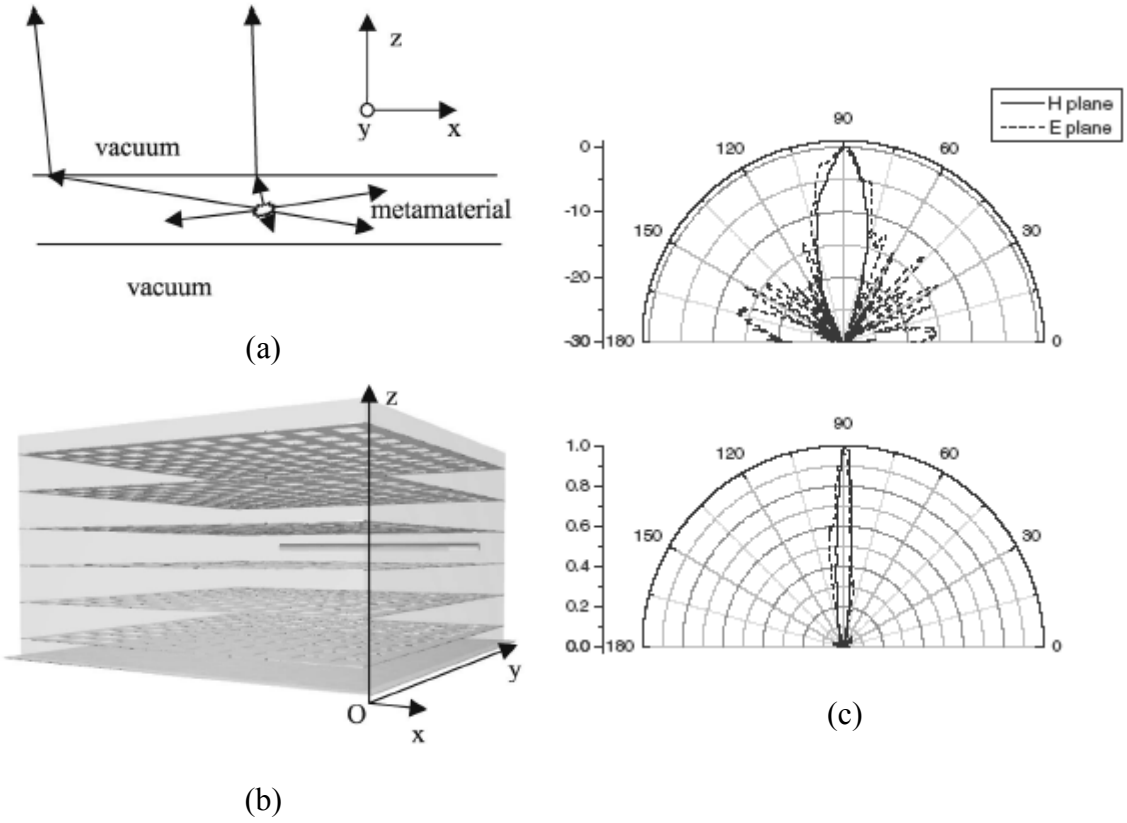

Figure 64: Directive antenna made of metamaterial with close to zero positive refractive index (from [184]): (a) geometrical image ; (b) image of the antenna: 6 grids of wires above a ground plane, excited by a monopole antenna placed between the 3rd and the 4th grid ; (c) measured radiation patterns at 14.65 GHz in log. scale (top) and lin. scale (bottom).

This antenna is effectively highly directive: the half-power beamwidth is about 8.9° in the H-plane and 12.5° in the E-plane. An estimation of the directivity D is 372 ($10\log D = 26$ dB)[3].

Similar results have been reported by the same group in [185], and some comments can be found in [186].

A 1D wire-mesh has also been used as an artificial lens in order to obtain compact directive antennas [187]. More precisely, the antenna is a half-wavelength dipole surrounded by an array of periodically cut wires. The use of cut wires offers the possibility of implementing an electrically controllable antenna, by inserting variable capacitances in the gaps (like varactors).

e) Multilayered structures with LHM as antenna radomes

Multi-layered structures containing LHM and dielectric slabs (RHM) present interesting transmission or reflection properties which are theoretically discussed in [188] (an idealized homogeneous isotropic LHM has been considered). It is proposed that such structures could be advantageously used as antenna radomes.

f) Cancellation of surface waves with a LHM substrate for microstrip antenna

Surface-wave propagation in a LHM grounded slab has been theoretically investigated in [189] (an idealized homogeneous isotropic LHM has been considered). It has been found that a complete suppression of surface waves can be achieved under certain conditions, which depend on the (negative) relative permittivity and permeability of the LHM slab and its height. These results suggest that LHM grounded slabs may find application as novel substrates for microstrip antennas and arrays, aimed at reducing edge diffraction effects due to the finite size of the structure and improving radiation efficiency.

7. Other antenna applications

a) Compact planar microstrip antenna based on a left-handed transmission line

The mushroom structure has been used to realize compact planar patch antennas based on transmission lines (Figure 65) [184], [190]. The structure is essentially a finite left-handed TL whose electrical length determines the resonant frequency of the antenna. It is known that this kind of resonant antenna radiates well at a frequency for which its length l_p corresponds to a half guided wavelength. With CRLH TL, it is possible to obtain a situation where this guided wavelength is

[3] At the operating frequency of 14.65 GHz, the free-space wavelength is only 3.5 times the lattice constant of the grid. Therefore it seems a little ambiguous to speak of an equivalent material for this wire-mesh.

significantly smaller than the free space wavelength, allowing then to obtain very small resonant patch antennas. These structures can be seen as periodically L-C loaded patch antennas.

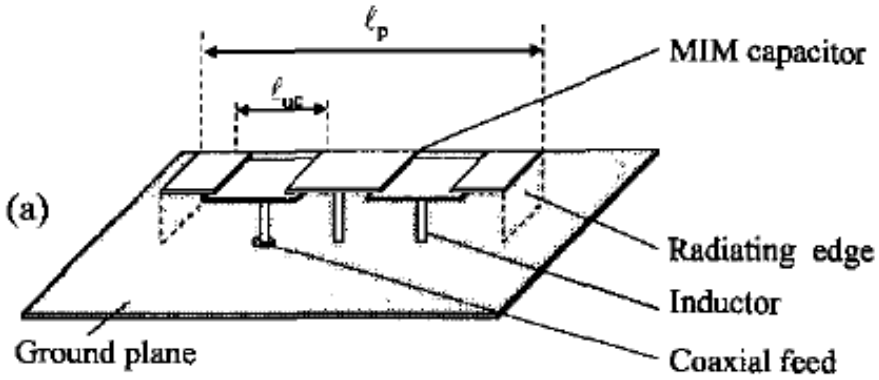

Figure 65: L-C loaded patch antenna based on the mushroom structure (3 unit cells) (from [190]).

A first prototype with four cells has been developed. It is $\lambda_0/6$ long, $\lambda_0/15$ wide and $\lambda_0/60$ high and it operates at the third resonance mode with a -10 dB bandwidth of 1.5 % at 1 GHz.

A second prototype with only two cells has been developed. It is $\lambda_0/40$ long, $\lambda_0/15$ wide and $\lambda_0/40$ high and it operates at the fundamental mode with a -10 dB bandwidth of 1.5 % at 0.5 GHz. For this antenna, the feeding method had to be modified, as explained in [184], [190].

b) Zero-th order resonator antenna [191]

The antenna presented here is based on Zero-th Order Resonators (ZOR). The resonance of such resonators is independent of its physical dimensions. The microstrip based unit cells of the antenna consist in an interdigital capacitor and a shunt meander line connected to a rectangular patch. The rectangular patch behaves as a virtual ground plane. Since resonance is independent of physical dimensions for the ZOR, the size of the antenna can be smaller than a half-wavelength. An example of a four-cell ZOR antenna has been proposed (Figure 66). It is designed to radiate at 4.88 GHz and its total length is 10 mm instead of 20.6 mm for a $\lambda/2$ microstrip patch antenna which operates at the same frequency. More details can be found in [192] and [193].

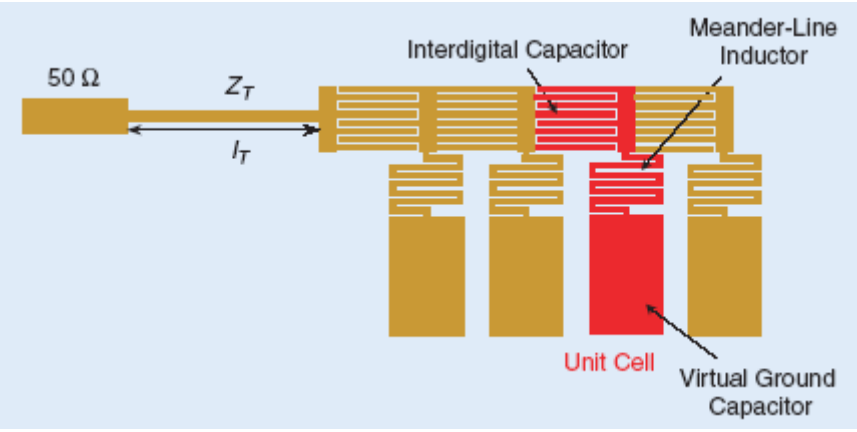

Figure 66: Four-cell zero-th order resonator (ZOR) microstrip antenna (from [191]).

c) Application to antenna feed-networks

The left-handed transmission line approach of LHM allows to build particular phase-shifting lines (as presented in [182]) which can be advantageously used in the feed-network of an antenna array [194]. Such a feed-network has the advantage of being compact, broadband and non-radiating, compared with conventional TL-based feed-networks (TL meander lines), which can be bulky, and narrowband.

d) Anisotropic reflector based on 2D loaded TL networks

Two-dimensional loaded TL networks realized as distributed textured surfaces could also be used as reflectors in antenna applications. With the flexibility offered by the loaded TL approach of metamaterials, it is possible to build anisotropic structures that exhibit a right-handed behaviour in one direction and a left-handed behaviour in another orthogonal direction [195]. Thus, a reflector made with such a structure would have distinct responses for orthogonal linear polarisations.

CONCLUSIONS

In this document, an assessment of the new trends in small terminal antennas was carried out. This included new and future applications as well as promising technological options for antenna implementation. Some practical examples were used to illustrate the different alternatives that may be of use in the future. The whole work was accompanied by an extensive review of the available literature, and of existing lines of research, that could serve as a guide to define new fields of interest.

This report can be used as basis to explore new possibilities in the design of small terminal antennas for future terminals in yet more applications. Indeed, it helps getting a better understanding of the future trends for mobile terminals and their use in a variatey of fields, which range from communications to medicine. Thus, the work carried out to produce this document helped clarify future lines of work, aiming at structuring European research in small antennas for terminals.

REFERENCES

[1] Diallo, A., Luxey, C., Le Thuc, P., Staraj, R. and Kossiavas, G., 'Reduction of the mutual coupling between two planar inverted-F antennas working in close radiocommunication standards', *18th International Conference on Applied Electromagnetics and Communications (IceCom),* Dubrovnik, Croatia, October 2005

[2] Ciais, P., Staraj, R., Kossiavas, G. and Luxey, C., 'Design of an Internal Quad-Band Antenna for Mobile Phones', *IEEE Microwave and Wireless Components Letters*, Vol. 14, no. 4, April 2004, pp. 148-150.

[3] Villanen, J., Suvikunnas, P., Sulonen, K., Ollikainen, J., Icheln, C. and Vainikainen, P., "Advances in Diversity Performance Analysis of Mobile Terminal Antennas", *International Symposium on Antennas and Propagation ISAP 2004*, Sendai, Japan, August 2004, pp. 649-652.

[4] Sharaiha, A., Toureilles, J.M., Terret, C. and Blot, J.P., "Quadrifilar helical antenna with integrated feeding network", Patent N° 96/142, 1985.

[5] Louvigne, J.-C.; Sharaiha, A., "Variable-pitch helical antenna, and corresponding method", Patent N° 20030184496.

[6] Alayon Glazunov, A., "UE antenna efficiency impact on UMTS system coverage/capacity", *R4-030546, 3GPP TSG-RAN Working Group 4 (Radio) meeting #27*, Paris, France 19-23 May, 2003.

[7] Alayon Glazunov, A., "Joint Impact of the Mean Effective Gain and Base Station Smart Antennas on WCDMA-FDD Systems Performance", *The Nordic Radio Symposium NRS 2004*, Oulu, Finland, August 2004.

[8] ACE Network of Excellence, Deliverable 2.2D1, *Report on the State of the Art in Small Terminal Antennas: Technologies. Requirements and Standards.*

[9] "Measurements of Radio Performances for UMTS Terminals in Speech Mode", *R4-040612,3GPP TSG-RAN Working Group 4 (Radio) meeting #3,3* Yokohama, Japan, 15-19 November 2004.

[10] American National Standards Institute (ANSI), *Method of Measurement of Compatibility between Wireless Communication Devices and Hearing Aids, C63.19*, http://www.ansi.org, 2001.

[11] Federal Communications Commission, *Order on Recon and FNPRM*, June 9, 2005, FCC 05-122, WT Docket No. 01-309, http://www.fcc.gov/cgb/dro.

[12] Mulvany, D. and Vickery, R,. "An Analysis of Inductive Coupling and Interference Issues in Digital Wireless Phones. Technically Feasible Solutions", *Hearing Loss Association News*, http://www.shhh.org/html/TC05.html.

[13] European Telecommunications Standards Institute, ETSI EN 300 401, http://www.etsi.org..

[14] European Information & Communications Technology Industry Association (EICTA), *Mobile and Portable DVB-T Radio Access. Part 1: Interface Specification, version 1.0.*

[15] Hannula, P., *Planning parameters for DVB-T portable indoor reception*, Diploma thesis, Espoo, Helsinki University of Technology, February 2004.

[16] Villanen, J., Ollikainen, J., Kivekäs, O. and Vainikainen, P., "Compact Antenna Structures for Mobile Handsets", *58th IEEE Vehicular Technology Conference VTC Fall 2003*, Orlando, Florida, USA, October 6-9, 2003.

[17] Yang, L. and Giannakis, G. B., "Ultra-Wideband Communications-An Idea whose Time has come", *IEEE Signal Processing Magazine*, Vol. 21, Issue 6, November 2004, pp. 26-54.

[18] Federal Communications Commission, *FCC First Report and Order: In the matter of Revision of Part 15 of the Commision's Rules Regarding Ultra-Wideband Transmission Systems, FCC 02-48*, April 2002.

[19] Electronic Communications Committee (ECC), *Final Report by the ECC to the EC in response to the EC Mandate to CEPT to Harmonise radio spectrum use for Ultra-wideband Systems in the European Union*, Europe's Information Society Thematic Portal, http://europa.eu.int/information_society/policy/radio_spectrum/docs/current/mandates/cept_response%20to%20_%20UWB.pdf

[20] Sörgel, W. and Wiesbeck, W., "Influence of the Antennas on the Ultra-Wideband Transmission", *EURASIP Journal on Applied Signal Processing*, Vol. 3, 2005, pp. 296-305.

[21] Sörgel, W., Waldschmidt, C. and Wiesbeck, W., "Transient responses of a vivaldi antenna and a logarithmic periodic dipole array for ultrawideband communication", *IEEE Antennas and Propagation Society Symposium*, Columbus, Ohio, June 2003.

[22] Kunisch, J. and Pamp, J. "UWB radio channel modeling considerations", *International Conference on Electromagnetics in Advanced Applications ICEAA'03*, Turin, September 2003.

[23] Martínez-Vázquez, M., "Small UWB Antenna for Mobile Handsets", *IEEE Antennas and Propagation Society Symposium*, Washington DC (USA), July 2005.

[24] Foschini, G.J. and Gans, M.J., "On Limits of Wireless Communications in a Fading Environment when Using Multiple Antennas", *Wireless Personal Communications*, Vol. 6, No. 3, March 1998, pp. 311-335.

[25] Steyskal, H. and Herd, J.S., "Mutual Coupling Compensation in Small Array Antennas", *IEEE Transactions on Antennas and Propagation*, Vol. 38, No. 12, December 1990, pp. 1971-1975.

[26] Antoniuk, J., Moreira, A. and Peixeiro, C., "Multi-Element Patch Antenna Integration into Laptops for Multi-Standard Applications", *IEEE Antennas and Propagation Society Symposium*, Washington DC, July 2005.

[27] Blanch, S., Romeu, J. and Corbella, J., "Exact representation of antenna system diversity performance from input parameter description", *Electronics Letters*, Vol. 39, No. 9, pp. 705-707, May 2003.

[28] Derneryd, A. and Kristensson, G., "Antenna signal correlation and its relation to the impedance matrix", *Electronics Letters*, Vol. 40, No. 7, April 2004, pp. 705-707.

[29] Fregoli, L. and Peixeiro, C., "Small Multi-band Planar Inverted-F Antenna for Mobile Communication Systems and WLAN/WPAN Applications", *URSI International Symposium on Electromagnetic Theory*, Pisa, Italy, May 2004.

[30] Bolin, T., Derneryd, A., Kristensson, G., Plicanic, V., and Ying, Z., "Two-antenna receive diversity performance in an indoor environment", *Electronics Letters*, Vol. 41, No. 22, October 2005, pp. 1205-1206.

[31] Finkenzeller, K, *RFID Handbook. Fundamentals and Applications in Contactless Smart Cards and Identification,* John Wiley & Sons Inc. Ltd, 2003.

[32] Colpitts B.G., and Boiteau, G., "Harmonic Radar Transceiver Design: Miniature Tags for Insect Tracking", *IEEE Transactions on Antennas and Propagation*, vol. 52, N° 11, November 2004, pp. 2825-2832.

[33] de Moura Presa, E, Zürcher, J.-F. and Skrivervik, A. K,. "A New Microwave Harmonic Direction-Finding System for Localization of Small Mobile Targets using Passive Tags", *Microwave and Optical Technology Letters*, vol. 47, Issue 2, 25 August 2005, pp. 134-137.

[34] Nikitin, P. V., Seshagiri Rao, K. V., Lam, S. F., Pillai, V., Martinez R. and Heinrich, H., "Power Reflection Coefficient Analysis for Complex Impedances in RFID Tag Design", *IEEE Transactions on Microwave Theory and Techniques*, vol. 53, N° 9, September 2005, pp. 2721-2725.

[35] Foster, P.R. and Burberry, R.A., "Antenna Problems in RFID Systems", *IEE Colloquium on RFID Technology,* London, UK, October 1999, pp. 3/1-3/5.

[36] Nikitin, P.V., Lam, S. and Rao, K.V.S., "Low Cost Silver Ink RFID Tag Antennas", *IEEE Antennas and Propagation Society Symposium*, Washington DC, 3-8 July 2005.

[37] Ukkonen, L., Engels, D., Sydänheimo, L. and Kivikoski, M., "Folded Microstrip Patch Antenna for RFID Tagging of Objects Containing Metallic Foil", *IEEE Antennas and Propagation Society Symposium*, Washington DC, 3-8 July 2005.

[38] Son, H.-W. and Pyo, C.–S., "Design of RFID Tag Antennas using an Inductively Coupled Feed", *Electronics Letters*, vol. 41, N°18, 2005, pp. 994-996.

[39] Cho, C., Choo H. and Park, I., "Broadband RFID Tag Antenna with Quasi-Isotropic Radiation Pattern", *Electronics Letters*, vol. 41, N°20, September 2005, pp. 1091-1092.

[40] Scheele, P., Tomescu, V., Giere, A., Mueller, S. and Jakoby, R., "Passive Ferroelectric Phase Modulators for RFID Backscatter Transponders", *35th European Microwave Conference*, Paris, 2005, pp. 645-648.

[41] Siwiak, K. *Radiowave Propagation and Antennas for Personnal Communications*. Second Edition. Norwood, MA: Artech House, 1998.

[42] McLean, J.S., *The Radiative properties of Electrically-Small Antennas,* IEEE Press, Wisconsin-Madison, 1994.

[43] Chu, L.J., “Physical Limitations of omni-directional Antennas", *Journal of Applied Physics*, 1948, Vol. 19, pp. 1163-1175.

[44] McLean, J.S., “A Re-examination of the Fundamental Limits on the Radiation Q of Electrically Small Antennas", *IEEE Transactions on Antennas and Propagation* , Vol 44, May 1996, pp. 672-676.

[45] Thiele, G.A., Detweiler, P.L., Penno, R.P., "On the Lower Bound of the Radiation Q for Electrically Small Antennas". *IEEE Transactions on Antennas and Propagation* Vol 51, pp. 1263-1269.

[46] Jofre, L., Cetiner, B.A. and De Flaviis, F., "Miniature Multi-Element Antenna for Wireles Communications". *IEEE Transactions on Antennas and Propagation* Vol. 50, May 2002, pp 658-669.

[47] Serkan Basat, S., Lim, K., Laskar, J. and Tentzeris, M., "Design and Modeling of Embedded 13.56 MHz RFID Antennas", *IEEE Antennas and Propagation Society Symposium*, Washington DC, 3-8 July 2005.

[48] Pozar D.M., Kaufman, B., "Comparison of Three Methods for the Measurement of Printed Antenna Efficiency". *IEEE Transactions on Antennas and Propagation* Vol 36, January 1988, pp 136-139.

[49] Ritamäki, M., Ruhanen, A., Kukko, V., Miettinen, J. and Turner, L.H., "Contactless Radiation Pattern Measurement Method for UHF RFID Transponders", *Electronics Letters*, vol. 41, N°13, June 2005, pp. 723-724.

[50] Lalis, S., Savidis, A. and Stephanidis, C., "Wearable Systems for Everyday Use", *ERCIM News* no 52, http://www.ercim.org/publication/Ercim_News/enw52/lalis.html, January 2003.

[51] http://www.sintef.com

[52] Nechayev, Y., Hall, P. Constantinou, C.C., Hao, Y., Owadally, A. and Parini, C.G., "Path loss measurements of on-body propagation channels", *International Symposium on Antennas and Propagation ISAP 2004*, Sendai, Japan, 2004, pp. 745-748.

[53] Alomainy, A., Hao, Y., Parini, C.G. and Hall, P.S., "Comparison Between Two Different Antennas for UWB On-Body Propagation Measurements", *IEEE Antennas and Wireless Propagation Letters*, vol. 4, 2005, pp. 31-34.

[54] Kamarudin, M.R., Nechayev, Y.I. and Hall, P. S., "Performance of Antennas in the On-Body Environment", *IEEE Antennas and Propagation Society Symposium*, Washington DC, 3-8 July 2005.

[55] "When technology gets personal", *BBC News Online*, http://news.bbc.co.uk/go/pr/fr/-/2/hi/technology/4059011.stm, December 2004.

[56] See, T. S. P. and Chen, T. N. "Effects of Human Body on Performance of Wearable PIFAs and RF Transmission", *IEEE Antennas and Propagation Society Symposium*, Washington DC, 3-8 July 2005.

[57] Yang, T., Davis, W.A. and Stutzman, W.L., "Wearable Ultra-Wideband Half-Disk Antennas", *IEEE Antennas and Propagation Society Symposium*, Washington DC, 3-8 July 2005.

[58] Salonen, P., Kim, J. and Rahmat-Samii, Y., "Dual-Band E-Shaped Wearable Textile Antenna", *IEEE Antennas and Propagation Society Symposium*, Washington DC, 3-8 July 2005.

[59] Durney, C.H., "Antennas and other electromagnetic applicators in biology and medicine", *Proceedings of the IEEE,* Vol. 80, N°1, January 1992, pp. 194-199.

[60] Johansson, A., *"Wireless Communication with Medical Implants"*, PhD thesis, 2005, Lund University, htt.p://www.es.lth.se

[61] Jaehoon Kim and Rahmat-Samii, Y., "Implanted Antennas Inside a Human Body: Simulations, Designs, and Characterizations", *IEEE Transactions on Microwave Theory and Techniques*, Vol 52, No 8, August 2004, pp. 1934-1943.

[62] *Popular Science Magazine*, Vol 263, #3, 2005

[63] R. Mackay, "Bio-Medical Telemetry", IEEE Press, ISBN 0-7803-4718-8

[64] Scanlon, W.G. Burns, J.B. and Evans, N.E., "Radiowave Propagation from a Tissue-Implanted, Source at 418 MHz and 916.5 MHz", *IEEE Transactions on Biomedical Engineering*, Vol. 47, No. 4, April 2000.

[65] Martin, G., Berthelot, P., Masson, J., Daniau, W., Blondeau-Patissier, V., Guichardaz, B. and Ballandras, S., "Measuring the Inner Body Temperature Using a Wireless Tempreature SAW-Sensor-Based System", *Proceedings of the Ultrasonics Symposium,* Rotterdam, 2005.

[66] Given Imaging, http://www.givenimaging.com/Cultures/en-US/Given/English/Professionals

[67] European Telecommunications Standards Institute, *ETSI EN 301 839-1*, http://www.etsi.org.

[68] Federal Communications Commission, *FCC 47 CFR 95.601-95.673 Subpart E*, http://www.fcc.gov

[69] Yun, X., Fear, E.C. and Johnston, R.H., "Compact Antenna for Radar-Based Breast Cancer Detection", *IEEE Transactions on Microwave Theory and Techniques*, vol. 53, N°8, August 2005, pp. 2374-2380.

[70] Kim, J. and Rahmat-Samii, Y., "Implanted Antennas Inside a Human Body: Simulations, Designs, and Characterizations", *IEEE Transactions on Microwave Theory and Techniques*, vol. 52, N°8, August 2004, pp. 1934-1943.

[71] Gosalia, K., Humayun, M.S. and Lazzi, G., "Impedance Matching and Implmentation of Planar Space-Filling Dipoles as Intraocular Implanted Antennas in a Retinal Prostesis", *IEEE Transactions on Microwave Theory and Techniques*, vol. 53, N°8, August 2005, pp. 2365-2373.

[72] Simons R.N. and Miranda, F.A., "Radiation Characteristics of Miniature Silicon Square Spiral Chip Antenna for Implatable Bio-MEMS Sensors", *IEEE Antennas and Propagation Society Symposium*, Washington DC, 3-8 July 2005.

[73] Saito, K., Yoshimura, H., Ito, K., Aoyagi Y. and Horita, H., "Clinical Trials of Interstitial Microwave Hyperthermia by Use of Coaxial-Slot Antenna with Two Slots", *IEEE Transactions on Microwave Theory and Techniques*, vol. 52, N°8, August 2004, pp. 1987-1991.

[74] Zwick, T., Fischer, C., Wiesbeck, W., "A Stochastic Multipath Channel Model Including Path Directions for Indoor Environments", *IEEE Journal on Selected Areas in Communications*, vol. 20, no. 6, August 2002, pp. 1178-1192.

[75] Waldschmidt, C., Fügen, T., Wiesbeck, W., "Spiral and Dipole Antennas for Indoor MIMO Systems", *IEEE Antennas and Wireless Propagation Letters*, vol. 1, 2002, pp. 176-178.

[76] Maurer, J., Knörzer, S., Wiesbeck, W., "Ray Tracing in Rich Scattering Environments for Mobile-to-Mobile Links", *International Conference on Electromagnetics in Advanced Applications ICEAA'05*, September 2005, pp. 1073-1076.

[77] Maurer, J., Waldschmidt, C., Kayser, T., Wiesbeck, W. "Characterisation of the time-dependent urban MIMO channel in FDD communication systems", *IEEE Vehicular Technology Conference VTC-Spring*, April 2003, pp. 544-548.

[78] Suvikunnas, P., Sulonen, K., Villanen, J., Icheln, C., Vainikainen, P., "Evaluation of performance of multi-antenna terminals using two approaches", *IEEE Instrumentation and Measurement Technology Conference IMTC'04*, Como, Italy, May 2004.

[79] Kalliola, K., Laitinen, H., Vaskelainen, L. and Vainikainen, P., "Real-time 3-D spatial-temporal dual-polarized measurement of wideband radio channel at mobile station", *IEEE Transactions on Instrumentation and Measurements*, vol. 49, 2000, pp. 439-448,.

[80] Kivinen, J., Suvikunnas, P., Perez, D., Herrero, C., Kalliola, K., Vainikainen, P., "Characterization system for MIMO channels", *4th International Symposium on Wireless Personal Multimedia Communications*, September 2001, pp. 159-162.

[81] Zhao J. and Raman, S. "Design of "Chip-Scale" Patch Antennas for 5-6 GHz Wireless Microsystems", *IEEE Antennas and Propagation Society Symposium*, Washington DC, 8-13 July 2001.

[82] Kuo, S.-W., Lin C.-C. and Chuang, H.-R., "A 2.4 GHz CMOS RFIC-on-Chip Antenna for RFID Application", *IEEE Antennas and Propagation Society Symposium*, Washington DC, 3-8 July 2005.

[83] Touati, F. And Pons, M., "On-Chip Integration of Dipole Antenna and VCO using Standard BiCMOS Technology for 10 GHz Applications", *29th Euopean Solid-State Circuits Conference*, 16-18 September 2003.

[84] Kim, K. and Kenneth, K. O., "Integrated Dipole Antennas on Silicon Substrates for Intra-Chip Communication", *IEEE Antennas and Propagation Society Symposium*, Vol.3, Orlando, FL, 11-16 July 1999, pp. 1582-1585.

[85] Seok, E. and Kenneth, K.O., " The Impact of Power Grid to the Performance of On-Chip Antennas", *IEEE Antennas and Propagation Society Symposium*, Washington DC, 3-8 July 2005.

[86] Nitta, M. and Kikkawa, T., "Interference of Digital Noise with Integrated Dipole Antenna for Inter-Chip Signal Transmission in ULSI", *IEEE Antennas and Propagation Society Symposium*, Washington DC, 3-8 July 2005.

[87] Kimoto, K. and Kikkawa, T., "Data Transmission Characteristics of Integrated Linear Dipole Antennas for UWB Communication in Si ULSI", *IEEE Antennas and Propagation Society Symposium*, Washington DC, 3-8 July 2005.

[88] Song, C.T.P., Hall, P.S., Ghafouri-Shiraz, H. and Wake, D., "Packaging Technique for Gain Enhancement of Electrically Small Antenna Designed on Gallium Arsenide", *Electronics Letters*, Vol. 36, 31st August 2000, pp. 1524-1525.

[89] Zhang, Y.P., "Integrated Circuit Ceramic Ball Grid Array Package Antenna", *IEEE Transaction on Antennas and Propagation*, Vol. 52, N°10, October 2004.

[90] Aberle, J.T., Zavosha, F. and Auckland, D.T.,."Reconfigurable Antenna Pushes MEMs Performance Specs", *EE Times,* http://www.commsdesign.com/story/OEG20011205S0052, December 5, 2001.

[91] Corey, L., "Phased Array Development at DARPA", *IEEE Int. Symposium On Phased Array Systems and Technology*, Boston, 2003.

[92] Schobel, J., Buck, T., Reimann, M., Ulm, M., Schneider, M., "W-band RF-MEMS subsystems for smart antennas in automotive radar sensors", *34th European Microwave Conference*, Vol 3, 11-15 October 2004, pp. 1305-1308.

[93] Sievenpiper, D., Song, H.J., Hsu, H.P., Tangonan, G., Loo, R.Y., Schaffner, J., "MEMS-based switched diversity antenna at 2.3 GHz for automotive applications", *5th International Symposium on Wireless Personal Multimedia Communications*, Vol 2, 27-30 October 2002, pp. 762-765.

[94] Cetiner, B.A., Jafarkhani, H., Jiang-Yuan Qian, Hui Jae Yoo, Grau, A., De Flaviis, F., "Multifunctional reconfigurable MEMS integrated antennas for adaptive MIMO systems", *IEEE Communications Magazine*, Vol. 42, Issue 12, December 2004, pp. 62-70.

[95] ACE Network of Excellence, Deliverable 2.1D3, *Report on facilities assessment*, Chapter 5.

[96] Hajimiri, A., Komijani, A., Natarajan, A., Chunara, R., Guan, X. and Hashemi, H., "Phased Array Systems in Silicon", *IEEE Communications Magazine*, vol. 42, August 2004, pp. 122-130.

[97] Sagkol, H., Topalli, K., Unlu, M., Civi, O.A., Koc, S., Demir, S., Akin, T., "A monolithic phased array with RF MEMS technology", *IEEE Antennas and Propagation Society Symposium*, Vol 4, 16-21 June 2002, pp. 760-763.

[98] Sabet, K.F., Katehi, L.P.B., Sarabandi, K., "Modeling and design of MEMS-based reconfligurable antenna arrays", *IEEE Aerospace Conference*, Vol. 2, 8-15 March 2003, pp. 2_1135-2_1141.

[99] Ferrero, F., Luxey, C., Jacquemod, G., Staraj, R., Kossiavas G., and Fusco, V., "Reconfigirable Phased-Arrays Based on Hybrid Couplers in Reflection mode", *International Symposium on Antenna Technology and Applied Electromagnetism (ANTEM)*, Saint-Malo, 15-17 June 2005.

[100] Kivekäs, O., Ollikainen, J. and Vainikainen, P., "Frequency-Tunable Internal Antenna for Mobile Phones", *13èmes Journées Internationales de Nice sur les Antennas JINA 2002*, Nice, 12-14 November 2002.

[101] Panaïa, P., Luxey, C., Jacquemod, G., Staraj, R., Kossiavas, G. and Dussopt, L., "Multistandard PIFA Antenna", *International Symposium on Antenna Technology and Applied Electromagnetism (ANTEM)*, Saint-Malo 15-17 June 2005.

[102] L. Le Garrec, I. Roch-Jeune, M. Himdi, R. Sauleau, O. Millet, L. Buchaillot, "Microactuators and microstrip antenna for polarisation diversity" *5th Workshop on MEMS for millimeterWAVE communications (MEMSWAVE), Uppsala (Sweden)*, 30 June-2 July 2004.

[103] Schaffner, J.H., Sievenpiper, D.F., Loo, R.Y., Lee, J.J., Livingston, S.W., "A wideband beam switching antenna using RF MEMS switches", *IEEE Antennas and Propagation Society Symposium*, Vol 3, 8-13 July 2001, pp. 658-661.

[104] Legay, H., Pinte, B., Charrier, M., Ziaei, A., Girard, E., Gillard, R., "A steerable reflectarray antenna with MEMS controls", *IEEE International Symposium on Phased Array Systems and Technology*, 14-17 October 2003, pp. 494-499.

[105] Laheurte, J-M., "A switchable CPW-fed slot antenna for multifrequency operation", *Electronics letters*, Vol.37, 2001, pp. 1498-1500.

[106] Luxey, C., Dussopt, D., Le Sonn, J., Laheurte, J., "Dual frequency operation of a CPW fed antena controlled by PIN diodes", *Electronics letters*, Vol.36, 2000, pp. 2-3.

[107] Pioch, S., Adellan, N., Laheurte, J.M., Blondy, P., Pothier, A., "Integration of MEMS in Frequency-Tuneable Cavity-Backed Slot Antennas", *JINA 2002*, Nice, November 2002

[108] Rose, J., Roy, L., Tait, N., "Development of a MEMS microwave switch and application to adaptive integrated antennas", *IEEE Canadian Conference on Electrical and Computer Engineering CCECE*, Vol. 3, 4-7 May 2003, pp. 1901-1904.

[109] Weedon, W.H., Payne, W.J., Rebeiz, G.M., "MEMS-switched reconfigurable antennas", *IEEE Antennas and Propagation Society International Symposium*, Vol. 3, 8-13 July 2001, pp. 654-657.

[110] Simons, R.N., Donghoon Chun; Katehi, L.P.B., "Reconfigurable array antenna using microelectromechanical systems (MEMS) actuators", *IEEE Antennas and Propagation Society Symposium*, Vol. 3, 8-13 July 2001, pp. 674-677.

[111] Le Garrec, L., Himdi, M., Sauleau, R., Mazenq, L., Grenier, K., Plana, R., "CPW-fed slot microstrip MEMS-based reconfigurable arrays", *IEEE Antennas and Propagation Society Symposium*, Vol. 2, 20-25 June 2004, pp. 1835-1838.

[112] Weedon, W.H., Payne, W.J., Rebeiz, G.M., Herd J.S. and Champion, M., "MEMS-Switched Reconfigurable Multi-Band Antenna: Design and Modeling", *Antenna Applications Symposium*, Monticello, IL, 15-17 September, 1999.

[113] Petit, L., Panaïa, P., Luxey, C., Jacquemod, G., Staraj, R., Dussopt L. and Laheurte J.-M., "MEMS-Switched Reconfigurable Antennas", *MEMSWAVE 2005 Conference*, Lausanne, 23-24 June 2005.

[114] Cetiner, B.A., Jafarkhani, H., Jiang-Yuan Qian, Hui Jae Yoo, Grau, A., De Flaviis, F., "Multifunctional reconfigurable MEMS integrated antennas for adaptive MIMO systems", *IEEE Communications Magazine*, Vol. 42, Issue 12, December 2004, pp. 62-70.

[115] Jung-Chih Chiao, Yiton Fu, Iao Mak Chio, DeLisio, M., Lih-Yuan Lin, "MEMS reconfigurable Vee antenna", *IEEE MTT-S International Microwave Symposium*, Vol. 4, 13-19 June 1999, pp. 1515-1518.

[116] Cho, Y.H., Ha, M.-L., Choi, W., Pyo, C., Kwon, Y.-S., "Floating-patch MEMS antennas on HRS substrate for millimetre-wave applications", *Electronics Letters*, Vol. 41, Issue 1, 6 January 2005, pp. 5-6.

[117] Anagnostou, D., Chryssomallis, M.T., Lyke, J.C., Christodoulou, C.G., "Re-configurable Sierpinski gasket antenna using RF-MEMS switches", *IEEE Antennas and Propagation Society Symposium*, Vol. 1, 22-27 June 2003, pp. 375-378.

[118] Simons, R.N., Donghoon Chun; Katehi, L.P.B., "Polarisation reconfigurable patch antenna using microelectromechanical systems (MEMS) actuators", *IEEE Antennas and Propagation Society Symposium*, Vol. 2, 16-21 June 2002, pp. 6-9.

[119] Simons, R.N., Donghoon Chun; Katehi, L.P.B., "Microelectromechanical systems (MEMS) actuators for antenna reconfigurability", *2001 IEEE MTT-S International Microwave Symposium*, Vol. 1, 20-25 May 2001, pp. 215-218.

[120] Rose, J., Roy, L., Tait, N., "Development of a MEMS microwave switch and application to adaptive integrated antennas", *IEEE Canadian Conference on Electrical and Computer Engineering CCECE 2003*, 2003. Vol. 3, 4-7 May 2003, pp. 1901-1904.

[121] Onat, S., Alatan, L., Demir, S., "Design of triple-band reconfigurable microstrip antenna employing RF-MEMS switches", *IEEE Antennas and Propagation Society Symp*osium, Vol. 2, 20-25 June 2004, pp. 1812-1815.

[122] Le Garrec, L. Himdi, M. Sauleau, R., "Antenne imprimée agile en fréquence à très large excursion continue ou discrète", french patent FR0307842.

[123] Skrivervik, A.K., Crespo-Valero, P., "MEMS in antennas", *MEMSWAVE 2005 Conference*, Lausanne, 23-24 June 2005, pp. 25-30.

[124] Sihvola, A., "Electromagnetic Emergence in Metamaterials", *NATO Advanced Workshop on Bianisotropics - 9th International Conference on Electromagnetics of Complex Media*, Marrakesh, Morocco, 2002.

[125] Veselago, V. G., "The Electrodynamics of Substances with Simultaneously Negative Values of epsilon and mu.", *Soviet Physics Uspekhi*, vol. 10, 1968, pp. 509-514.

[126] McCall, M. W. Lakhtakia, A. and Weiglhofer, W. S., "The negative index of refraction demystified", *European Journal of Physics*, vol. 23, 2002, pp. 353-359.

[127] Pendry, J. B. Holden, A. J. Stewart, W. J. and Youngs, I., "Extremely Low Frequency Plasmons in Metallic Mesostructures", *Physical Review Letters*, vol. 76, 1996, pp. 4773-4776.

[128] Pendry, J. B., Holden, A. J., Robbins, D. J. and Stewart, W. J., "Low frequency plasmons in thin-wire structures", *J. Phys.: Condens. Matter*, vol. 10, 1998, pp. 4785-4809.

[129] Belov, P. A., Marqués, R., Maslovski, S. I. Nefedov, I. S. Silveirinha, M. Simovski, C. R. and Tretyakov, S. A., "Strong spatial dispersion in wire media in the very large wavelength limit", *Physical Review B*, vol. 67, 2003, pp. 113103.

[130] Gay-Balmaz, P., Maccio, C. and Martin, O. J. F., "Microwire arrays with plasmonic response at microwave frequencies", *Applied Physics Letters*, vol. 81, 2002, pp. 2896-2898.

[131] Maslovski, S. I., Tretyakov, S.A., and Belov, P. A., "Wire media with negative effective permittivity: a quasi-static model", *Microwave and Optical Technology Letters*, vol. 35, 2002, pp. 47-51.

[132] Pitarke, J. M., Garcia-Vidal, F. J. and Pendry, J. B., "Effective electronic response of a system of metallic cylinders", *Physical Review B*, vol. 57, 1998, pp. 15261-15266.

[133] Smith, D. R., Vier, D. C., Padilla, W., Nemat-Nasser, S. C. and Schultz, S., "Loop-wire medium for investigating plasmons at microwave frequencies", *Applied Physics Letters*, vol. 75, 1999, pp. 1425-1427.

[134] Sievenpiper, D. F., Sickmiller, M. E. and Yablonovitch, E., "3D Wire Mesh Photonic Crystals", *Physical Review Letters*, vol. 76, 1996, pp. 2480-2483.

[135] Marqués, R., Martel, J,. Mesa, F. and Medina, F., "Left-Handed-Media Simulation and Transmission of EM Waves in Sub-wavelength Split-Ring-Resonator-Loaded Metallic Waveguides", *Physical Review Letters*, vol. 89, 2002, pp. 183901.

[136] Marqués, R., Medina, F., Mesa, F. and Martel, J., "On the electromagnetic modelling of Left-handed metamaterials", *NATO Advanced Workshop on Bianisotropics 2002-9th International Conference on Electromagnetics of Complex Media*, Marrakesh, Morocco, 2002.

[137] Pendry, J. B., Holden, A. J., Robbins, D. J. and Stewart, W. J., "Magnetism from Conductors and Enhanced Nonlinear Phenomena", *IEEE Transactions on Microwave Theory and Techniques*, vol. 47, p, 1999p. 2075-2084.

[138] Zhang, F., Zhao, Q., Liu, Y., Luo, C. and Zhao, X., "Behaviour of Hexagonal Split Ring Resonators and Left-Handed Metamaterials", *Chinese Phyics. Letters,* vol. 21, 2004, pp. 1330-1332.

[139] Marqués, R., Medina, F. and Rafii-El-Idrissi, R., "Role of bianisotropy in negative permeability and left-handed metamaterials", *Physical Review B*, vol. 65, 2001, pp. 144440.

[140] Marqués, R., Mesa, F., Martel, J. and Medina, F., "Comparative Analysis of Edge- and Broadside-Coupled Split Ring Resonators for Metamaterial Design-Theory and Experiments", *IEEE Transactions on Antennas and Propagation*, vol. 51, 2003, pp. 2572-2581.

[141] Katsarakis, N., Koschny, T., Kafesaki, M., Economou, E. N. and Soukoulis, C. M., "Electric coupling to the magnetic resonance of split ring resonators", *Applied Physics Letters*, vol. 84, 2004, pp. 2943-2945.

[142] Baena, J. D., Marqués, R., Medina, F. and Martel, J., "Artificial magnetic metamaterial design by using spiral resonators", *Physical Review B*, vol. 69, 2004, pp. 014402.

[143] Pendry, J. B. and O'Brien, S., "Magnetic activity at infrared frequencies in structured metallic photonic crystals", *Journal Phys.: Condens. Matter*, vol. 14, pp. 6383-6394, 2002.

[144] Yen, T. J., Padilla, W. J., Fang, N., Vier, D. C., Smith, D. R., Pendry, J. B., Basov, D. N. and Zhang, X., "Terahertz Magnetic Response from Artificial Materials", *Science*, vol. 303, 2004, pp. 1494-1496.

[145] Linden, S., Enkrich, C., Wegener, M,. Zhou, J., Koschny, T. and Soukoulis, C.M., "Magnetic Response of Metamaterials at 100 Terahertz", *Science*, vol. 306, 2004, pp. 1351-1353.

[146] Hsu, A.-C., Cheng, Y.-K., Chen, K.-H., Chern, J.-L., Wu, S.-C., Chen, C.-F., Chang, H., Lien, Y.-H. and Shy, J.-T., "Far-Infrared Resonance in Split Ring Resonators", *Japanese Journal of Applied Physics*, vol. 43, 2004, pp. L176-L179.

[147] Shamonin, M., Shamonina, E., Kalinin, V. and Solymar, L., "Properties of a metamaterial element: Analytical solutions and numerical simulations for a singly split double ring", *Journal of Applied Physics*, vol. 95, 2004, pp. 3778-3784.

[148] Huang, Y.-C., Hsu, Y.-J., Lih, J.-S.and Chern, J.-L., "Transmission Characteristics of Deformed Split-Ring Resonators", *Japanese Journal of Applied Physics*, vol. 43, 2004, pp. L190-L193.

[149] Hsu, Y.-J., Huang, Y.-C., Lih, J.-S.and Chern, J.-L., "Electromagnetic resonance in deformed split ring resonators of left-handed meta-materials", *Journal of Applied Physics*, vol. 96, 2004, pp. 1979-1982.

[150] Hsu, Y.-J. and Chern, J.-L., "Transmission Characteristics of Smiling Pattern Resonators", *Japanese Journal of Applied Physics*, vol. 43, 2004, pp. L669-L672.

[151] Gay-Balmaz, P. and Martin, O. J. F., "Efficient isotropic magnetic resonators", *Applied Physics Letters*, vol. 81, 2002, pp. 939-941.

[152] Smith, D. R., Padilla, W. J., Vier, D. C., Nemat- Nasser, S. C. and Schultz, S., "Composite Medium with Simultaneously Negative Permeability and Permittivity", *Physical Review Letters*, vol. 84, 2000, pp. 4184-4187.

[153] Shelby, R. A., Smith, D. R., Nemat-Nasser, S. C. and Schultz, S., "Microwave transmission through a two-dimensional, isotropic, left-handed metamaterial", *Applied Physics Letters*, vol. 78, 2001, pp. 489-491.

[154] Grbic, A. and Eleftheriades, G. V., "Experimental verification of backward-wave radiation from a negative refractive index metamaterial", *Journal of Applied Physics*, vol. 92, 2002, pp. 5930-5935.

[155] Luxey, C. and Laheurte, J.-M., "Simple Design of Dual-Beam Leaky-Wave in Microstrips", *IEE Proceedings of Microwave and Antennas Propagation, Part. H,* Vol. 144, N° 6, December 1997, pp. 397-402.

[156] Liu, L., Caloz, C. And Itoh, T., "Dominant mode leaky-wave antenna with backfire-to-endfire scanning capability", *Electronics Letters*, vol. 38, 2002, pp. 1414-1416.

[157] Grbic, A. and Eleftheriades, G. V., "A Backward-Wave Antenna Based on Negative Refractive Index L-C Networks", *IEEE Antennas and Propagation Society Symposium*, San Antonio, Texas, 2002.

[158] Martin, F., Bonache, J., Falcone, F., Sorolla, M. and Marqués, R., "Split ring resonator-based left-handed coplanar waveguide", *Applied Physics Letters*, vol. 83, 2003, pp. 4652-4654.

[159] Flores, M., Falcone, F., Martín, F., Bonache, J., Baena, J.D., Lopetegi, T., Laso, M. A. G., Marcotegui, J.A., García, J., Marqués, R. and Sorolla, M., "Radiation phenomena in coplanar waveguide metamaterial structures", *27th ESA Antenna Workshop on Innovative Periodic Antennas, Santiago de Compostela*, Spain, 2004.

[160] Caloz, C. and Itoh, T., "Array Factor Approach of Leaky-Wave Antennas and Application to1-D/2-D Composite Right/Left-Handed (CRLH) Structures", *IEEE Microwave and Wireless Components Letters*, vol. 14, pp. 274-276, 2004.

[161] Caloz, C. and Itoh, T., "Transmission Line Approach of Left-Handed (LH) Materials and Microstrip Implementation of an Artificial LH Transmission Line", *IEEE Transactions on Antennas and Propagation*, vol. 52, 2004, pp. 1159-1166.

[162] Lim, S., Caloz, C. And Itoh, T., "Novel Arbitrary Angle Leaky-Wave Reflector using Heterodyne Mixing", *33rd European Microwave Conference*, Munich, 2003.

[163] Lim, S., Caloz, C. And Itoh, T., "A Reflecto-Directive System Using a Composite Right/Left-Handed (CRLH) Leaky-Wave Antenna and Heterodyne Mixing", *IEEE Microwave and Wireless Components Letters*, vol. 14, 2004, pp. 183-185.

[164] Kang, M., Caloz, C. And Itoh, T., "Miniaturized MIM CRLH Transmission Line Structure and Application to Backfire-to-Endfire Leaky-Wave Antenna", *IEEE Antennas and Propagation Society Symposium*, 2004.

[165] Gómez Tornero, J.L., Álvarez Melcón, A. and Pardo, M. P., "Design of backfire to endfire periodic leaky-wave antennas for millimeter-wave band applications", *27th ESA Antenna Workshop on Innovative Periodic Antennas*, Santiago de Compostela, Spain, 2004.

[166] Lim, S., Caloz, C. and Itoh, T., "Electronically Scanned Composite Right/Left Handed Microstrip Leaky-Wave Antenna", *IEEE Microwave and Wireless Components Letters*, vol. 14, 2004, pp. 277-279.

[167] Lim, S., Caloz, C. and Itoh, T., "Electronically-Controlled Metamaterial-Based Transmission Line as a Continuous-Scanning Leaky-Wave antenna", *IEEE MTT-S International Microwave Symposium*, 2004.

[168] Lim, S., Caloz, C. and Itoh, T., "Metamaterials-Based Electronically Controlled Transmission-Line Structure as a Novel Leaky-Wave Antenna With Tunable Radiation Angle and Beamwidth", *IEEE Transactions on Microwave Theory and Techniques*, vol. 52, pp. 2678-2690, 2004.

[169] Luxey, C. and Laheurte, J.-M., " Effect of a Reactive Loading in Microstrip Leaky Wave Antennas", *Electronics Letters,* Vol. 36, N°15*,* pp. 1259-1260, July 2000.

[170] Caloz, C. and Itoh, T., "1D and 2D Leaky-Wave Antennas based on Metamaterials Concepts", *27th ESA Antenna Workshop on Innovative Periodic Antennas*, Santiago de Compostela, Spain, 2004.

[171] Sanada, A., Caloz, C. and Itoh, T., "Characteristics of the Composite Right/Left-Handed Transmission Lines", *IEEE Microwave and Wireless Components Letters*, vol. 14, 2004, pp. 68-70.

[172] Allen, C., Caloz, C. and Itoh, T., "Leaky-Waves in a Metamaterial-Based Two-Dimensional Structure for a Conical Beam Antenna Application", *IEEE MTT-S Digest*, 2004.

[173] Sievenpiper, D. F., Schaffner, J. H., Song, H. J., Loo, R. Y. and Tangonan, G., "Two-Dimensional Beam Steering Using an Electrically Tunable Impedance Surface", *IEEE Transactions on Antennas and Propagation*, vol. 51, 2003, pp. 2713-2722.

[174] Alu, A. and Engheta, N., "Radiation from a traveling-wave current sheet at the interface between a conventional material and a metamaterial with negative permittivity and permeability", *Microwave and Optical Technology Letters*, vol. 36, 2002, pp. 460-463.

[175] Lu, J., Grzegorczyk, T.M., Zhang, Y., Pacheco Jr, J., Wu, B.-I. and Kong, J. A., "Cherenkov radiation in materials with negative permittivity and permeability", *Optics Express*, vol. 11, 2003, pp. 723-734.

[176] Ziolkowski, R. W. and Kipple, A. D., "Application of Double Negative Materials to Increase the Power Radiated by Electrically Small Antennas", *IEEE Transactions on Antennas and Propagation*, vol. 51, 2003, pp. 2626-2640.

[177] Khodier, M. M., "Radiation Characteristics of an Infinite Line Source Surrounded by Concentric Shells of Metamaterials", *IEEE Antennas and Propagation Society Symposium*, 2004.

[178] Kildal, P.-S., "Comments on 'Application of double negative materials to increase the power radiated by electrically small antennas'" (the authors of the original paper are R. W. Ziolkowski and A. D. Kipple), *IEEE Transactions on Antennas and Propagation*, accepted for publication.

[179] Mahmoud, S. F., "A New Miniaturized Annular Ring Patch Resonator Partially Loaded by a Metamaterial Ring With Negative Permeability and Permittivity", *IEEE Antennas and Wireless Propagation Letters*, vol. 3, 2004, pp. 19-22.

[180] Saenz, E., Gonzalo, R., Ederra, I. and De Maagt, P., "Metamaterials as super-substrate to enhance dipole antenna performances", *11th International Student Seminar on Microwave Applications of Novel Physical Phenomena*, St.-Petersburg, Russia, 2004.

[181] Saenz, E., Gonzalo, R., Ederra, I. and De Maagt, P., "High Efficient Dipole Antennas by Using Left-Handed Superstrates", *14èmes Journées Internationales de Nice sur les Antennas JINA 2004,* Nice, France, November 2004.

[182] Antoniades, M. A. and Eleftheriades, G. V., "Compact Linear Lead/Lag Metamaterial Phase Shifters for Broadband Applications", *IEEE Antennas and Wireless Propagation Letters*, vol. 2, 2003, pp. 103-106.

[183] Enoch, S., Tayeb, G., Sabouroux, P., Guérin, N. and Vincent, P., "A Metamaterial for Directive Emission", *Physical Review Letters*, vol. 89, 2002, pp. 213902.

[184] Schüssler, M., Oertel, M., Fritsche, C., Freese, J. and Jakoby, R., "Design of Periodically L-C Loaded Patch Antennas", *27th ESA Antenna Workshop on Innovative Periodic Antennas*, Santiago de Compostela, Spain, 2004.

[185] Tayeb, G., Enoch, S., Sabouroux, P,. Guérin, N. and Vincent, P., "Compact Directive Antennas Using Metamaterials", *13èmes Journées Internationales de Nice sur les Antennas JINA 2003*, Nice, France, November 2002.

[186] Dardenne, X. and Craeye, C., "Numerical study of low-profile directive antennas based on metamaterials", *11th International Student Seminar on Microwave Applications of Novel Physical Phenomena*, St.-Petersburg, Russia, 2004.

[187] Ikonen, P., Simovski, C. R. and Tretyakov, S. A., "Compact Directive Antennas With a Wire-Medium Artificial Lens", *Microwave and Optical Technology Letters*, vol. 43, 2004, pp. 467-469.

[188] Cory, H. and Zach, C., "Wave propagation in metamaterial multi-layered structures", *Microwave and Optical Technology Letters*, vol. 40, 2004, pp. 460-465.

[189] Baccarelli, P., Burghignoli, P., Lovat, G. and Paulotto, S., "Surface-Wave Suppression in a Double-Negative Metamaterial Grounded Slab", *IEEE Antennas and Wireless Propagation Letters*, vol. 2, 2003, pp. 269-272.

[190] Schüssler, M., Freese, J. and Jakoby, R., "Design of Compact Planar Antennas using LH-Transmission Lines", *IEEE MTT-S International Microwave Symposium*, 2004.

[191] Lai, A., Caloz, C. And Itoh, T., "Composite Right/Left-Handed Transmission Line Metamaterials", *IEEE Microwave Magazine*, 2004, pp. 34-50.

[192] Sanada, A. Caloz, C. and Itoh, T. "Zeroth order resonance in composite right/left-handed transmission line resonators", *Asia-Pacific Microwave Conference*, Seoul, Korea, vol. 3, pp. 1588–1592, 2003.

[193] Sanada, A., Kimura, M. Awai, I. Kubo, H. Caloz, C. and Itoh, T., "A planar zeroth order resonator antenna using left-handed transmission line", *European Microwave Conference,* Amsterdam, The Netherlands, 2004.]

[194] Eleftheriades, G. V., Antoniades, M. A., Grbic, A., Iyer, A. K. and Islam, R., "Electromagnetic Applications of Negative-Refractive-Index Transmission-Line Metamaterials", *27th ESA Antenna Workshop on Innovative Periodic Antennas*, Santiago de Compostela, Spain, 2004.

[195] Grbic, A. and Eleftheriades, G. V., "Dispersion Analysis of a Microstrip-Based Negative Refractive Index Periodic Structure", *IEEE Microwave and Wireless Components Letters*, vol. 13, 2003, pp. 155-157.

[196] Baccarelli, P. and Burghignoli, P., "The nature of radiation from leaky waves on single- and double-negative metamaterial grounded slabs", *IEEE MTT-S International Microwave Symposium*, 2004.

LIST OF ILLUSTRATIONS

LIST OF TABLES

LIST OF ACRONYMS

2G: Second Generation systems

3G: Third Generation

3.5G: 3.5 Generation systems

3GPP: Third Generation Partnership Project

3GPP2: Third Generation Partnership Project

A

ANSI: American National Standards Institute

ASIC: Application-Specific Integrated Circuits

B

BAN: Body Area Network

BiCMOS: Bipolar CMOS

BTE: Behind-The-Ear

BW. Backward Wave

C

CBGA: Ceramic Ball Grid Array

CDMA: Code Division Multiple Access

CI: Cochlear Implant

CIC: Completely-In-the-Canal

CMOS: Complementary Metal Oxide Semiconductor

CPW: CoPlanar Waveguide

CRLH: Composite Right/Left-Handed

CS: Circuit Switched

D

DAB: Digital Audio Broadcasting

DVB-H: Digital Video Broadcasting for Handsets

DVB-T: Digital Video Broadcasting, Terrestrial

DC: Direct Current

DCS: Digital Communications System

DECT: Digital Enhanced Cordless Telecommunications

DNG: Double NeGative media

E

EBG: Electromagnetic BandGap

ECC: Electronic Communications Committee

EDGE: Enhanced Data rates for the GSM Evolution

EIRP: Effective Isotropic Radiated Power

EM: ElectroMagnetic

EMC: ElectroMagnetic Compatibility

EMI: ElectroMagnetic Interference

EPWBM: Experimental Plane-Wave Based Method

ETSI: European Telecommunications Standards Institute

EICTA: European Information & Communications Technology Industry Association

F

FCC: Federal Communications Commission

FDD: Frequency Division Duplex

FET: Field Effect Transistor

FHWM: Full Half Width Maximum

FSS: Frequency Selective Surface

G

GaAs: Gallium Arsenide

GSM: Global System for Mobiles

H

HA: Hearing Aid

HAC: Hearing Aid Compatible

HF: High Frequency

HPBW: Half-Power BeamWidth

HSCA: Horn shaped Self-Complementary Antenna

HSDPA: High Speed Downlink Packet Access

HSUPA: High-Speed Uplink Packet Access

I

ICPA: Integrated Circuit Package Antenna

IEEE: Institute of Electrical and Electronics Engineers

IF: Intermediate Frequency

IFA: Invertef-F Antenna

IMT-2000: International Mobile Telecommunications-2000

ISO: International Organization for Standardization

ITE: In-The-Ear

ITU: I nternational Telecommunication Union

L

LF: Low Frequency

LH: Left Handed

LHM: Left Handed Media

LPDA: Logarithmic-Periodic Dipole Array

LTI: Linear Time Invariant

M

MEG: Mean Effective Gain

MEMS: Micro-Electro-Mechanical Systems

MICS: Medical Implants Communications System

MIMO: Multiple Input, Multiple Output

MLA: Meander Line Antennas

MT: Mobile Terminal

N

NLOS: Non Line Of Sight

NRI: Negative Refractive Index

P

PBG: Photonic BandGap

PCB: Printed Circuit Board

PICA: Planar Inverted Cone Antenna

PIFA: Planar Inverted-F Antenna

PQHA: Printed Quadrifilar Helical Antenna

PS: Packet Switched

PSD: Power Spectrum Density

R

RF: Radio Frequency

RF-SoC: RF System-on-a Chip

RH: Right Handed

RHM: Right Handed Media

RFID: Radio Frequency IDentification

S

SDA: Scratch Drive Actuator

SDR: Software-Defined Radio

Si: Silicon

SISO: Single-Input, Single Output

T

TDD: Time Division Duplex

TDMA: Time Division Multiple Access

TD-SCDMA: Time Division Synchronous Code Division Multiple Access

TL-LW: Transmission Line-Leaky Wave

TRP: Total Radiated Power

U

UHF: Ultra High Frequency

ULSIC: Ultra Large Scale Integrated Circuits

UMTS: Universal Mobile Telecommunications System

UTD: Uniform geometrical Theory of Diffraction

UWB: Ultra Wide Band

UWC-136: Universal Wireless Communications-136

V

VCO: Voltage-Controlled Oscillator

VSWR: Voltage Standing Wave Ratio

W

WARC: World Administrative Radio Conference

W-CDMA: Wideband-CDMA

Z

ZOR: Zero-th Order Resonators